MOLECULAR MECHANISMS OF RADIATION-INDUCED BRAIN INJURY

Won Hee Lee

Dissertation submitted to the faculty of the Virginia Polytechnic Institute and State University in fulfillment of the requirements for the degree of

DOCTOR OF PHILOSOPHY
In
Biomedical Engineering and Sciences

Committee Members:

Yong Woo Lee, Chairman
Aaron S. Goldstein
Liwu Li
Marion Ehrich
M. Nichole Rylander

November 3, 2010
Blacksburg, VA

Keywords: Whole brain irradiation, brain inflammation, aging, extracellular matrix, angiogenesis

Molecular Mechanisms of Radiation-Induced Brain Injury

Won Hee Lee

ABSTRACT

Radiation therapy has been most commonly used modality in the treatment of brain tumors. About 200,000 patients with brain tumors are treated with either partial large field or whole brain irradiation every year in the United States. The use of radiation therapy for treatment of brain tumor, however, can subsequently lead to devastating functional deficits several months to years after treatment. Unfortunately, there are no known successful treatments and effective strategies for mitigating radiation-induced brain injury. In addition, the specific mechanisms by which irradiation causes brain injury in normal tissues are not fully understood. A deeper understanding of the molecular mechanisms underlying these phenomena could enable the development of more effective therapies to contribute to long-term disease suppression or even cure. Therefore, the primary goal of this research project was to determine the molecular mechanisms responsible for radiation-induced brain injury in normal tissues. In the first study, the effects of whole brain irradiation on pro-inflammatory pathways in the brain were examined. Results demonstrated that brain irradiation induces regionally specific alterations in pro-inflammatory environments through activation of pro-inflammatory transcription factors (e.g., activator protein-1 (AP-1), nuclear factor-κB (NF-κB), and cAMP response element-binding protein (CREB)) and overexpression of pro-inflammatory mediators (e.g., tumor necrosis factor-α (TNF-α), interleukin-1β (IL-1β), and monocyte chemoattractant protein-1 (MCP-1)) in brain. This study provides evidence for a differential induction of pro-inflammatory mediators in specific brain regions that have importance for the neurological/neuropathological consequences of irradiation.

In the second study, a mathematical model describing radiation-induced mRNA and protein expression kinetics of TNF-α in hippocampus was reconstructed. This study demonstrated that the reaction kinetic model could predict protein expression levels of TNF-α in cortex, suggesting that this model could be used to predict protein expression levels of pro-inflammatory mediators in other parts of the brain.

In the third study, the effects of aging on radiation-mediated impairment of immune responses in brain were examined. Results showed that radiation-induced acute inflammatory responses, such as overexpression of pro-inflammatory cytokines (e.g., TNF-α, IL-1β, and IL-6), adhesion molecules (e.g., intercellular adhesion molecule-1 (ICAM-1), vascular cell adhesion molecule-1 (VCAM-1), and E-selectin), chemokine MCP-1, and matrix metalloproteinase-9 (MMP-9), are significantly impaired in aged brain. This study suggests that reduced production of pro-inflammatory mediators in response to irradiation compromises the normal host defense mechanisms in damaged brain tissue and subsequently leads to impaired repair/remodeling responses in old individuals.

In the fourth study, the effects of irradiation on MMPs/tissue inhibitor of metalloproteinases (TIMPs) and extracellular matrix (ECM) degradation in brain were examined. Results demonstrated that whole brain irradiation induces an imbalance between MMPs and TIMPs expression, increases gelatinase activity, and degrades collagen type IV in the brain. This study suggests that a radiation-induced imbalance between MMP-2 and TIMP-2 expression may have an important role in the pathogenesis of brain injury by degrading ECM components of the blood-brain barrier (BBB) basement membrane.

In the fifth study, the effects of irradiation on angiogenic factors and vessel rarefaction in brain were examined. Results demonstrated that whole brain irradiation decreases endothelial cell (EC) proliferation, increases EC apoptosis, and differentially regulates the expression of angiogenic factors such as angiopoietin-1 (Ang-1), Ang-2, Tie-2, and vascular endothelial growth factor (VEGF) in brain. This study suggests that radiation-induced differential regulation of angiogenic factors may be responsible for vessel rarefaction.

In summary, the results from these studies demonstrated that whole brain irradiation induces brain injury by triggering pro-inflammatory pathways, degrading extracellular matrix, and altering physiologic angiogenesis. Therefore, this work may be beneficial in defining a new cellular and molecular basis responsible for radiation-induced brain injury. Furthermore, it may provide new opportunities for prevention and treatment of brain tumor patients who are undergoing radiotherapy.

AUTHOR'S ACKNOWLEDGMENTS

I would first like to thank my advisor Dr. Yong Woo Lee for his support, ceaseless guidance, and patience throughout my graduate carrier. His dedication to achieve excellence and his belief to be a constructive part of the whole have inspired me to put that extra effort and motivated me to keep going in spite of failures. Dr. Lee, I have been very fortunate to have an advisor like you. Thanks for everything.

I want to acknowledge Dr. Aaron S. Goldstein, Dr. Liwu Li, Dr. Marion Ehrich, and Dr. M. Nichole Rylander for providing their valuable suggestions and reviewing my work. I appreciate your time and help. I appreciate the help from our collaborators, Dr. William E. Sonntag, Han Yan, and Matthew Mitschelen, in the Reynolds Oklahoma Center on Aging, Department of Geriatric Medicine at University of Oklahoma Health Sciences Center.

I would also thank all my labmates, Anjali Hirani, Hyungjoon Cho, Katelyn Colacino, and Paul Kim for their unconditional support, encouragement, and kind friendship. It is nice to have lifelong friends.

Our graduate and department administrative staff, Tess Sentelle, Pam Stiff, Jo Thomason, and Kathy Creggar, will always have my thanks and good wishes for helping me.

Finally, I am profoundly grateful to my parents, sisters, brother, Dr. Yun's family who have been a constant source of love, support, and encouragement at all times for longer than I can remember.

DECLARATION OF WORK PERFORMED

I declare that with the exception of the items indicated below, all work reported in this dissertation was performed by me.

All irradiation procedures (*in vivo* and *in vitro*) and collection of tissue samples were done at University of Oklahoma Health Sciences Center (OUHSC), Oklahoma City, OK. All animal protocols were approved by the Institutional Animal Care and Use Committees of OUHSC. Dr. William E. Sonntag supervised all irradiation procedures. Irradiation procedures, blood perfusion, and brain tissue collection from rats and mice were conducted by Junie P. Warrington, Han Yan, and Matthew Mitschelen at OUHSC. Han Yan and Julie Farley also assisted me with cell culture and *in vitro* irradiation.

TABLE OF CONTENTS

LIST OF FIGURES

LIST OF TABLES

LIST OF ABBREVIATIONS

3D-CRT	Three-dimensional conformal radiation therapy
Aβ	Amyloid β
AD	Alzheimer's disease
Ang	Angiopoietin
ANOVA	Analysis of variance
AP-1	Activator protein-1
BBB	Blood-brain barrier
BED	Biologically effective dose
BSA	Bovine serum albumin
cAMP	Cyclic adenosine monophosphate
CBTRUS	Central brain tumor registry of the United States
CNS	Central nervous system
COX	Cyclooxygenase
CREB	cAMP response element-binding protein
CRT	Cranial irradiation
CSF	Cerebrospinal fluid
DMEM	Dulbecco’s modified eagle medium
DVT	Deep venous thrombosis
ECM	Extracellular matrix
ELISA	Enzyme linked immunosorbent assay
EMSA	Electrophoretic mobility shift assays
FBS	Fetal bovine serum
GAPDH	Glyceraldehydes-3-phosphate dehydrogenase
GRNs	Genetic regulatory networks
Gy	Gray
HSV	Herpessimplex virus
ICAM-1	Intercellular adhesion molecule-1
IFN-γ	Interferon-γ
IL-1β	Interleukin-1β

IL-6	Interleukin-6
LINAC	Linear accelerator
LPS	Lipopolysaccharide
LQ	Linear quadratic
MCP-1	Monocyte chemoattractant protein-1
MMP	Metalloproteinase
MPTP	1-methyl-4-phenyl-1,2,3,6-tetrahydropyridine
mRNA	Messenger RNA
NF-κB	Nuclear factor-kB
NSAIDs	Non-steroidal anti-inflammatory drugs
ODE	Ordinary differential equation
OUHSC	University of Oklahoma health sciences center
PBS	Phosphate buffered saline
PD	Parkinson's disease
PGE_2	Prostaglandin E_2
RT-PCR	Reverse transcriptase-polymerase chain reaction
SI	International system of units
SNpc	Substantia nigra pars compacta
SOCS	Suppressors of cytokine signaling
TBI	Traumatic brain injury
TIMP	Tissue inhibitors of metalloproteinase
TNF-α	Tumor necrosis factor-α
VCAM-1	Vascular cell adhesion molecule-1
VEGF	Vascular endothelial growth factor

CHAPTER 1: INTRODUCTION

1.1 Significance and Hypothesis

Radiation therapy has been shown to be of major significance in tumor control and survival rate of brain tumor patients (1). According to the Central Brain Tumor Registry of the United States (CBTRUS), about 200,000 patients with brain tumors are treated with either partial large field or whole brain irradiation every year in the United States (2). The use of radiotherapy for treatment of brain tumors, however, is limited by the risk of radiation-induced injury to normal brain tissue that can subsequently lead to devastating functional deficits several months to years after treatment (1-3). Recent randomized, prospective clinical trials also provide evidence that the addition of whole brain irradiation to stereotactic radiosurgery may cause a significant reduction in learning and memory in patients with brain tumors (4). However, very limited information on the etiology of radiation-induced damage to normal brain tissue is currently available. At present, there are no successful treatments or effective preventive strategies for radiation-induced brain injury. Additionally, the specific mechanisms by which radiation causes brain injury in normal tissues have not yet been fully understood.

The main hypothesis tested by this doctoral study was that **whole brain irradiation induces brain injury in normal tissues by triggering pro-inflammatory pathways, degrading extracellular matrix, and altering physiologic angiogenesis (Figure 1.1).** To fully address our hypothesis, we pursued the following five specific aims: (1) to determine the effect of irradiation on pro-inflammatory environments in the brain, (2) to construct a mathematical model of radiation-induced brain inflammation, (3) to determine the effect of aging on radiation-mediated impairment of immune response in the brain, (4) to determine the effect of irradiation on matrix metalloproteinases (MMPs)/tissue inhibitor of metalloproteinases (TIMPs) and extracellular matrix (ECM) degradation in the brain, and (5) to determine the effect of irradiation on angiogenic factors and vessel rarefaction in the brain.

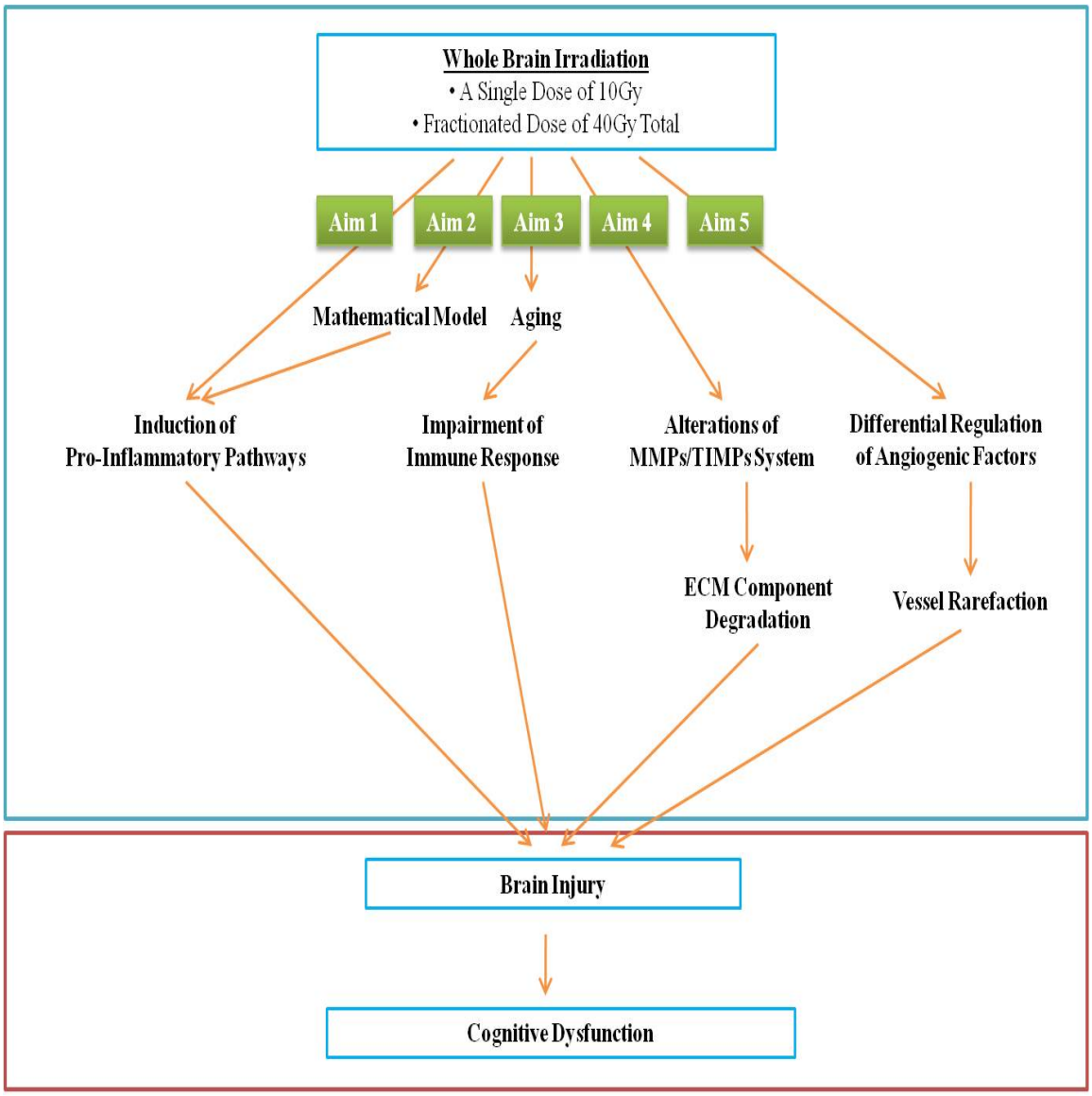

Figure 1.1. Schematic Diagram of the Main Hypothesis.

In the present study, we determined mechanisms of radiation-induced brain injury at the cellular and molecular level by investigating five specific aims. In addition, we have made a collaborative arrangement with Dr. William E. Sonntag at University of Oklahoma Health Sciences Center (OUHSC) to address the effect of whole brain irradiation on cognitive dysfunction in animal models.

1.2 Specific Aims and Justification

1.2.1 ***Specific Aim 1:*** *To determine the effect of irradiation on pro-inflammatory environments in the brain.*

Recent evidence has identified inflammation as one of the most important pathways leading to radiation-induced brain injury (5-9). These studies raise the possibility that a pro-inflammatory environment resulting from overexpression of pro-inflammatory mediators may be responsible for the risk of life-threatening complications occurring in brain after irradiation. Effects of irradiation on pro-inflammatory pathways in the brain, however, have not yet been fully elucidated. Therefore, we examined the effects of whole brain irradiation on pro-inflammatory pathways in the brain.

1.2.2 ***Specific Aim 2:*** *To construct mathematical model of radiation-induced brain inflammation.*

Multiple interactions of gene products are involved in molecular pathways of a variety of human diseases. Therefore, understanding of the factors responsible for the gene regulation is critical to understand general biological systems and to develop new strategies for prevention and treatment of diseases. Various mathematical models have been proposed to describe the behavior of the networks being modeled and make predictions corresponding with experimental observations (10, 11). Dynamic system approach using ordinary differential equations (ODEs) is the most prominent method to analyze genetic regulatory system. In the present study, we constructed a mathematical model describing radiation-induced mRNA and protein expression kinetics of tumor necrosis factor-α (TNF-α) in the hippocampus by modifying a nonlinear model based on reaction kinetics (12).

1.2.3 ***Specific Aim 3:*** *To determine the effect of aging on radiation-mediated impairment of immune response in the brain.*

It has been suggested that acute inflammatory responses in cancer patients undergoing radiation therapy may have beneficial effects. A number of previous studies have demonstrated that an enhanced production of pro-inflammatory cytokines in response to radiation is a necessary component of normal tissue repair processes (13, 14). Although it is generally accepted that the immune responses and the effectiveness of radiation therapy decline with age, the association among aging, inflammation, and radiation therapy remains to be further investigated. Therefore, the present study was designed to examine the effect of aging on radiation-induced expression of pro-inflammatory mediators, such as cytokines, adhesion molecules, chemokine, and MMP-9 in rat brain.

1.2.4 ***Specific Aim 4:*** *To determine the effect of irradiation on MMPs/TIMPs and ECM degradation in the brain.*

The blood-brain barrier (BBB) exists primarily as a selective barrier between the systemic circulation and the brain. The ECM, forming a basal laminar underlying vasculature, is critical to maintaining the integrity of the BBB. The gelatinases MMP-2 and MMP-9, the most commonly investigated MMPs in the central nervous system (CNS), are able to degrade ECM components including collage type IV which is essential for maintaining BBB integrity. The activity of MMP-2 and MMP-9 is prone to be blocked by TIMPs. Therefore, the balance between MMPs and TIMPs is considered as an important homeostatic regulation in the development and plasticity of the CNS. Previous reports have demonstrated that BBB breakdown is one of major consequences of irradiation and may be responsible for the radiation-induced brain injury in normal tissues (15, 16). The cellular and molecular mechanisms of radiation-induced BBB disruption, however, remain to be further investigated. In the present study, we examined the critical role of MMPs/TIMPs system in radiation-induced ECM degradation in rat brain to define the molecular mechanisms of the BBB disruption and subsequent brain injury by whole brain irradiation.

1.2.5 ***Specific Aim 5:*** *To determine the effect of irradiation on angiogenic factors and vessel rarefaction in the brain.*

Vessel rarefaction has been implicated in the onset and progression of various pathological processes (17-19). Previous studies have shown that irradiation induces both acute and late changes in the vasculature (20-22). It has been also hypothesized that radiation-induced early and persistent damages to the microvasculature may be responsible for vessel rarefaction leading to the late delayed brain injury. The molecular mechanisms of radiation-induced vessel rarefaction in brain, however, remain to be further investigated. In the present study, we determined the critical role of radiation-induced differential regulation of angiogenic factors in vessel rarefaction in rat brain.

The significance of the present study is that this work may provide a foundation for defining a new cellular and molecular basis related to the etiology of cognitive impairment that occurs in response to whole brain irradiation. Additionally, it may lead to new opportunities for preventive and therapeutic interventions for brain tumor patients who are undergoing radiotherapy.

1.3 Experimental Design and Methods

The present study was designed to test our main hypothesis that whole brain irradiation induces brain injury in normal tissues by triggering pro-inflammatory pathways, degrading extracellular matrix, and altering physiologic angiogenesis.

1.3.1 Experimental Design

1.3.1.1 Effect of Irradiation on Pro-Inflammatory Environments in the Brain

Four month old F344×BN rats received either whole brain irradiation with a single dose of 10Gy γ-rays or sham-irradiation, and were maintained for 4, 8, and 24 h following irradiation. The mRNA and protein expression levels of pro-inflammatory mediators (e.g., TNF-α, interleukin-6 (IL-6), IL-1β, and monocyte chemoattractant protein-1 (MCP-1)) in both hippocampus and cortex were examined by real-time reverse transcriptase-polymerase chain reaction (RT-PCR), enzyme-linked immunosorbent assay (ELISA), and immunofluorescence staining. TNF-α mRNA and protein expression were also determined *in vitro*. Additionally, the DNA binding activity of pro-inflammatory transcription factors, such as activator protein-1 (AP-1), nuclear factor-κB (NF-κB), and cAMP response element-binding protein (CREB), was assessed by electrophoretic mobility shift assays (EMSA) to define the molecular mechanisms of radiation-induced brain inflammation.

1.3.1.2 Construction of Mathematical Model of Radiation-Induced Brain Inflammation

A mathematical model describing radiation-induced mRNA and protein expression kinetics of TNF-α in the hippocampus was constructed by modifying a nonlinear model consisting of ordinary differential equations (ODEs) based on reaction kinetics. As a regulation function, a positive Hill curve function was used. To estimate four unknown model parameters, experimental data measured in rat hippocampus and Matlab's "fminsearch" command were employed. The model was simulated using the command "ODE113" in Matlab. Additionally,

values between model predictions and measured protein expression levels of TNF-α were compared to confirm the accuracy of the model.

1.3.1.3 Effect of Aging on Radiation-Mediated Impairment of Immune Response in the Brain

Male F344×BN rats (4, 16, and 24 months of age) received either whole brain irradiation with a single dose of 10Gy γ-rays or sham-irradiation, and were maintained for 4, 8, and 24 h post-irradiation. The mRNA expression levels of various pro-inflammatory mediators, including cytokines (e.g., TNF-α, IL-1β, and IL-6), adhesion molecules (e.g., intercellular adhesion molecule-1 (ICAM-1), vascular cell adhesion molecule-1 (VCAM-1), and E-selectin), chemokine MCP-1, and MMP-9, were analyzed by quantitative real-time RT-PCR.

1.3.1.4 Effect of Irradiation on MMPs/TIMPs and ECM Degradation in the Brain

Rats received either a single dose of 10Gy γ-rays or sham-irradiation, and mice received a fractionated dose of 40Gy γ-rays total or sham-irradiation. Animals were then maintained for 4, 8, and 24 h following irradiation. The mRNA expression levels of MMPs (e.g., MMP-2, -3, -7, -9, -10, and -12) and TIMPs (e.g., TIMP-1, and TIMP-2) in the brain were analyzed by real-time RT-PCR. In addition, the functional activity of MMPs was measured by *in situ* zymography and degradation of ECM was visualized by collagen type IV immunofluorescence staining.

1.3.1.5 Effect of Irradiation on Angiogenic Factors and Vessel Rarefaction in the Brain

Rats received either whole brain irradiation with a single dose of 10Gy γ-rays or sham-irradiation, and were maintained for 4, 8, and 24 h following irradiation. To determine vessel rarefaction, endothelial cell proliferation and apoptosis were visualized by double immunofluorescence staining. The mRNA and protein expression levels of various angiogenic factors (e.g., vascular endothelial growth factor (VEGF), angiopoietin (Ang-1), Ang-2, and Tie-2) were analyzed by real-time RT-PCR, ELISA, and immunofluorescence staining.

1.3.2 Experimental Methods

This section provides the general description of common experimental methods used throughout this dissertation. A more detailed, project-specific materials and methods are included in chapters 3-7.

1.3.2.1 Animals

Fisher 344-Brown Norway (F344×BN) male rats (4, 16, and 24 months old) and C57BL/6 male mice were purchased from Harlan Laboratories (Indianapolis, IN) and Jackson Laboratory (Bar Harbor, ME), respectively. The F344×BN rat is a recommended strain by the National Institutes on Aging in studying aging-associated pathophysiological changes. It appears to have a longer life span (average life span is 137 weeks), a lower level of aging-related pathological conditions, and less biological variability than inbred rats (23). Therefore, the F344×BN rat has been a common and useful model to examine age-related cognitive and behavioral deficits in the presence of maintained physical function (24). In addition, C57BL/6 is the most widely used inbred strain as models of human diseases because of the easy breeding, the availability of congenic strains, and robustness. Furthermore, these two types of animals have been most commonly used as models for studying radiation response (25-29). Rats were used for single dose irradiation studies and mice were used when fractionated doses of irradiation were given.

In this study, animals were housed on a 12/12 light-dark cycle with food and water provided *ad libitum*. Animal care was conducted in accordance with the NIH Guide for the Care and Use of Laboratory Animals and this study was approved by the Institutional Animal Care and Use Committee.

1.3.2.2 Whole Brain Irradiation

Following an acclimatization period of one week, the animals received either whole brain irradiation (a single dose of 10Gy γ-rays for rats or a fractionated dose of 40Gy γ-rays total for mice) or sham-irradiation (**Figure 1.2**).

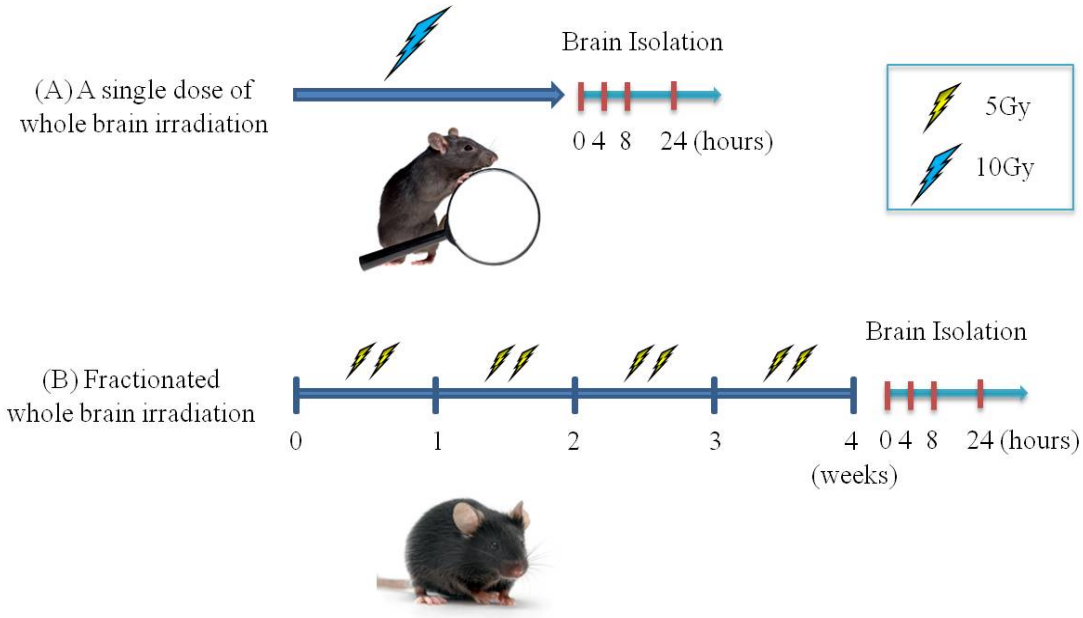

Figure 1.2. Whole Brain Irradiation Schedules. Animals received either (A) a single dose of 10Gy γ-rays (rats), (B) a fractionated dose of 40Gy γ-rays total (mice), or sham-irradiation, and were maintained for 4, 8, and 24 h following whole brain irradiation.

In the present study, a rat model of whole brain irradiation with a single dose of 10Gy was chosen for three reasons: (1) it is known as the lowest dose to have a radiation effect (30, 31), (2) it is well below the threshold for vascular changes, demyelination or radionecrosis (32-34), and (3) it is close to a clinically relevant dose in humans because rat brain is more resistant to radiation injury than human brain (32, 35). Whole brain irradiation procedures were carried out as described previously (26, 36) with minor modifications. The photographs of irradiation procedures (**Figure 1.3**) and sample preparation for immunofluorescence staining (**Figure 1.5**) were provided by OUHSC. Rats were anesthetized using a 350 μl mixture of ketamine/xylazine (80/12 mg/kg body weight). Whole brain irradiation was performed in a 12,000 Ci self-shielded ^{137}Cs irradiator (Gammacell 40 Exactor, Nordion International Inc; Kanata, Ontario, Canada) using lead and Cerrobend shielding devices to collimate the beam so that the whole rat brain, including the brain stem, was irradiated. Dosimetry was performed using thermoluminescent dosimeters placed in the skull of dead rats, and confirmed with ionization chambers in tissue equivalent phantoms. The average dose rate to the midline of the brain for the two positions was

~ 4Gy/min with an 8 % difference between the two positions. To ensure that each rat received the same midline brain dose, each lightly anesthetized animal had 5Gy delivered to alternate sides of the head. A total dose of 10Gy γ-rays is at an average dose rate of 4.23Gy/min. The eyes received about 15 % of the brain dose, and the body received 1-3 % of the brain dose. Control rats were anesthetized but not irradiated. The animals were maintained for 4, 8, and 24 h post-irradiation.

Step 1: Intramuscular injection with ketamine/xylazine for anesthesia.

Step 2: Putting rat in the mold to protect body during whole brain irradiation.

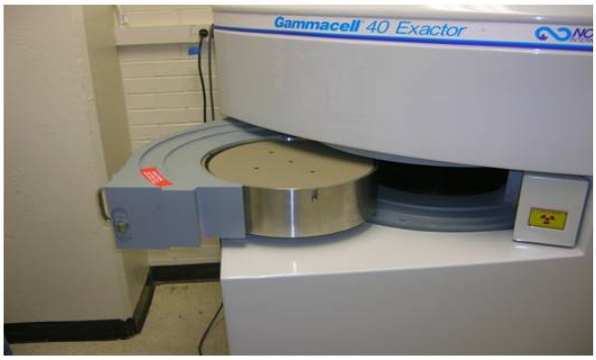

Step 3: Placing the rat in the irradiator.

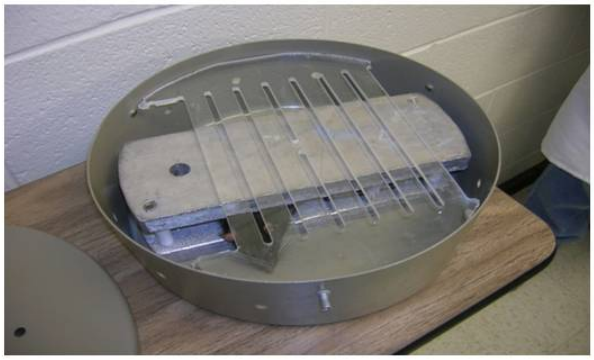

Step 4: Pulling them out of the irradiator. Plastic disc was used to prevent the basket from collapsing.

Figure 1.3. Irradiation Procedures.

In vitro irradiation was performed to provide results reported in Chapter 3. The murine microglial cell line, BV-2 cells, were grown to 80-90 % confluence and irradiated with a single dose of 10Gy γ-rays using a ^{137}Cs irradiator (**Figure 1.4**). All irradiations were performed at room temperature and control cells received sham-irradiation. After irradiation, the cells were returned to the CO_2 incubator and maintained at 37 °C in 5 % CO_2/95 % air for 4 and 24 h post-irradiation.

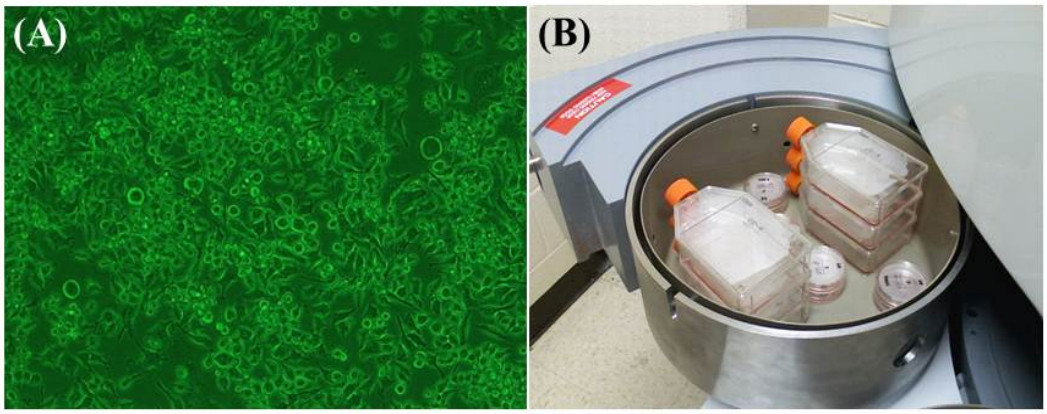

Figure 1.4. *In Vitro* Irradiation. BV-2 cells (A) were irradiated with a single dose of 10 Gy γ-rays (B).

In addition, a fractionated dose of whole brain irradiation was employed to provide a clinical relevance. The calculated biologically effective dose (BED) of the fractionated whole brain irradiation in this study was close to the corresponding BED for conventional whole brain irradiation regimen used clinically for the treatment of brain tumor patients (37, 38). Fractionated whole brain irradiation was performed in mice as described previously (**Figure 1.2B**) (39). Briefly, mice were anesthetized using intraperitoneal injections of 100 µl of a ketamine/xylazine mixture (20/3 mg/kg body weight). Mice received a clinical fractionated dose of whole brain irradiation (total cumulative dose of 40Gy in eight fractions of 5Gy, twice a week for four weeks) using a ^{137}Cs γ-irradiator. The bodies of the mice were shielded by Cerrobend so that only the head received the full irradiation dose. Mice in the control group were only

anesthetized. The mice were maintained for 4, 8, and 24 h after the last fractionated dose of whole brain irradiation.

1.3.2.3 Tissue Sample Preparation

For real-time RT-PCR, the rat brains were rapidly removed and two different rat brain regions (hippocampus and cortex) were dissected, immediately frozen in liquid nitrogen, and stored at -80 °C until analysis. For immunofluorescence staining and *in situ* zymography, rats were given ketamine/xylazine (80/12 mg/kg body weight) immediately prior to perfusion. Rats were then transcardially perfused with ice-cold phosphate buffered saline (PBS) containing 6unit/ml heparin and the whole brains were rapidly removed, immediately frozen in liquid nitrogen, and stored at -80 °C until analysis (**Figure 1.5**).

Mice were given ketamine/xylazine (20/3 mg/kg body weight) and perfused transcardially using heparinized PBS. The mouse brains were rapidly removed after perfusion and hemisected at the midline. Brains were then immediately frozen in liquid nitrogen and stored at -80 °C until analysis.

1.3.2.4 Statistical Analysis

The statistical analysis of data was completed using SigmaStat 3.5 (SPSS Inc., Chicago, IL). One-way analysis of variance (ANOVA) was used to compare mean responses among the treatments. For each endpoint, the treatment means were compared using the Bonferroni least significant difference procedure. Statistical probability of $p<0.05$ was considered significant.

Step 1: Intramuscular injection with ketamine/xylazine for anesthesia.

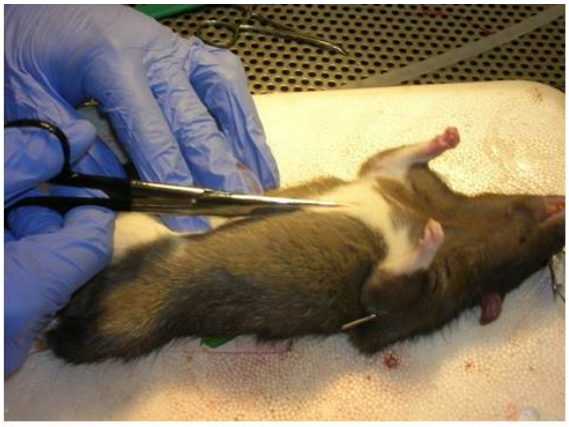

Step 2: Cutting the chest and retracting the ribs.

Step 3: Making a small incision in the left side of the posterior left ventricle, cannulating the aorta, and pumping ice-cold heparinized PBS.

Step 4: Extracting the brain from the skull and freezing them in dry ice-chilled isopentane.

Figure 1.5. Sample Preparation for Immunofluorescence Staining.

CHAPTER 2: BACKGROUND

2.1 Treatment Options for Brain Tumors

Brain tumors are categorized as two types: glial and non-glial tumors. Astrocytomas, oligodendrogliomas, and ependymomas are the most common gliomas that develop from glial tissues such as astrocytes and oligodendrocytes. The majority of gliomas are characterized by their tendency to diffusely infiltrate into white matter tracts. It is almost impossible to extirpate nearly all gliomas, partly because of their growth pattern (40). Non-glial brain tumors, such as meningioma, germ cell tumor, and pituitary adenoma, develop in areas other than glial tissues including glands, blood vessels and nerves. Both glial and non-glial brain tumors can be either malignant or benign (non-malignant). Although the exact cause of brain tumors is still unknown, several risk factors have been identified such as certain genetic disorders, environmental factors, and electromagnetic fields (41). Treatment options for brain tumors are selected based on factors including tumor type, location and size of tumor, tumor grade, age, and general health of the patient. The most widely used treatments include surgery, chemotherapy, and radiation therapy.

2.1.1 Surgery

Surgical procedure is usually the first line of therapy for patients with primary brain tumors. It is necessary to perform a biopsy for diagnosis or eliminate accessible brain tumors at the primary site. Clinical data have shown that a near-total resection is important in improving survival in patients with high-grade gliomas (42, 43). Even though surgery serves as an initial therapy and can often be curative for intracranial tumors that occur on the outer portion of the brain, it may not be efficient for all malignant brain tumors. Deeply-seated tumors within the brain or near critical regions such as the brain stem cannot be removed surgically because of the risk of severe nervous system damage during the operation (44-46). Depending greatly on the extent of the procedure, surgery poses various risks and side effects such as infection, blood clots, temporary or permanent neurological deficits, unstable blood pressure and bleeding. Although these are relatively uncommon, additional risks, associated with the location of the tumor, are also possible. These include seizures, muscle weakness, balance/coordination difficulties, stroke, and hydrocephalus (excessive fluid in the brain). Furthermore, deep venous

thrombosis (DVT), a significant cause of morbidity and mortality, was observed in 29 % to 43 % of brain tumor patients who underwent surgery (47). It is also reported the perioperative morbidity and mortality in patients with supratentorial gliomas exceeded the potential benefit of the surgical procedure (48).

2.1.2 Chemotherapy

Chemotherapy uses drugs to kill the cancer cells by interrupting cell division. Even though chemotherapy alone gives mild advantage to treat brain tumors, it provides an adjuvant outcome in treating with surgery and radiation therapy. In fact, survival benefit in the patients with high-grade gliomas has been observed when they were treated with a combination of chemotherapy and radiation therapy (49, 50). However, chemotherapeutic drugs can also affect normal cells leading to significant side effects, especially in fast growing cells, including cells in the hair, digestive system, and blood (51). In addition, the presence of the BBB has been proved to be a major obstacle for chemotherapeutic treatment of brain tumors. Many efforts have been made to administer chemotherapy to central nervous system tumors using methods that circumvent the BBB in order to improve delivery of drugs. Intrathecal chemotherapy, direct injection of drugs into cerebrospinal fluid (CSF), and interstitial chemotherapy, addition of drugs to tissue involved with tumor, appear to be efficient methods for patients with CNS tumors (40). Intrathecal chemotherapy, however, still needs the added effect of radiation therapy to control tumor nodules (52).

2.1.3 Radiation Therapy

Radiation therapy continues to be a major treatment modality in the therapeutic management of brain tumors (40). In radiation therapy, controlled high energy rays, such as X-ray and γ-ray, are delivered to damage the DNA found inside cells making them unable to divide and reproduce. Radiation can be given either by external or internal means; external therapy is a critical component to treat brain tumors in many patients (40). Stereotactic radiosurgery delivers a high dose of radiation during a single session from an external source, such as a gamma knife

and linear accelerator (LINAC), to treat brain tumors. Whole brain radiotherapy is another way of providing external therapy and is often used to treat multiple brain tumors by administering a dose of radiation to the entire brain.

Based on tumor type and normal tissue limitations, the appropriate total dose of radiation is typically delivered in fractionated protocols over a period of several weeks. The radiation quantity and the relationships between the old and the International System of units (SI) units are listed in **Table 2.1**. The dose at any given point is the energy deposited in a small fixed weight of the material surrounding that point (medium). Radiation doses are measured in a unit called the gray (Gy), which is defined as 1 J/kg (transferred or absorbed radiation energy/mass). The unit in which the dose is calculated is traditionally the rad, which is defined as energy deposition of 0.01 J/kg or 100 erg/g (1 erg = 10^{-7} J). Biological dose is specified using the linear-quadratic (LQ) model in terms of BED to quantify biological effects for radiotherapy (53). BED is the dose which is required for a certain effect at an infinitesimally small dose rate. This parameter is useful to compare the biological effects of different fractionation schedules and different types of radiotherapy.

Quantity	Definition	SI unit	Old unit	Conversion
Dose (D)	$D = \frac{\Delta E_{ab}}{\Delta m}$	$1Gy = 1\frac{J}{kg}$	$1\ rad = 100\frac{erg}{g}$	$1Gy = 100\ rad$

ΔE_{ab} is the absorbed energy Δm is the mass of medium

Table 2.1. Radiation Quantity, Units, and Conversion between Old and SI Unit.

Radiation therapy can be applied to shrink tumors before surgery or target residual tumors which cannot be removed safely by surgery. As the primary treatment modality, it is often used for patients with metastatic brain tumors. It is also beneficial for tumors that have recurred, tumors that are inoperable, or infiltrative tumors. Some benign gliomas that are life-threatening because of uncontrolled growth conditions may also be treated. Walker et al. (54) suggested dose-dependent effects of radiation on malignant gliomas by demonstrating the relationship

between increased radiotherapy dose and increased survival. Other trials have demonstrated that post-operative radiotherapy provides significant survival benefits compared with surgery alone or chemotherapy (55, 56). In addition, advances in neuroimaging sophisticated three-dimensional computerized treatment planning system, and three-dimensional conformal radiation therapy (3D-CRT) have markedly enhanced efficacy and safety of radiotherapy (57). Therefore, radiation therapy plays a central role in the management of most brain tumors, whether benign or malignant.

2.2 Radiation-Induced Brain Injury

The use of radiotherapy for treatment of brain tumors is limited by the risk of radiation-induced injury to normal brain tissue that can subsequently lead to devastating functional deficits several months to years after irradiation (1, 2, 58). Radiation-induced brain injury is classified as acute, early delayed (subacute), and late delayed reactions based on the timing of onset of symptoms in response to whole brain irradiation (1, 59). Acute injury, occurring within 48 hours or weeks after irradiation, is fairly mild to moderate in severity and characterized by fatigue, hair loss, skin erythema, headache, and emesis. Early delayed injury is observed 1-6 months after irradiation and is associated with the clinical symptoms of fatigue and somnolence. Even though acute and early delayed injuries can lead to severe conditions, it is generally believed that most of the symptoms and signs of these injuries are reversible. In contrast, late delayed injury, occurring from 6 months to several years post-irradiation, is considered irreversible and progressive, and is characterized by demyelination, vascular abnormalities, and ultimately white matter necrosis (60). Recent studies have demonstrated that late delayed injury is largely responsible for cognitive impairment, focal neurological signs, seizures, and increased cranial pressure. For example, significant side effects including progressive impairments in learning and memory were observed in 20-50 % of brain tumor patients as long-term consequences of radiotherapy. Progressive deterioration of memory function was observed in aged rats over a 7-month period post-radiation therapy (61). Yoneoka et al. (62) employed the Morris water maze and passive avoidance tasks to show a similar, late onset of cognitive impairment in adult rats at 12 months following cranial irradiation. Structural modifications, occlusion, alterations in

vascular permeability, loss of microvasculature, and increased inter-capillary distance have all been reported in response to a single exposure to 10Gy radiation (22). Furthermore, some studies showed that diminished blood flow in response to radiation decreases microvascular density (63). However, the specific mechanisms by which radiation cause brain injury in normal tissues have not yet been fully understood.

2.3 Radiation, Inflammation, and Brain Injury

2.3.1 Inflammation and Brain Injury

Inflammatory reactions are generally considered a self-defense mechanism in response to extracellular stimuli. In some cases inflammatory responses can lead to severe tissue damages if the immune system reacts improperly. It is widely accepted that a pro-inflammatory environment is critically associated with the pathophysiological process of brain injury and subsequent progression of neurological disorders (64, 65). For example, amyloid β (Aβ) peptides contribute to pathogenesis in Alzheimer's disease (AD) through an inflammatory cascade in the brain *via* secretion of interferon-γ (IFN-γ), IL-1β, and CD40 (66, 67). Aβ also increases the ability of blood monocytes/macrophages to infiltrate into brain tissue across the BBB (68, 69). Furthermore, brain inflammation has been suggested to actively participate in the neurodegenerative process of Parkinson's disease (PD) (70, 71). Degeneration of nigral dopaminergic neurons was observed in both an inflammation-mediated rat model and an *in vitro* cell culture model of PD (72). It was also found that cyclooxygenase (COX-2) expression is induced specifically within the substantia nigra pars compacta (SNpc) dopaminergic neurons in human postmortem PD specimens and in the 1-methyl-4-phenyl-1,2,3,6-tetrahydropyridine (MPTP) mouse model of PD during the destruction of the nigrostriatal pathway (73). In addition, increasing evidence has suggested that anti-inflammatory therapy, such as treatment with non-steroidal anti-inflammatory drugs (NSAIDs), may be beneficial in delaying the onset or slowing the progression of neurodegenerative diseases including AD and PD (64, 66). These findings provide robust evidence that an inflammatory process in the brain plays a significant role in the pathogenesis of CNS diseases.

In general, a cascade of inflammatory events occurs in response to external stimuli and this cascade is mediated through the production of pro-inflammatory mediators. Pro-inflammatory cytokines, chemokines, and adhesion molecules facilitate pro-inflammatory pathways by recruiting and transmigrating inflammatory cells from blood to tissues (74-76). A number of previous *in vivo* and *in vitro* studies have demonstrated that TNF-α and IL-1β are the most important pro-inflammatory cytokines and they play a central role in acute and chronic inflammation. It is well known that TNF-α and IL-1β strongly promote inflammatory responses in a wide spectrum of cell types, and overproduction of these cytokines has been implicated in a variety of human diseases (77, 78). IL-6 is another multifunctional pro-inflammatory cytokine that plays a major role in the mediation of the inflammatory and immune responses initiated by infection or injury (79). In addition to pro-inflammatory cytokines, chemokines are known to directly promote inflammatory responses. MCP-1 is a member of the CC chemokine family and plays a critical role in monocyte chemotaxis and transmigration (80).

It is generally accepted that the expression of inflammatory mediators is regulated at the transcriptional level through activation of pro-inflammatory transcription factors, including AP-1, NF-κB, and CREB (74, 81-84). Activation of AP-1 and NF-κB is considered part of the general regulation of a number of pro-inflammatory gene expressions in response to various extracellular stimuli (85-89).

2.3.2 Radiation, Inflammation, and Tissue Injury

It has been proposed that the acute inflammatory responses triggered by overexpression of pro-inflammatory mediators may be responsible for the radiation-induced tissue injury (3). For example, a marked elevation of COX-1 and COX-2 activity and prostaglandin E_2 (PGE_2) synthesis in the mouse brain following ionizing radiation augments brain inflammation through up-regulation of gene expression of a variety of pro-inflammatory molecules (90, 91). Evidence from previous *in vitro* and *in vivo* studies has demonstrated that radiation-induced overexpression of adhesion molecules, such as ICAM-1 and vascular cell adhesion molecule-1 VCAM-1, exerts a crucial role in leukocyte recruitment and infiltration which leads to

subsequent inflammatory injuries of a variety of tissues including intestine and lung, as well as to various cell types such as vascular endothelial cells (8, 92-96). Enhanced expression of adhesion molecules was also observed in irradiated brains (5, 7-9) and may contribute to either brain damage or subsequent cognitive impairment.

In addition to up-regulating adhesion molecules, irradiation has also been reported to up-regulate expression of pro-inflammatory cytokines and chemokines. For example, a rapid induction of gene expression of the pro-inflammatory cytokines TNF-α and IL-1β in response to radiation has been implicated in radiotherapy-associated damages to the lung and brain (5, 7, 97, 98). It was also found that both total-body irradiation and localized irradiation of the right hind leg lead to a significant increase in IL-6 levels in serum of rats (99). Furthermore, Johnston et al. (100) suggested potential mechanisms of radiation-induced pulmonary fibrosis based on their findings that the mRNA levels of chemokines, including MCP-1, and chemokine receptor families were elevated in fibrosis-sensitive C57BL/6 mice by thoracic irradiation.

2.4 Radiation, Inflammation, and Aging

It is commonly accepted that chronic overexpression of pro-inflammatory mediators has detrimental effects on the brain (7). However, evidence also suggests that acute overexpression of pro-inflammatory mediators may exert beneficial effects on tissue injury (101, 102). For example, neuroprotective effects of pro-inflammatory cytokines, such as promotion of neuronal differentiation and survival, induction of neurotropic factors, and induction of anti-inflammatory mediators, have been observed after acute traumatic brain injury (TBI) (103). The beneficial role of cytokines in the pathophysiology of TBI is also supported by animal studies indicating that cytokine knockout mice and cytokinereceptor knockout mice exhibited higher mortality and enhanced tissue damage after experimental TBI (103, 104). In addition, the protective role of pro-inflammatory mediators in the early stages of wound healing has been extensively reported. For example, enhanced production of cytokines (e.g., IL-6, TNF-α, and IL-1β) (105), adhesion molecules (e.g., ICAM-1 and VCAM-1) (106), chemokines (e.g., MCP-1) (107), and matrix metalloproteinases (e.g., MMP-9) (108) at the wound site promotes healing processes of injured

brain tissues. These studies provide compelling evidence that the acute induction of pro-inflammatory mediators in the brain is an essential part of a pathway that induces a protective response to brain injury.

It is well documented that basal expression levels of pro-inflammatory mediators including TNF-α, IL-1β, and IL-6 are significantly elevated in the aged brain compared with younger subjects (109). In contrast, advancing age results in a marked decrease in inflammatory responses induced by extracellular stimuli. Gon et al. (110) demonstrated that the serum concentrations of pro-inflammatory cytokines including TNF-α and IL-1β were significantly lower in elderly patients with pneumonia compared with those in young patients. They also found that peripheral blood monocytes from healthy normal elderly subjects produce less amounts of these cytokines than those from healthy normal young subjects in response to lipopolysaccharide (LPS) stimulation (110). In addition, IL-1 production by LPS-stimulated co-cultures of peritoneal macrophages and splenic T cells from old mice was markedly reduced when compared with cells of young mice (111) and TNF-α-induced MMP-9 expression was decreased in aortic smooth muscle cells derived from old mice (112). It was also found that LPS administration resulted in a significant attenuation of TNF-α and IL-6 mRNA expression in brains of old mice compared with those of young mice (109). Finally, mononuclear cells from elderly patients displayed a marked decrease in mitogen-stimulated production of IFN- γ and IL-2 (113). These studies provide evidence that an age-dependent impairment of immune response results in diminished inflammatory responses to extracellular stimuli.

The prevailing evidence suggests that aging is an important prognostic factor in determining the response of brain tumors to radiation therapy (114). Previous clinical studies have shown that the use of high dose radiation therapy for brain tumors resulted in significantly lower survival rates for patients older than 70 years of age compared with those for patients aged 70 and younger (115, 116). In addition, Rosenblum et al. (117) reported that stem cells obtained from patients over the age of 50 with brain tumors were less sensitive to radiation than those from patients 50 years old or younger. Although the mechanisms for this effect have not been

established, these studies clearly demonstrate that aging exerts a profound effect on the efficacy of radiation therapy for treatment of brain tumors.

2.5 Radiation, Extracellular Matrix, and Brain Injury

2.5.1 Radiation, BBB Disruption, and Brain Injury

The BBB is a complex neuroprotective system consisting of brain microvascular endothelial cells, astrocytes, pericytes, and basement membrane (118). It provides a highly selective barrier that regulates the exchange of materials and cells between the circulation and brain tissue (119). Under physiological conditions, the BBB restricts and controls the movement of various chemical substances and macromolecules to maintain the brain homeostasis that is essential for the normal operation of the nervous system (120, 121). In some cases, however, the BBB becomes disrupted or modified not only in response to different stresses such as irradiation but also as a consequence of the pathological insult (122). Indeed, dysfunction of the BBB is a key feature in common neurological disorders including stroke, trauma, and Alzheimer's disease (120). Previous studies have shown that alterations in the BBB may be responsible for tissue injury in brain after irradiation. For example, irradiation mediates disruption of the BBB by damaging the structural and functional integrity of the microvasculature in brain (15, 16). In addition, Delattre *et al*. (123) demonstrated that cranial irradiation (CRT) markedly increased regional capillary permeability and capillaries of normal brain tissue are more sensitive to the acute effects of CRT than capillaries found in brain tumors. It was also found that BBB permeability was significantly increased in rat brain after whole brain and whole body irradiation (122, 124). Furthermore, other *in vivo* studies have demonstrated a rapid increase in BBB breakdown in response to interstitial brachytherapy (125-127). The cellular and molecular mechanisms by which irradiation induces BBB disruption, however, are not fully understood.

2.5.2 ECM Degradation, BBB Disruption, and Brain Injury

The ECM forms a basal lamina underlying vasculature and is critical to maintaining the integrity of the BBB (128). Besides performing as a barrier to macromolecules and cells, it also provides structural framework for the tissue and serves as an anchor for the endothelium *via* cell-matrix interactions, stimulating a number of intracellular signaling pathways (129). The ECM is a complex of various proteins and proteoglycans, including collagens, laminin, fibronectin, and tenascin which constitute the basal lamina of the BBB (129-131). Compelling evidence indicates that degradation and consequent rearrangement of ECM are critically involved in the breakdown of the BBB. For example, the injection of bacterial collagenase to rat brain resulted in degradation of ECM, disruption of basal lamina, and an increase in BBB permeability (132). In addition, the increased gelatinolytic activity and collagen type IV degradation were found to be significantly associated with BBB disruption in a rat model of bacterial meningitis (133) and a mouse model of herpes simplex virus (HSV) encephalitis (134), respectively. Tilling *et al*. (135) also reported that ECM constituents such as collagen type IV, fibronectin, and laminin significantly increased the transcellular electrical resistance of primary brain microvascular endothelial cells in an *in vitro* model of BBB, indicating that these proteins play an important role in enhancing barrier properties. Despite a crucial role for ECM degradation in the BBB breakdown, the involvement of ECM remodeling in the pathophysiology of radiation-induced brain injury has not yet been investigated.

2.5.3 Radiation, MMPs, and TIMPs

MMPs are a large family of ECM-degrading enzymes. Depending on substrate specificity and structural differences, MMPs are subdivided into gelatinase (MMP-2 and -9), collagenases (MMP-1, -8, -13, and -18), stromelysins (MMP-3, -10, and -11), matrilysins (MMP-7 and -26), elastases (MMP-12), and MT-MMPs (MMP-14, -15, -16, and -17) (136-138).

In a variety of physiologic and pathophysiologic conditions, MMPs become activated and play a key role in degradation of the ECM proteins (139). Recent evidence from *in vivo* and *in vitro* studies has identified that ionizing irradiation up-regulates MMPs expression in various

tissues. For example, enhanced activity of MMP-2 and MMP-9 was observed in lung after thoracic irradiation (140). Araya *et al.* (141) have reported a significant elevation of MMP-2 production in human airway epithelial cells after irradiation. Additionally, previous clinical studies have shown that use of pelvic radiation therapy for prostate cancer patients resulted in significant increases in MMP-2 and MMP-9 activity in rectal mucosa (142). It was also found that abdominal irradiation led to a significant elevation in MMP-2 and MMP-14 levels in rat ileum (138). These findings are supported by an *in vitro* study from Nirmala *et al*. (143) demonstrating that radiation-induced expression of MMP-2 and MMP-9 may be involved in the alteration of the CNS microvasculature by regulating glial-endothelial cell interaction.

The enzymatic activity of MMPs is inactivated by TIMPs, the endogenous inhibitors with a higher affinity for specific MMPs (144, 145). For example, TIMP-1 forms a specific complex with MMP-9, whereas MMP-2 is bound by TIMP-2 (144, 146). Therefore, the balance between MMPs and TIMPs is considered necessary for normal homeostasis during periods of development and plasticity in the CNS (133, 134). TIMP-1 mRNA expression was found to be up-regulated in the irradiated rat colon while the mRNA level of TIMP-2 was unchanged (147). In lung epithelial cells, radiation increased MMP-2 mRNA but had no effect on TIMP-2 indicating the balance between the MMP-2 and TIMP-2 was in favor of MMP-2 promoting proteolysis (141).

2.6 Radiation, Physiologic Angiogenesis, and Brain Injury

2.6.1 Angiogenic Factors and Vessel Rarefaction

Angiogenesis plays critical roles not only in many physiological processes such as embryonic development and wound healing, but also in the development of a number of pathological conditions including inflammation and progression of tumors. These events are characterized by dynamic temporally and spatially coordinated interactions among endothelial cells, angiogenic factors, and surrounding ECM proteins (148). One of the most important angiogenic factors is VEGF which has a potent and specific activity for the vascular endothelium (149). VEGF and its

receptors serve to initiate endothelial cell proliferation, migration, and production of new capillary sprouts, which promote vasculogenesis and angiogenesis (150, 151). Angiopoietins are a second family of vascular regulatory molecules that are also specific for the vascular endothelium involving in both physiological and pathological blood vessel generation (152). There are four identified angiopoietin families: Ang-1, Ang-2, Ang-3, and Ang-4. Although Davis et al. (152) reported that Ang-1 does not directly affect proliferation of cultured endothelial cells, it has a great effect in mediating interactions between the endothelium and the surrounding matrix, stimulating endothelial migration (153), sprouting (154), and tubule formation (155). Indeed, Ang-1 is necessary for subsequent vascular remodeling as well as vessel maturation and stabilization, while VEGF plays an active role during the early stages of vessel development (156). All angiopoietin families bind to the endothelial receptor Tie-2 which is typically expressed by vascular endothelial cells (157). The balance of Ang-1/Tie-2 system has been known to be necessary for vessel maturation and stabilization (156). Ang-2 serves as a functional antagonist of Ang-1. By blocking Tie-2 signaling, Ang-2 leads to a loosening of tight vascular structure (158, 159). This loosening of cell-matrix and cell-cell interactions allows the endothelial cells to be more sensitive and responsible toward the other angiogenic factors such as VEGF. For example, in the absence of the activating signal from VEGF, Ang-2 promotes endothelial cell death and finally rarefaction of vessels (159). In the presence of high levels of VEGF, however, new capillary sprouting is facilitated by Ang-2. The dynamic interaction among VEGF, Ang-1, and Ang-2 in angiogenesis is shown in **Figure 2.1**. An intimate and coordinated relationship of Ang-1, Ang-2, Tie-2, and VEGF plays a key role in regulating various aspects of physiological angiogenesis.

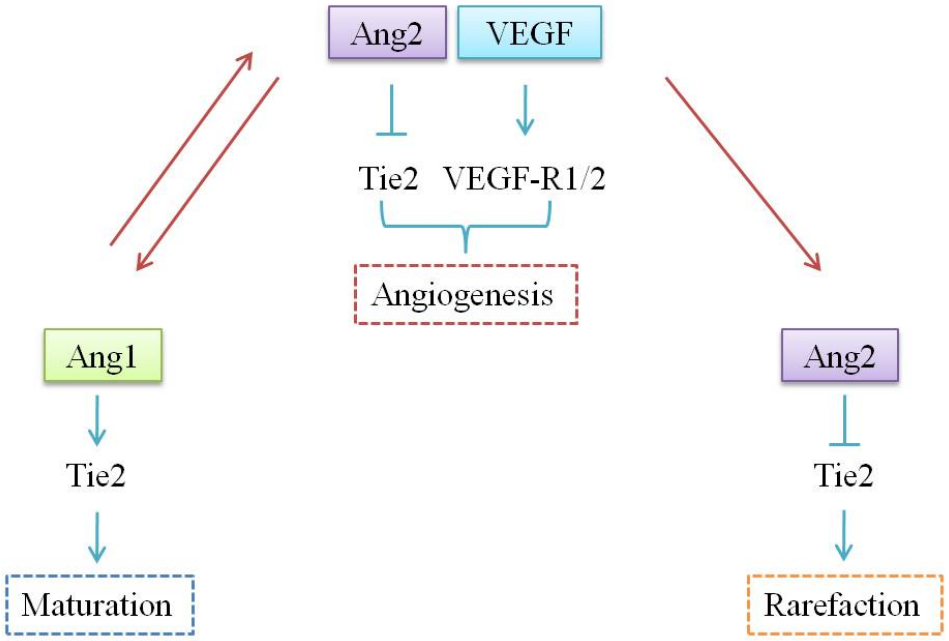

Figure 2.1. Schematic Diagram of Dynamic Interplay between Ang-1, Tie-2, Ang-2, and VEGF.

2.6.2 Radiation and Vessel Rarefaction

Vessel rarefaction, defined as a decrease in vascular density, has been implicated in the onset and progression of various pathological processes (17-19). Previous studies have shown that irradiation induces both acute and late changes in the vasculature (20-22). For example, Ljubimova et al. (20) found a decrease in endothelial cell density in rat brain within 24 h after large single doses of irradiation. In addition, an initial marked decline and a subsequent slow loss of endothelial cell number were observed after 24 h and between 26 and 52 weeks after a single dose of X-rays to the rat brains, respectively (160). Irradiation also has been shown to enhance acute vascular responses including vascular permeability, endothelial cell apoptosis, and endothelial swelling within 24 h (15, 161). Furthermore, 10 weeks after fractionated whole brain irradiation, a substantial decrease in vessel density and length was detected in irradiated rat brains (38). These studies provide evidence indicating that radiation-induced early and persistent

damages to the microvasculature may be responsible for vessel rarefaction leading to late delayed brain injury. The molecular mechanisms of radiation-induced vessel rarefaction in brain, however, remain to be further investigated.

2.7 Mathematical Models of Genetic Regulatory System

Gene expression refers to the process by which cells synthesize proteins from the information encoded in a gene (**Figure 2.2**). Several stages are involved in regulating the gene expression process, including transcription, translation, and post-translational modification of proteins (162, 163). During these stages, gene expression is controlled by regulatory molecules such as any of the intermediate products (RNA, polypeptides, or proteins), suggesting a network of gene regulation. Genetic regulatory networks (GRNs) consist of regulatory interactions among DNA, RNA, protein, and other molecules. Their function is to specify identity as well as control mRNA expression levels in a group of targeted genes (164). However, numerous challenges have been reported in the area of a reconstruction of a GRN. For example, there are limited amounts of experimental data due to high levels of noise, limited data size from the cost of experiments and the complexity of gene regulatory process (165). Despite many difficulties to reconstruct GRNs, various mathematical models have been proposed to understand the behavior of the networks being modeled and make predictions corresponding with experimental observations (10, 11).

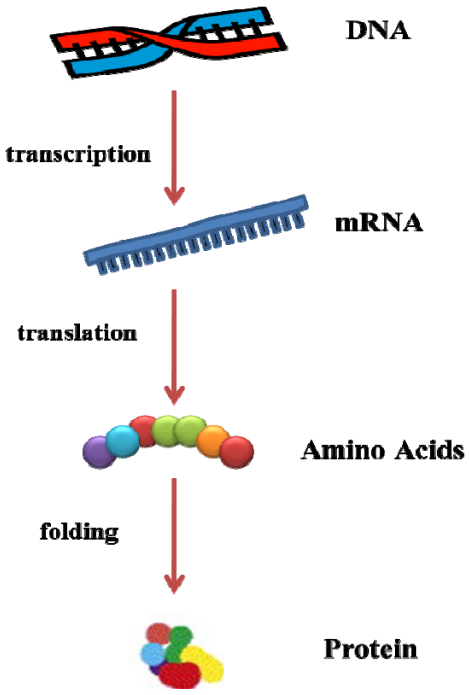

Figure 2.2. Regulation of Gene Expression. (1) DNA is transcribed into mRNA. (2) mRNA is translated into a chain of amino acids. (3) The amino acid chain is folded up into a final three-dimensional protein structure.

In general, mathematical models can be categorized into two types: Boolean network based models (166, 167) and dynamic system using differential equations (168, 169). The Boolean method simply describes the state of a gene as binary on/off switches and use Boolean logical rules to approximate the regulatory control of gene expression, functioning in discrete time steps. This method, however, shows a disadvantage in expressing continuous aspects of gene regulation occurring in the cell environment. The dynamic system approach using ODEs is the most prominent method to analyze genetic regulatory system. In ODEs, each state describes the concentrations of protein or mRNA. And changes of each state are assumed to be continuous and deterministic. Therefore, this method provides more intensive mathematical interpretations and greater physical accuracy for biological pathways than the Boolean approach (170).

CHAPTER 3:

IRRADIATION INDUCES REGIONALLY SPECIFIC ALTERATIONS IN PRO-INFLAMMATORY ENVIRONMENTS IN RAT BRAIN

*Reprinted from **Lee WH**, Sonntag WE, Mitschelen M, Yan H, Lee YW. *International Journal of Radiation Biology*, 86(2):132-144 (2010), with permission from Informa Healthcare Communications publishers (171).

IRRADIATION INDUCES REGIONALLY SPECIFIC ALTERATIONS IN PRO-INFLAMMATORY ENVIRONMENTS IN RAT BRAIN

3.1 Abstract

Purpose: Pro-inflammatory environments in the brain have been implicated in the onset and progression of neurological disorders. In the present study, we investigate the hypothesis that brain irradiation induces regionally specific alterations in cytokine gene and protein expression.

Materials and methods: Four month old F344×BN rats received either whole brain irradiation with a single dose of 10Gy γ-rays or sham-irradiation, and were maintained for 4, 8, and 24 h following irradiation. The mRNA and protein expression levels of pro-inflammatory mediators were analyzed by real-time reverse transcriptase-polymerase chain reaction (RT-PCR), enzyme-linked immunosorbent assay (ELISA), and immunofluorescence staining. To elucidate the molecular mechanisms of irradiation-induced brain inflammation, effects of irradiation on the DNA-binding activity of pro-inflammatory transcription factors were also examined.

Results: A significant and marked up-regulation of mRNA and protein expression of pro-inflammatory mediators, including tumor necrosis factor-α (TNF-α), interleukin-1β (IL-1β), and monocyte chemoattractant protein-1 (MCP-1), was observed in hippocampal and cortical regions isolated from irradiated brain. Cytokine expression was regionally specific since TNF-α levels were significantly elevated in cortex compared to hippocampus (57% greater) and IL-1β levels were elevated in hippocampus compared to cortical samples (126% greater). Increases in cytokine levels also were observed after irradiation of mouse BV-2 microglial cells. A series of electrophoretic mobility shift assays (EMSA) demonstrated that irradiation significantly increased activation of activator protein-1 (AP-1), nuclear factor-κB (NF-κB), and cAMP response element-binding protein (CREB).

Conclusion: The present study demonstrated that whole brain irradiation induces regionally specific pro-inflammatory environments through activation of AP-1, NF-κB, and CREB and

overexpression of TNF-α, IL-1β, and MCP-1 in rat brain and may contribute to unique pathways for the radiation-induced impairments in tissue function.

Key words: R*adiation; brain inflammation; cytokines; AP-1; NF-κB; CREB*

3.2 Introduction

It has been proposed that the acute inflammatory responses triggered by overexpression of pro-inflammatory mediators may be responsible for radiation-induced tissue injury (3). For example, a marked elevation of cyclooxygenase (COX-1 and COX-2) activity and prostaglandin E_2 (PGE_2) synthesis in the mouse brain following ionizing radiation augments brain inflammation through up-regulation of gene expression of a variety of pro-inflammatory molecules (90, 91). Evidence from previous *in vitro* and *in vivo* studies has demonstrated that radiation-induced overexpression of adhesion molecules, including intercellular adhesion molecule-1 (ICAM-1) and vascular cell adhesion molecule-1 (VCAM-1), exerts a crucial role in leukocyte recruitment and infiltration that lead to subsequent inflammatory injuries to a variety of tissues including intestine and lung, as well as various cell types such as vascular endothelial cells (8, 92-96). Enhanced expression of adhesion molecules was also observed in irradiated brain (5, 7-9) and may contribute to brain damage and/or subsequent cognitive impairment.

Irradiation also has been reported to up-regulate expression of pro-inflammatory cytokines and chemokines. For example, a rapid induction of gene expression of the pro-inflammatory cytokines tumor necrosis factor-α (TNF-α) and interleukin-1β (IL-1β) in response to radiation has been implicated in radiotherapy-associated damage to both lung and brain (5, 7, 97, 98). It was also found that both total-body irradiation and localized irradiation of the right hind leg led to a significant increase in interleukin-6 (IL-6) levels in serum of rats (99). Furthermore, Johnston et al. (100) suggested potential mechanisms of radiation-induced pulmonary fibrosis based on their findings that the mRNA levels of chemokines, including monocyte chemoattractant protein-1 (MCP-1), and chemokine receptor families were elevated in fibrosis-sensitive C57BL/6 mice by thoracic irradiation.

These data provide robust but only partial evidence indicating that inflammation is one of the major consequences of irradiation and has a pivotal role in subsequent radiation-induced tissue injury. Unfortunately, in the majority of the aforementioned studies, the cytokine analyses are limited to gene expression (mRNA levels) without analysis of the corresponding protein levels, the time-course for the effects of irradiation are limited or differential changes in expression of cytokines in specific brain regions are not considered. Importantly, radiation has been shown to impair performance on spatial memory tasks that are hippocampally-dependent and analysis of the potential specific effects of irradiation on this tissue requires a clear understanding of the consequences of radiation on this important brain region.

In the present study, we examined the effects of whole brain irradiation on mRNA and protein expression of several pro-inflammatory mediators, (e.g., TNF-α, IL–6, IL-1β, and MCP-1) in both hippocampus and cortex. The potential contribution of microglia to radiation-induced TNF-α expression was also determined *in vitro*. Additionally, the DNA-binding activity of pro-inflammatory transcription factors, such as activator protein-1 (AP-1), nuclear factor-κB (NF-κB), and cAMP response element-binding protein (CREB), was assessed to define the molecular mechanisms of radiation-induced brain inflammation. Our results provide a clear time course for the acute effects of radiation on both cytokine and chemokine gene and protein expression in hippocampus and cortex. In addition, our results provide evidence for a differential induction of cytokines in specific brain regions that have importance for the neurological/neuropathological consequences of irradiation.

3.3 Materials and Methods

3.3.1 Animals

Four month old Fisher 344-Brown Norway (F344×BN) male rats were purchased from Harlan Laboratories, Inc. (Indianapolis, IN). Animals were housed on a 12/12 light-dark cycle with food and water provided *ad libitum*. Animal care was conducted in accordance with the NIH Guide for the Care and Use of Laboratory Animals and this study was approved by the Institutional Animal Care and Use Committee.

For real-time reverse transcriptase-polymerase chain reaction (RT-PCR) and enzyme-linked immunosorbent assay (ELISA), the brains were rapidly removed and two different brain regions (hippocampus and cortex) were dissected, immediately frozen in liquid nitrogen, and stored at -80°C until analysis. For immunofluorescence staining, animals were given 350 μl of ketamine/xylazine (80/12 mg/ml, respectively) immediately prior to perfusion. Animals were then transcardially perfused with ice-cold phosphate buffered saline (PBS) and 6 unit/ml heparin (a total of 700 μl per animal), and the whole brains were rapidly removed, immediately frozen in liquid nitrogen, and stored at -80 °C until analysis.

3.3.2 Cell Cultures

The murine microglial cell line, BV-2 cells, was a generous gift from Dr. Michael E. Robbins (Wake Forest University Medical Center, Winston-Salem, NC). BV-2 cells are an immortalized cell line obtained by infecting mouse primary microglial cells with a v-raf/v-myc oncogene-carrying retrovirus (172). BV-2 cells were cultured in Dulbecco's modified eagle medium (DMEM) with 5 % fetal bovine serum (FBS), 100 unit/ml of penicillin, and 100 μg/ml of streptomycin at 37 °C in a humid atmosphere of 5 % CO_2 and 95 % air.

3.3.3 Irradiation

Following an acclimatization period of one week, the animals received either whole brain irradiation with a single dose of 10Gy γ-rays or sham-irradiation. In the present study, a rat model of whole brain irradiation with a single dose of 10Gy was chosen for three reasons: (1) it is known as the lowest dose to have a radiation effect (31, 173), (2) it is well below the threshold for vascular changes, demyelination or radionecrosis (32-34) and (3) it is close to a clinically relevant dose in humans because rat brain is more resistant to radiation injury than human brain (32, 35). Whole brain irradiation procedures were carried out as described previously (26, 36) with minor modifications. Rats were anesthetized using a 350 μl mixture of ketamine/xylazine (80/12 mg/kg body weight). Whole brain irradiation was performed in a 12,000 Ci self-shielded ^{137}Cs irradiator (Gammacell 40 Exactor, Nordion International Inc; Kanata, Ontario) using lead and Cerrobend shielding devices to collimate the beam so that the whole rat brain, including the

brain stem, was irradiated. Dosimetry was performed using thermoluminescent dosimeters placed in the skull of dead rats, and confirmed with ionization chambers in tissue equivalent phantoms. The average dose rate to the midline of the brain for the two positions was ~ 4Gy/min with an 8% difference between the two positions. To ensure that each rat received the same midline brain dose, each lightly anesthetized (ketamine/xylazine) animal had 5Gy delivered to alternate sides of the head. A total dose of 10Gy γ-rays was at an average dose rate of 4.23Gy/min. The eyes received about 15 % of the brain dose, and the body received 1-3 % of the brain dose. Control rats were anesthetized but not irradiated. The animals were maintained for 4, 8, and 24 h post-irradiation.

BV-2 cells were grown to 80-90 % confluence and irradiated with a single dose of 10Gy γ-rays using a ^{137}Cs irradiator. All irradiations were performed at room temperature and control cells received sham-irradiation. After irradiation, the cells were returned to the CO_2 incubator and maintained at 37 °C in 5 % CO_2/95 % air for 4 and 24 h post-irradiation.

3.3.4 Real-time Reverse Transcriptase-Polymerase Chain Reaction (RT-PCR)

Quantitative real-time RT-PCR using fluorogenic 5'nuclease assay technology with TaqMan® probes and primers (Applied Biosystems, Foster City, CA) were employed for gene expression analyses. Rat brains were homogenized with 1 ml of TRI Reagent (Sigma-Aldrich, St. Louis, MO) in a tissue homogenizer and total RNA was isolated from tissue homogenates as described previously (84). In addition, total RNA was isolated from BV-2 using RNeasy Mini Kit (Qiagen, Valencia, CA) according to the protocol of the manufacturer. 1 μg of total RNA was reverse transcribed at 25 °C for 15 min, 4 2°C for 45 min, and 99 °C for 5 min in 20 μl of 5 mM $MgCl_2$, 10 mM Tris-HCl, pH 9.0, 50 mM KCl, 0.1 % Triton X-100, 1 mM dNTP, 1 unit/μl of recombinant RNasin, 15 unit/μg of Avian Myeloblastosis Virus (AMV) reverse transcriptase, and 0.5 μg of random hexamers. Amplification of individual genes was performed on the Applied Biosystems 7300 Real-Time PCR System using TaqMan® Universal PCR Master Mix and a standard thermal cycler protocol (50 °C for 2 min before the first cycle, 95 °C for 15 sec and 60 °C for 1 min, repeated 45 times). TaqMan® Gene Expression Assay Reagents for rat TNF-α, rat IL-1β, rat IL-6, rat MCP-1, rat glyceraldehydes-3-phosphate dehydrogenase

(GAPDH), mouse TNF-α, and mouse GAPDH were used for specific probes and primers of PCR amplifications. The threshold cycle (C_T), which indicates the fractional cycle number at which the amount of amplified target gene reaches a fixed threshold, was determined from each well using the Applied Biosystems Sequence Detection Software v1.2.3 and relative quantification was calculated by the comparative C_T method as described previously (74, 174, 175). The data were analyzed using the equation $2^{-\Delta\Delta C_T}$, where $\Delta\Delta C_T$ = [C_T of target gene - C_T of housekeeping gene] $_{\text{treated group}}$ − [C_T of target gene - C_T of housekeeping gene] $_{\text{untreated control group}}$. For the treated samples, evaluation of $2^{-\Delta\Delta C_T}$ indicates the fold change in gene expression, normalized to a housekeeping gene (GAPDH), and relative to the untreated control.

3.3.5 Enzyme-Linked Immunosorbent Assay (ELISA)

Tissue homogenates from rat brain were prepared using the method recommended by R&D Systems (Minneapolis, MN). Both hippocampus and cortex were homogenized in 1 ml of ice-cold PBS and stored overnight at -80 °C. After three freeze-thaw cycles were performed, the homogenates were centrifuged for 5 min at 5,000 × g at 4 °C. Supernatants were frozen immediately on dry ice and stored at -80 °C until analysis. Protein concentrations of brain tissue homogenates were determined as described by Bradford (176). The protein expression levels of pro-inflammatory mediators in brain tissue homogenates were determined by using Quantikine® Rat Immunoassay Kits for TNF-α, IL-1β, and IL-6 (R&D Systems) and Rat MCP-1 Immunoassay Kit (Biosource International, Camarillo, CA) following to the manufacturer's protocols. TNF-α concentrations in cell culture supernatants were measured by using a Mouse TNF-α Quantikine® Immunoassay Kit (R&D Systems).

3.3.6 Immunofluorescence Staining

Frozen tissues were cut into 20-μm sections using a Microm HM 550 cryostat (MICROM International GmbH, Walldorf) and mounted on Superfrost/Plus microscope slides (Fisher Scientific, Pittsburgh, PA). Sections were fixed in 4% paraformaldehyde for 15 min at room temperature, rinsed with PBS three times for 5 min each, and incubated in 0.5 % Triton X-100 for 15 min to permeabilize tissues for optimal staining. After washing with PBS three times, the

sections were then incubated with 3 % bovine serum albumin (BSA) in PBS for 1 h at room temperature to block non-specific binding of the antibodies, followed by incubation with the primary antibody, goat anti-TNF-α polyclonal antibody (Santa Cruz Biotechnology, Santa Cruz, CA) diluted 1/40 in 1.5 % BSA, overnight at 4 °C. Negative controls were prepared by incubation of tissue sections with non-immune goat serum (normal goat-IgG, Santa Cruz Biotechnology) instead of the primary antibody. Sections were washed three times with PBS and incubated with secondary antibody, bovine anti-goat IgG conjugated with Texas Red (Santa Cruz Biotechnology), diluted 1/100 in PBS in the dark for 1 h. Vectashield mounting medium (Vector Laboratories Inc, Burlingame, CA) was added to prevent fading, and the slides were sealed with a cover slip. The slides were examined on a Zeiss AXIO Imager A1m fluorescence microscope (Carl Zeiss MicroImaging, Inc., Thornwood, NY). Images were acquired with 10× objective by AxioCam MRc5 Digital Imaging System. Texas Red was assigned to the red channel of the generated RGB image.

3.3.7 Electrophoretic Mobility Shift Assay (EMSA)

Nuclear extracts from hippocampus of each rat brain were prepared according to the method of Beg et al. (177) with minor modification as described earlier (84). The tissues were homogenized in 1 ml of lysis buffer (10 mM Tris-HCl, pH 8.0, 60 mM KCl, 1 mM ethylenediaminetetraacetic acid (EDTA), 1 mM dithiothreitol, 100 μM phenylmethylsulfonyl fluoride, 0.1% NP-40), lysed for 5 min on ice, and centrifuged at 600 × g for 4 min at 4°C to collect nuclei. Then, the nuclear pellets were washed with 1 ml of lysis buffer without NP-40, lysed in 75 μl of nuclear extract buffer (20 mM Tris-HCl, pH 8.0, 420 mM NaCl, 1.5 mM $MgCl_2$, 0.2 mM EDTA, 25 % glycerol) for 10 min on ice, and centrifuged at 18,300 × g for 15 min at 4 °C. Supernatants, which contain nuclear extracts, were frozen immediately on dry ice and transferred to -80 °C until analysis. Protein concentrations of isolated nuclear extracts were determined as described by Bradford (176).

Double-stranded oligonucleotides containing the consensus sequences of the binding sites for pro-inflammatory transcription factors AP-1, NF-κB, or CREB were purchased from Promega (Madison, WI, USA) and labeled with [γ-^{32}P]-ATP using bacteriophage T4 polynucleotide

kinase. The reaction mixture consisted of 70 mM Tris-HCl, pH 7.6, 10 mM $MgCl_2$, 5 mM dithiothreitol (DTT), 1.75 pmoles of double-stranded oligonucleotides, 30μCi of [γ-^{32}P]-ATP (GE Healthcare Bio-Sciences, Piscataway, NJ, USA), and 20 units of T4 polynucleotide kinase (Promega) in a total volume of 20 μl. The reaction was incubated for 1 h at 37 °C. Following incubation, T4 polynucleotide kinase was inactivated by placing the tube for 10 min at 68 °C. Unlabeled nucleotides were removed by gel filtration chromatography using mini Quick Spin Oligo Columns (Roche Applied Science, Indianapolis, IN).

Binding reactions were performed in a 20 μl volume containing 6-10 μg of nuclear protein extracts, 10 mM Tris-Cl, pH 7.5, 50 mM NaCl, 1 mM EDTA, 0.1 mM dithiothreitol, 10 % glycerol, and 2 μg of poly[dI-dC]. After adding the reagents, the mixture was incubated for 25 min at room temperature. Then, 40,000 cpm of ^{32}P-labeled specific oligonucleotide probe was added, and the binding mixture was incubated for 25 min at room temperature. Competition studies were performed by the addition of a molar excess of unlabeled oligonucleotide to the binding reaction. Resultant protein-DNA complexes were electrophoresed on a non-denaturing 5 % polyacrylamide gel using 0.25 × TBE buffer (50 mM Tris-Cl, 45 mM boric acid, 0.5 mM EDTA, pH 8.4) for 3 h at 150 V. The gel was transferred to Whatman® 3MM paper, dried on a gel dryer, and exposed to a X-ray film overnight at -80 °C with an intensifying screen. All experiments were repeated using nuclear extracts from 4 rat hippocampi of each group and relative intensities of the bands corresponding to specific transcription factors were measured using UN-SCAN-IT gel™ image analysis software (Silk Scientific, Inc., Orem, UT). The values of relative pixel intensity were subjected to statistical analyses.

3.3.8 Statistical Analysis

The statistical analysis of data was completed using SigmaStat 3.5 (SPSS Inc., Chicago, IL). One-way analysis of variance (ANOVA) was used to compare mean responses among the treatments. For each endpoint, the treatment means were compared using the Bonferroni least significant difference procedure. Statistical probability of $p<0.05$ was considered significant.

3.4 Results

3.4.1 Irradiation Up-regulates TNF-α Expression in Rat Brain

Quantitative real-time RT-PCR demonstrated a significant and marked increase in the mRNA expression levels of the pro-inflammatory cytokine, TNF-α, in hippocampus and cortex isolated from rat brains at 4, 8, and 24 h after a single dose of whole brain irradiation (**Figure 3.1A**). Up-regulation of TNF-α mRNA expression reached maximal levels within 4 h after irradiation (15-fold induction in hippocampus and 19-fold induction in cortex compared to the sham-irradiated control rats). Expression of GAPDH (a housekeeping gene), however, was not affected by irradiation (data not shown).

The quantitative sandwich enzyme immunoassay technique was employed to determine whether irradiation-mediated increases in TNF-α mRNA levels translate to elevated protein expression in hippocampal and cortical regions isolated from rat brains. As indicated in **Figure 3.1B**, very low expression levels of TNF-α protein were found in sham-irradiated control rats (3.6 pg/mg protein in hippocampus and 4.4 pg/mg protein in cortex). However, consistent with the gene expression data (**Figure 3.1A**), brain irradiation resulted in a significant and marked increase in TNF-α protein expression in hippocampus and cortex at 4 h (23 and 30 fold), 8 h (8.3 and 13 fold) and 24 h (3.6 and 4.1 fold) after irradiation (**Figure 3.1B**). TNF-α levels were significantly elevated in cortex compared to hippocampus at 4 h and 8 h post-irradiation. In addition, the irradiation-mediated overexpression of TNF-α protein in rat brain was further confirmed by immunofluorescence staining. As shown in **Figure 3.1C**, no immunoreactivity of TNF-α protein was detected in sham-irradiated control rat brains. A marked increase in TNF-α immunoreactivity, however, was observed in rat brains at 4, 8, and 24 h after irradiation (**Figure 3.1D-3.1F**). In agreement with the results from ELISA (**Figure 3.1B**), the maximal immunoreactivity of TNF-α protein was formed 4 h after irradiation and maintained at a high level 8 h after irradiation. The TNF-α immunoreactivity was then decreased 24 h after irradiation. In contrast, negative control experiments did not show any positive staining for TNF-α protein at all studied time points (**Figure 3.1G-3.1J**).

3.4.2 Irradiation Up-regulates TNF-α Expression in Microglia

To investigate the potential contribution of microglia to the induction of TNF-α expression in the brain after irradiation, BV-2, murine microglial cells, were exposed directly to a single dose of 10Gy or sham-irradiation and maintained for 4 and 24 h post-irradiation. The mRNA and protein expression levels of TNF-α were analyzed by real-time RT-PCR and ELISA. A significant up-regulation of mRNA and protein expression of TNF-α was observed in microglia at 4 and 24 h after irradiation compared with those determined in sham-irradiated control cells (**Figure 3.2**).

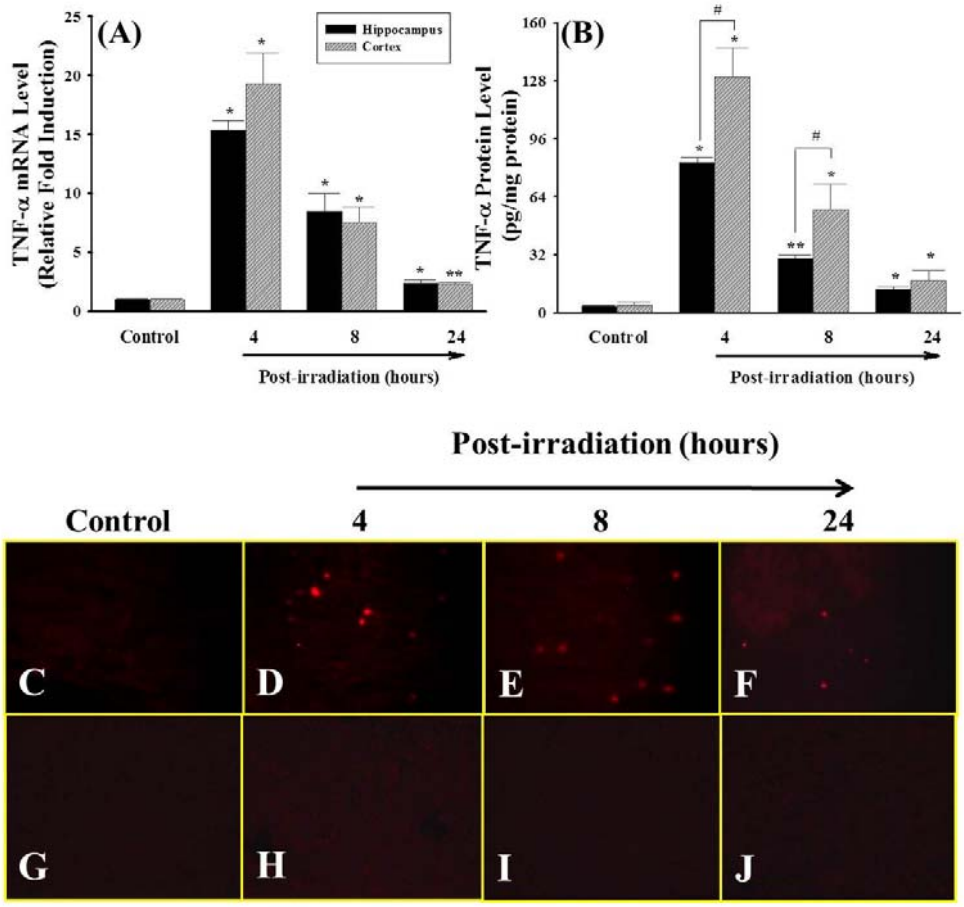

Figure 3.1. Irradiation Up-regulates mRNA and Protein Expression of TNF-α in Rat Brain. F344×BN rats (n=4) received either whole brain irradiation with a single dose of 10 Gy or sham-irradiation. The animals were maintained for 4, 8, and 24 h post-irradiation, and the brains were rapidly removed and two different brain regions (hippocampus and cortex) were dissected. The mRNA expression levels of TNF-α in hippocampus and cortex were determined by quantitative real-time RT-PCR (panel A). Using the $2^{-\Delta\Delta CT}$ method as described in *Materials and Methods*, the data are presented as fold change in gene expression normalized to a housekeeping gene, glyceraldehyde 3-phosphate dehydrogenase (GAPDH), and relative to the sham-irradiated control. The protein expression levels of TNF-α in hippocampus and cortex were analyzed by ELISA (panel B) and fluorescence microscopy (panel C-J). Panel C: sham-irradiation (Control); panel D: 4 h post-irradiation; panel E: 8 h post-irradiation; panel F: 24 h post-irradiation; panel G-J: negative controls. Magnification of the images (panel C-J) is 100×. Data shown are mean ± SEM for each group. *, **Statistically significant from control (*$p<0.05$ and **$p<0.001$). #Statistically significant from hippocampus ($p<0.05$).

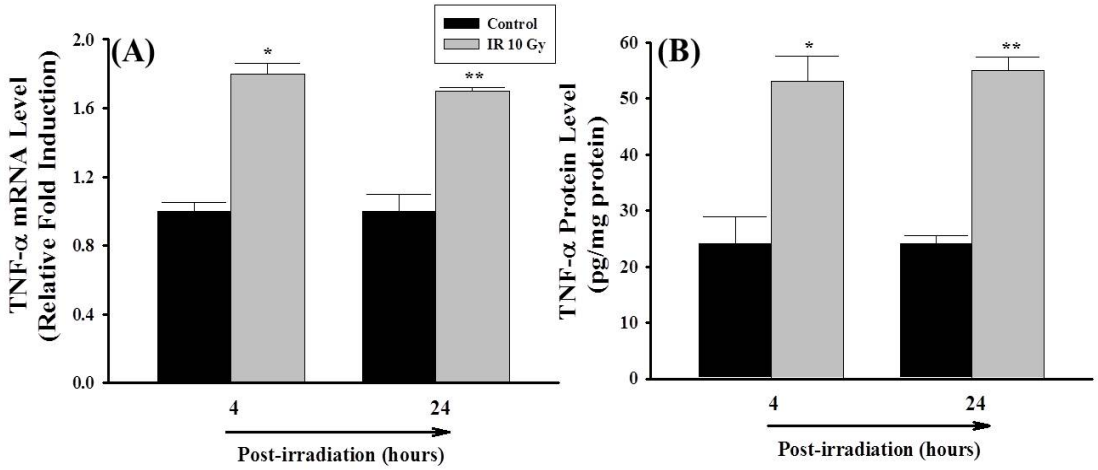

Figure 3.2. Irradiation Up-Regulates mRNA and Protein Expression of TNF-α in Microglia. BV-2 cells received irradiation with a single dose of 10 Gy (*IR 10 Gy*) or sham- irradiation (*Control*). Cells were maintained for 4 and 24 h post-irradiation, and the mRNA and protein expression levels of TNF-α were analyzed by quantitative real-time RT-PCR (panel A) and ELISA (panel B), respectively. Data shown are mean ± SEM for each group. *, **Statistically significant from control (*$p<0.05$ and **$p<0.001$).

3.4.3 Irradiation Up-regulates Expression of IL-1β and MCP-1 in Rat Brain

The effects of irradiation on mRNA and protein expression of IL-1β, IL-6, and MCP-1 were also investigated in rat brain. **Figure 3.3A** demonstrates that mRNA expression levels of the pro-inflammatory cytokine IL-1β were significantly higher in both hippocampal and cortical regions of irradiated rats compared to those of sham-irradiated controls at any time point. The greatest response was detected at 4 h after irradiation in hippocampus (a 20-fold induction) and 8 h after irradiation in cortex (a 19-fold induction). Significantly higher expression levels of IL-1β protein that remained for up to 24 h after irradiation were also observed in hippocampal and cortical regions isolated from irradiated rat brains (**Figure 3.3B**). IL-1β levels were markedly elevated in hippocampus compared to cortical samples. In addition, irradiation significantly up-regulated mRNA expression of another pro-inflammatory cytokine IL-6 in rat brain while an increased IL-6 mRNA expression was not translated to actual changes in protein levels (**Figure 3.4**). Furthermore, irradiation significantly and dramatically up-regulated mRNA expression of the pro-inflammatory chemokine MCP-1 in rat brain. The mRNA levels of MCP-1 in hippocampus and cortex were increased by 395- and 581-fold at 4 h, 252- and 347-fold at 8 h, and 11- and 22-fold at 24 h after irradiation (**Figure 3.5A**). Furthermore, expression levels of MCP-1 protein at 4 h and 8 h after irradiation were significantly greater in hippocampus and cortex than those of sham-irradiated control rat brains (**Figure 3.5B**).

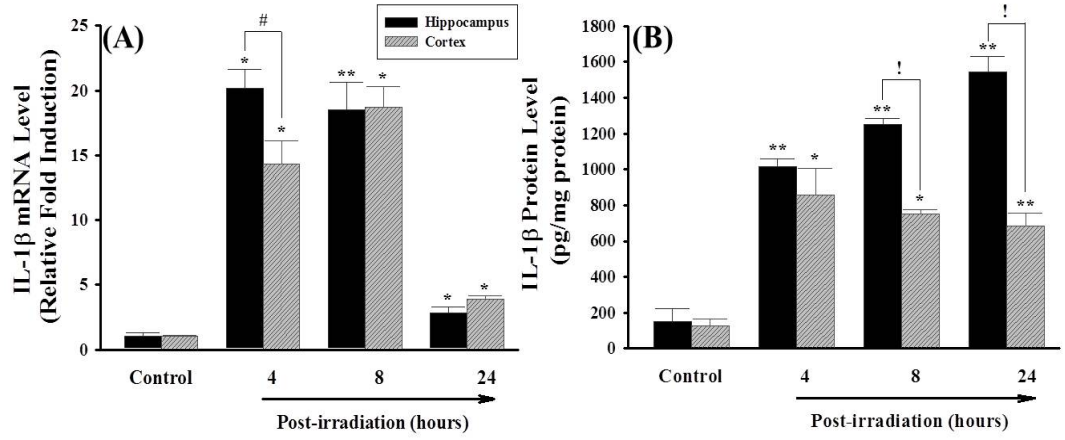

Figure 3.3. Irradiation Up-Regulates mRNA and Protein Expression of IL-1β in Rat Brain. Experiments were carried out as described in Figure 3.1. The mRNA expression levels of IL-1β in hippocampus and cortex were determined by quantitative real-time RT-PCR (panel A). The protein expression levels of IL-1β in hippocampus and cortex were determined by ELISA (panel B). Data shown are mean ± SEM for each group. *, **Statistically significant from control (*$p<0.05$ and **$p<0.001$). $^{\#}$, $^{!}$Statistically significant from hippocampus ($^{\#}p<0.05$ and $^{!}p < 0.001$).

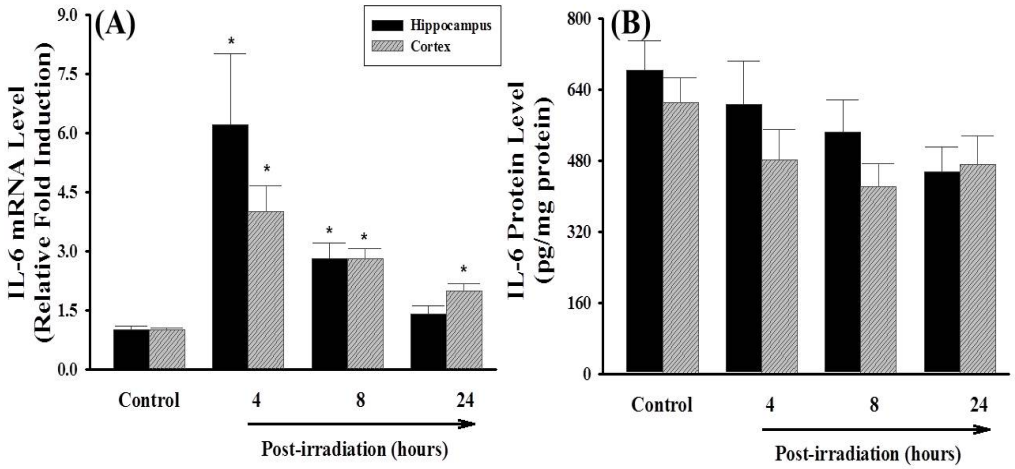

Figure 3.4. Effects of Irradiation on mRNA and Protein Expression of IL-6 in Rat Brain. Experiments were carried out as described in Figure 3.1. The mRNA expression levels of IL-6 in hippocampus and cortex were determined by quantitative real-time RT-PCR (panel A). The protein expression levels of IL-6 in hippocampus and cortex were determined by ELISA (panel B). Data shown are mean ± SEM for each group. *Statistically significant from control ($p<0.05$).

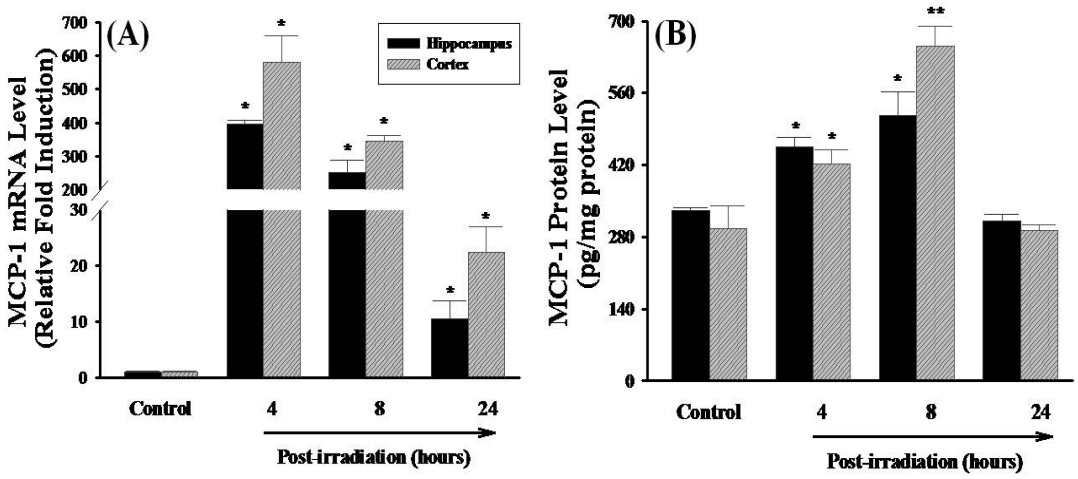

Figure 3.5. Irradiation Up-regulates mRNA and Protein Expression of MCP-1 in Rat Brain. Experiments were carried out as described in Figure 3.1. The mRNA expression levels of MCP-1 in hippocampus and cortex were determined by quantitative real-time RT-PCR (panel A). The protein expression levels of MCP-1 in hippocampus and cortex were determined by ELISA (panel B). Data shown are mean ± SEM for each group. *, **Statistically significant from control (*$p<0.05$ and **$p<0.001$).

3.4.4 Irradiation Activates Pro-Inflammatory Transcription Factors in Rat Brain

To elucidate the molecular mechanisms of irradiation-induced brain inflammation, the effects of irradiation on the DNA-binding activity of pro-inflammatory transcription factors in rat brain were examined by a series of EMSAs. These analyses were performed on nuclear protein extracts from hippocampal regions isolated from either irradiated rat brains or sham-irradiated controls. The effects of irradiation on the DNA-binding activity of AP-1 in rat brain are shown in **Figure 3.6**. A slight endogenous activity of AP-1 was observed in sham-irradiated control rat brains. In contrast, a significant increase in AP-1 DNA-binding activity was detected in irradiated rat brains (**Figure 3.6A**). AP-1 activation increased by 2.5-fold at 4 h and 2.8-fold at 8 h after irradiation compared to the sham-irradiated control rats and returned to the control levels at 24 h after irradiation (**Figure 3.6B**). The specificity of AP-1 DNA-binding was determined by competition experiments with molar excess of unlabeled oligonucleotide containing the consensus AP-1 binding sequence. As depicted in **Figure 3.6A** (*lane 6*), an excess amount of competitor oligonucleotide completely abolished the AP-1 DNA-binding activity.

In addition to AP-1, the effects of irradiation on other pro-inflammatory transcription factors, including NF-κB and CREB, were studied. As illustrated in **Figure 3.7** and **3.8**, a prominent and significant stimulation of DNA-binding activities of NF-κB (3.3-fold increase) and CREB (2.0-fold increase) was observed 4 h after irradiation. This activation was maintained at a high level 8 h after irradiation, and no activation of NF-κB and CREB was detected 24 h after irradiation. The molar excess of each unlabeled oligonucleotide probe completely diminished the specific band that corresponded to either NF-κB (**Figure 3.7A**, *lane 6*) or CREB DNA-binding (**Figure 3.8A**, *lane 6*).

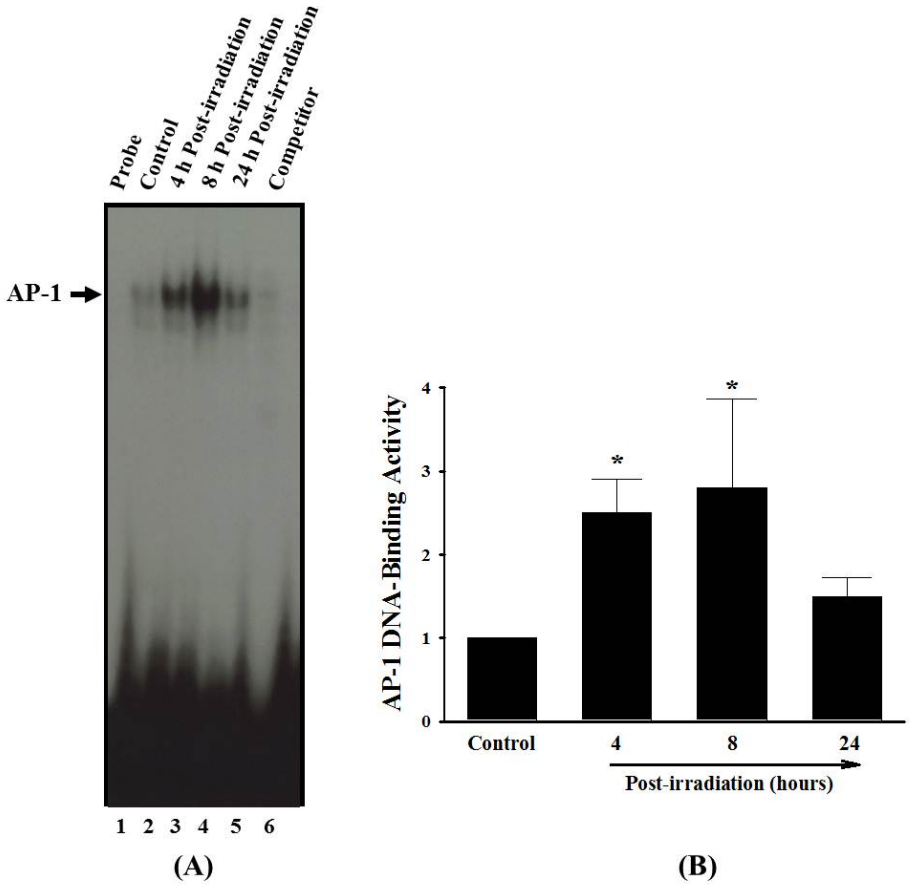

Figure 3.6. Representative Autoradiogram of EMSA of the Effects of Irradiation on AP-1 DNA-Binding Activity in Rat Brain (panel A). F344×BN rats (n=4) received either whole brain irradiation with a single dose of 10 Gy or sham-irradiation. The animals were maintained for 4, 8, and 24 h post-irradiation and nuclear extracts were prepared from the brain hippocampus regions and analyzed by EMSA. Competition studies were performed by adding excess unlabeled AP-1 probe. Densitometric quantification of the effects of irradiation on AP-1 DNA-binding activity in rat brain (panel B). Experiments were repeated four times, and the intensities of the AP-1-specific bands were measured and statistically analyzed. The results are expressed as fold increase over control values. Data shown are the mean ± SEM for each group. *Statistically different from control ($p<0.05$).

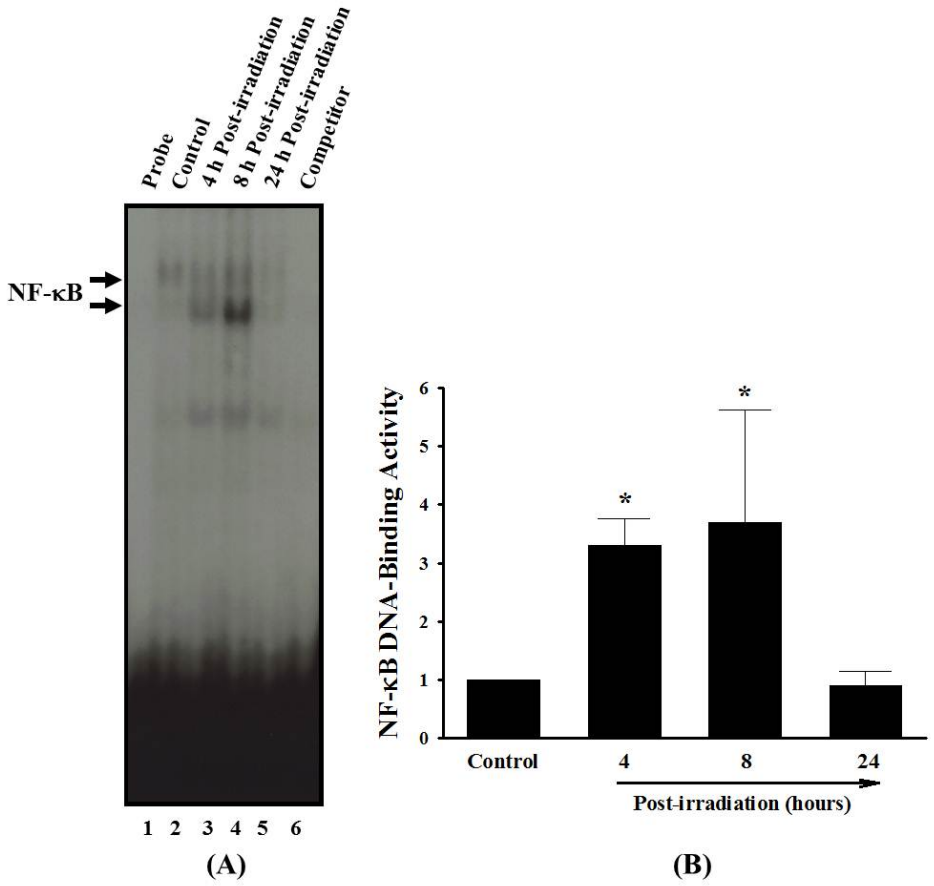

Figure 3.7. Representative Autoradiogram of EMSA of the Effects of Irradiation on NF-κB DNA-Binding Activity in Rat Brain (panel A). Experiments were carried out as described in Figure 3.6. Competition studies were performed by adding excess unlabeled NF-κB probe. Densitometric quantification of the effects of irradiation on NF-κB DNA-binding activity in rat brain (panel B). Experiments were repeated four times, and the intensities of the NF-κB-specific bands were measured and statistically analyzed. The results are expressed as fold increase over control values. Data shown are the mean ± SEM for each group. *Statistically different from control ($p<0.05$).

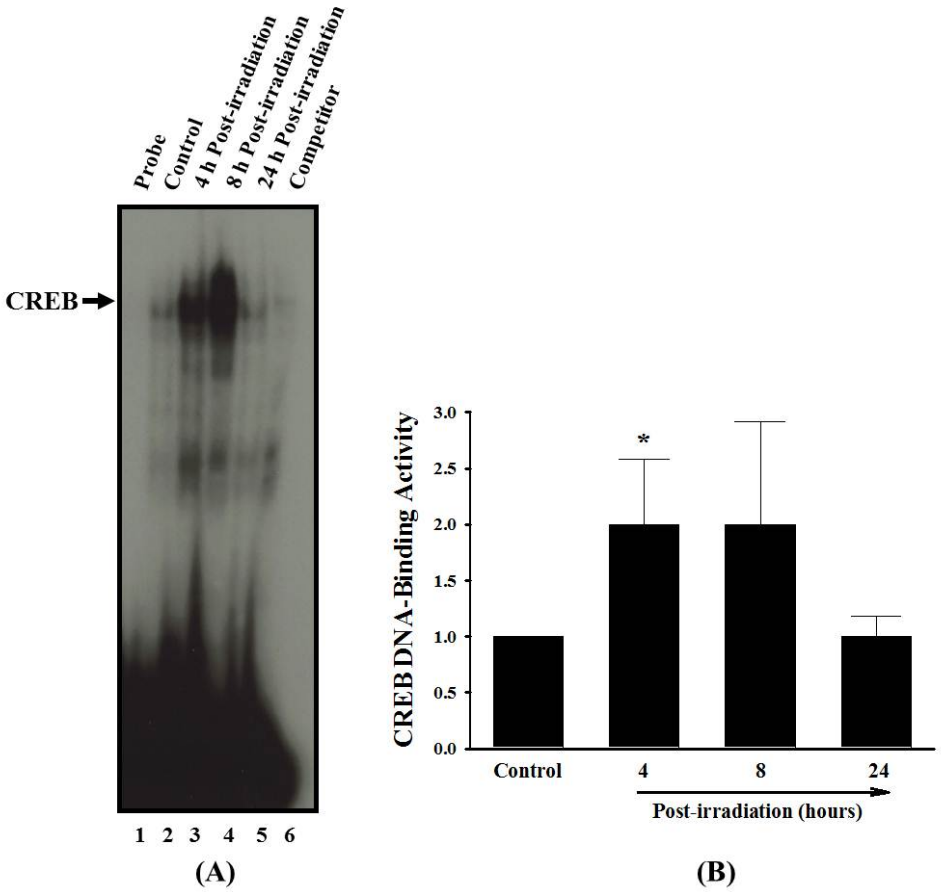

Figure 3.8. Representative Autoradiogram of EMSA of the Effects of Irradiation on CREB DNA-Binding Activity in Rat Brain (panel A). Experiments were carried out as described in Figure 3.6. Competition studies were performed by adding excess unlabeled CREB probe. Densitometric quantification of the effects of irradiation on CREB DNA-binding activity in rat brain (panel B). Experiments were repeated four times, and the intensities of the CREB-specific bands were measured and statistically analyzed. The results are expressed as fold increase over control values. Data shown are the mean ± SEM for each group. *Statistically different from control ($p<0.05$).

3.5 Discussion

Recent evidence has identified inflammation as one of the important pathways leading to radiation-induced brain injury (5-9). These early studies raise the possibility that a pro-inflammatory environment resulting from overexpression of inflammatory mediators may be responsible for many of the neurological/neuropathological complications occurring after irradiation (e.g., vascular rarefaction, necrosis, demyelination, vascular abnormality) (1-3, 60). However, subsequent studies on the effects of irradiation on pro-inflammatory pathways in the brain are limited by the absence of a clear time course for cytokine induction, incomplete analyses of gene and protein expression and/or lack of regional specificity that may contribute to selective biochemical pathways to neurodegeneration. In the present study, we demonstrate that irradiation activates AP-1, NF-κB, and CREB and overexpression of TNF-α, IL-1β, and MCP-1 throughout the rat brain. Nevertheless, the time course for induction and maximal response were regionally specific with hippocampus exhibiting higher levels of IL-1β and cortex exhibiting elevated levels of TNF-α. Our results are consistent with the conclusion that elevated levels of specific cytokines and chemokines within each brain region are unique and may contribute to specific pathways for the decline in tissue function after whole brain irradiation.

In general, a cascade of inflammatory events is regulated through the production of pro-inflammatory mediators. Enhanced expression of pro-inflammatory cytokines, chemokines, and adhesion molecules, and their close interactions facilitate pro-inflammatory pathways by recruiting and transmigrating inflammatory cells from blood to tissues (74-76). Several previous *in vivo* and *in vitro* studies have demonstrated that TNF-α and IL-1β are the most important pro-inflammatory cytokines that exert a central role in acute and chronic inflammation. It is well known that TNF-α and IL-1β strongly promote inflammatory responses in a wide spectrum of cell types, and overproduction of these cytokines has been implicated in a variety of human diseases including atherosclerosis, autoimmune disorders, and cancer (77, 78). In addition, there are several reports demonstrating that overexpression of TNF-α and IL-1β genes may be associated with the molecular responses of the brain to irradiation. Whole brain irradiation significantly up-regulated TNF-α gene expression in the mouse brain (7). Additionally, increased

levels of TNF-α and IL-1β gene expression were observed as an initial response of the mouse and rat brains to brain irradiation (5) and partial-body irradiation (178). Furthermore, Chiang et al. (6) reported that TNF-α mRNA was overexpressed 6 months after brain irradiation, suggesting that TNF-α may be involved in the late brain responses to irradiation. Up-regulation of TNF-α and IL-1β expression was also found in lung and intestine after irradiation (98, 179, 180). Despite the reports of increased gene expression, levels of TNF-α and IL-1β protein levels have not been reported. Importantly, the present study demonstrated for the first time a marked and significant increase in gene and protein expression of TNF-α and IL-1β in rat brain after whole brain irradiation and determined their specific time-courses. Since TNF-α and IL-1β are recognized as the crucial mediators of inflammatory events in brain, irradiation-mediated overexpression of these cytokines is likely to be an important contributing factor in the pathophysiological sequelae that occurs after whole brain irradiation.

The potential contribution of specific types of cells to the overexpression of pro-inflammatory mediators in the brain after irradiation, however, remains unclear. Microglia are the primary immune cells in the brain that release pro-inflammatory cytokines when they are activated by various environmental stimuli (181). Therefore, we performed an *in vitro* study to further examine the role of microglia in irradiation-induced TNF-α expression in brain. The results of this analysis indicate a significant up-regulation of the mRNA and protein expression of TNF-α in irradiated microglia suggesting that irradiation-induced pro-inflammatory environments in the brain may be, at least in part, mediated through activation of microglia.

IL-6 is another multifunctional pro-inflammatory cytokine that plays a major role in the mediation of the inflammatory and immune responses initiated by infection or injury (79). Recent studies have suggested that elevated levels of IL-6 mRNA and protein expression may be responsible for the radiation-induced inflammation in the intestine and whole brain (178-180). Additionally, both total-body and localized irradiation resulted in a small but significant increase in IL-6 levels in serum from rat blood (99). Consistent with the previous studies, irradiation significantly up-regulated mRNA expression of IL-6 in rat brain, however, we did not find that increased IL-6 gene expression translated to actual changes in protein levels. Potentially, this translational block or delay may be due to different protein expression kinetics for pro-

inflammatory cytokines in response to irradiation. Linard et al. (179) demonstrated that no change in IL-6 protein expression was observed in rat ileal muscularis layer at 6 h after abdominal irradiation, while the IL-6 content increased significantly 3 days after irradiation. The potential biochemical mechanism(s) for the delayed protein expression of IL-6 in response to irradiation remain to be determined.

In addition to pro-inflammatory cytokines, chemokines are known to directly promote inflammatory responses. MCP-1 is a member of the CC chemokine family and has a critical role in monocyte chemotaxis and transmigration (80). Although recent evidence indicates that irradiation induces dermatitis and fibrosis in skin and lung by elevating the levels of MCP-1 (100, 182), the molecular basis for the induction of this chemokine in irradiated brain has not yet been elucidated. Therefore, the results of the present study showing that irradiation significantly induced mRNA and protein expression of MCP-1 in hippocampus and cortex appear to be the first to document the stimulatory effects of irradiation on MCP-1 expression in the brain. Whether the irradiation-induced increase in MCP-1 results in fibrotic changes within the brain and contributes to neuropathology remains unknown.

Activation of AP-1 and NF-κB is considered to be a part of the general regulation of a number of pro-inflammatory gene expressions in response to various extracellular stimuli (85-89). Evidence indicates that irradiation can cause an increase in AP-1 and/or NF-κB DNA-binding activity in several different types of cells including A549 lung epithelial cells, HeLa cells, KG-1 myeloid leukemia cells, astrocytes, and glioblastoma cells (183-187). Additionally, both whole-body and abdominal irradiation increased inflammatory gene expression and activated NF-κB in rat intestine (96, 179, 180). It was also reported that exposure of mice to total-body irradiation selectively activated NF-κB in the spleen, lymph nodes, and bone marrow, and subsequently increased mRNA expression of TNF-α, IL-1α, IL-1β, and IL-6 (188). Furthermore, enhanced DNA-binding activities of AP-1 and NF-κB were found in the cerebral cortex collected from rat brains after whole brain irradiation (189). In agreement with these *in vivo* and *in vitro* studies, the present study further demonstrated a significant activation of AP-1 and NF-κB in rat hippocampus after irradiation. Recent evidence has also suggested that not only AP-1 and NF-κB but also CREB may belong to the family of transcription factors that play an

important role in the expression of pro-inflammatory mediators (190, 191). There are, however, no reports showing effects of irradiation on CREB activity in brain. Therefore, in the present study, DNA-binding activity of CREB was examined. To our knowledge, this is the first report to demonstrate that activation of CREB may be involved in irradiation-mediated cellular effects in the brain. Although these results provide evidence that activation of AP-1, NF-κB, and CREB may be responsible for irradiation-induced overexpression of pro-inflammatory mediators in brain, detailed signal transduction pathways leading to activation of these transcription factors in response to irradiation remain to be determined. In addition, it is necessary to find out whether radiation-mediated early inflammatory responses observed in the present study have a causal relationship with delayed injury to the brain.

3.6 Conclusions

The present study demonstrated that irradiation induces pro-inflammatory environments through activation of AP-1, NF-κB, and CREB and overexpression of inflammatory mediators throughout the brain but that the absolute levels of each cytokine and chemokine are unique to each brain region. Because brain inflammation is critically involved in the onset and progression of neurological disorders, these results may contribute to a deeper understanding of the pathophysiological mechanisms responsible for radiation-induced brain injury at the cellular and molecular levels. Furthermore, the present study may provide a foundation for the development of novel strategies for prevention and treatment of irradiation-induced brain injury specifically targeted against pro-inflammatory pathways.

3.7 Acknowledgments

The editorial assistance of MaryAnn Sonntag in preparation of the manuscript is greatly appreciated. The project described was supported by Grant Number R01NS056218 from the National Institute of Neurological Disorders and Stroke.

CHAPTER 4:

CONSTRUCTION OF A NONLINEAR DYNAMIC MODEL OF RADIATION-INDUCED TNF-α EXPRESSION IN BRAIN

CONSTRUCTION OF A NONLINEAR DYNAMIC MODEL OF RADIATION-INDUCED TNF-α EXPRESSION IN BRAIN

4.1 Abstract

Purpose: Mathematical models provide a useful conceptual framework for interpreting data and gaining insights into the static and dynamic behaviors of complex biological system such as gene regulatory networks. In the present study, we constructed a mathematical model describing radiation-induced mRNA and protein expression kinetics of tumor necrosis factor-α (TNF-α) in the hippocampus by modifying a nonlinear model based on reaction kinetics.

Materials and methods: A mathematical model describing radiation-induced mRNA and protein expression kinetics of TNF-α in the hippocampus was constructed by modifying a nonlinear model consisting of ordinary differential equations (ODEs) based on reaction kinetics. As a regulation function, a positive Hill curve function was used. To estimate four unknown model parameters, experimental data measured in rat hippocampus and Matlab's "fminsearch" command were employed. The model was simulated using the command "ODE113" in Matlab. Additionally, values between model predictions and measured protein expression levels of TNF-α were compared to confirm the accuracy of the model.

Results: Unknown parameters in the modified model were optimized with experimental data for the hippocampus. However, the model did not closely fit the data for TNF-α mRNA and protein levels at 4 and 8 h. This suggests that an additional factor is regulating TNF-α mRNA transcription.

Conclusion: We modified the proposed nonlinear model based on reaction kinetics and reconstructed the model in time series experimental data of binding activity of transcription factor, mRNA expression, and protein expression in hippocampus following irradiation.

Key words: *Mathematical model; reaction kinetic; TNF-α; ODEs; parameter estimation*

4.2 Introduction

The classic view of the central dogma of molecular biology indicates that genetic information is stored in DNA, transcribed to messenger RNA (mRNA), and translated into proteins. Proteins play an essential role in the development and function of organisms. For example, they may function as enzymes, receptors responding to extracellular signals, or transcription factors regulating gene expression. Although nearly all cells in an organism contain the same DNA, there are fundamental differences between cell types, such as where, when, and which genes are expressed in the organism. In addition, multiple interactions of gene products are involved in molecular pathways of various diseases. Therefore, understanding the factors responsible for the gene regulation is critical to understand general biological systems and to develop new strategies for the prevention and treatment of diseases.

Gene expression refers to the process by which cells synthesize proteins from the information encoded in a gene. Several stages are involved in regulating the gene expression process, including transcription, translation, and post-translational modification of proteins (162, 163). During these stages, gene expression is controlled by regulatory molecules such as any of the intermediate products (RNA, polypeptides, or proteins), suggesting a network of gene regulation. Genetic regulatory networks (GRNs) consist of regulatory interactions among DNA, RNA, protein, and other molecules. They play an important role in the evolution and development of biological systems (164). However, numerous challenges have been reported in the area of modeling and simulating GRNs. For example, there are limited amounts of experimental data due to high levels of noise, limited data size from the cost of experiments, and the complexity of gene regulatory process (165). Despite many difficulties to reconstruct GRNs, various mathematical models have been proposed to understand the behavior of the networks being modeled and make predictions corresponding with experimental observations (10, 11).

In general, mathematical models can be categorized into two types: Boolean network based models (166, 167) and a dynamic system approach using ordinary differential equations (ODEs) (168, 169). The Boolean method simply describes the state of a gene as binary on/off switches and uses Boolean logical rules to approximate the regulatory control of gene expression,

functioning in discrete time steps. This method, however, possesses a disadvantage in expressing continuous aspects of gene regulation occurring in the cell environment. The dynamic system approach using ODEs is the most prominent method to analyze the genetic regulatory system. In ODEs, each state describes the concentrations of mRNA or protein and changes of each state are assumed to be continuous and deterministic; therefore, this method provides more extensive mathematical interpretations and greater physical accuracy for biological pathways than the Boolean approach (170).

In Chapter 3, we demonstrated that irradiation significantly up-regulates mRNA and protein expression of pro-inflammatory mediators including TNF-α in rat brain and activation of transcription factors such as NF-κB may be responsible for radiation-induced overexpression of pro-inflammatory mediators (171). In the present study, we constructed a mathematical model describing radiation-induced mRNA and protein expression kinetics of TNF-α in the hippocampus by modifying the nonlinear model consisting of ordinary differential equations based on reaction kinetics (12).

4.3 Methods

4.3.1 Modified Ordinary Differential Equation Model

In a reaction kinetic model, the expression of mRNA, protein, or small metabolites changes over time (12). The expression at any given time is described by the balance between its rate of synthesis and rate of degradation. In a previous report, Goodwin (192) developed a simple kinetic model for a genetic regulation process by employing the following set of differential equations proposed by Tyson and Othmer (12).

$$\frac{dx_1}{dt} = \kappa_{1n} r(x_n) - \gamma_1 x_1, x_1 \geq 0,$$

Equation [1]

$$\frac{dx_i}{dt} = \kappa_{i,i-1} x_{i-1} - \gamma_i x_i, \; x_i \geq 0, \quad 1 < i \leq n$$

In Equation [1], x_1 is the mRNA concentration for a particular gene and x_i is the protein or the metabolite concentration. The parameters κ_{1n}, $\kappa_{21},\ldots,$ $\kappa_{n,n-1} > 0$ are production rate constants and $\gamma_1,\ldots,\gamma_n > 0$ are degradation rate constants. In the case of x_1, the synthesis term includes a nonlinear regulation function $r(x_n)$. The function $r(x_n)$ embodies either activation or repression of x_n synthesis.

In general, gene expression is regulated at the transcriptional level through activation of some outside signals such as transcription factors. Therefore, in the present study, the function $r(x_n)$ was replaced with the function $f([TF])$, where an increase in concentration of transcription factor [TF] will activate or repress the transcription rate of x_1. A kinetic model of a genetic regulation process used in the present study is shown in **Figure 4.1.**

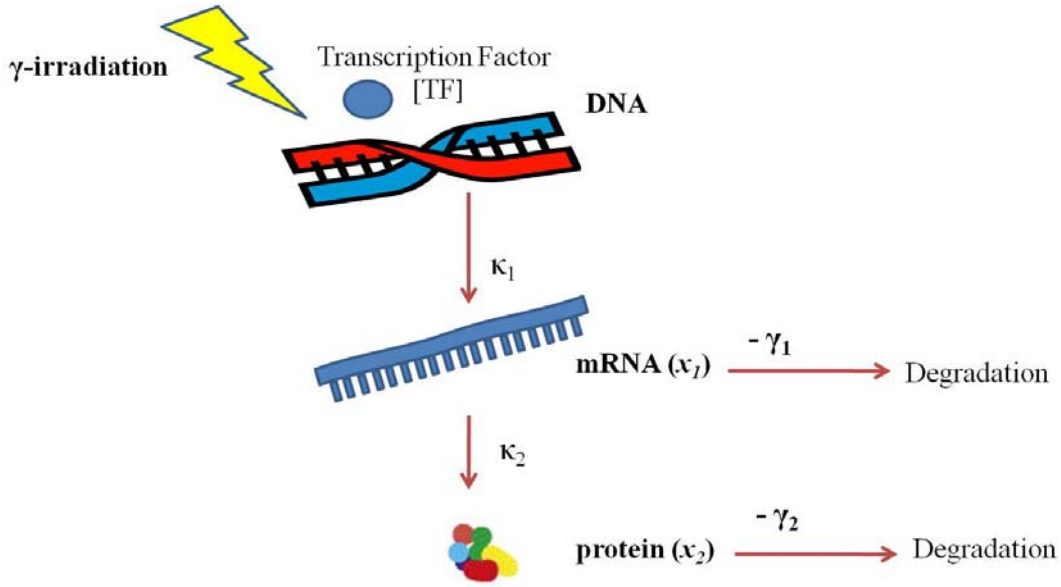

Figure 4.1. Model Schematic for a Genetic Regulatory System

The genetic regulatory system modeled by reaction kinetic can be expressed as the following set of ODEs.

$$\frac{dx_1}{dt} = \kappa_1 f([\mathrm{TF}]) - \gamma_1 x_1 \, , x_1 \geq 0 \qquad \text{Equation [2-a]}$$

$$\frac{dx_2}{dt} = \kappa_2 x_1 - \gamma_{2,} x_{2,}, \; x_2 \geq 0 \qquad \text{Equation [2-b]}$$

where the variables (x_1 and x_2) and [TF] are functions of time t, while the parameters (κ_1, κ_2, γ_1, and γ_2) are constants. They are defined as follows:

$x_1 =$ mRNA concentration

$x_2 =$ protein concentration

$\kappa_1, \kappa_2 > 0$, production rate constants of mRNA and protein, respectively

$\gamma_1, \gamma_2 > 0$, degradation rate constants of mRNA and protein, respectively

$f([\text{TF}])$ = the corresponding regulation function

As shown in Equation [2], the description of mRNA and protein kinetic involves the synthesis and degradation of molecules per unit time. Specifically, transcription is governed by the transcription rate $\kappa_1 f([\text{TF}])$ where $\kappa_1$is the mRNA synthesis rate. Each mRNA is translated into protein at a rate κ_2 per mRNA molecule. In addition, mRNA and proteins are constantly being degraded at a rate γ_1 and γ_2, respectively. As a regulation function, a Hill curve function which formulates relative intensity of gene regulation was used. A Hill curve has been recently employed to model the transcription factor binding/unbinding to the promoter region at equilibrium (45, 193). In Equation [2], $f([\text{TF}])$ is the relative promoter activity as a function of the TF concentration [TF]. In Chapter 3, transcription factor NF-κB acts as an activator in TNF-α mRNA expression suggesting that the transcription rate increases as the concentration of transcription factor [TF] increases. Thus, we choose $f([\text{TF}])$ to be an increasing function, i.e. $\frac{\mathrm{d}f}{\mathrm{d}[\text{TF}]} > 0$ and the corresponding regulation function $f([\text{TF}])$ can be written as follows:

$$f([\text{TF}]) = \frac{[\text{TF}]^m}{\theta^m + [\text{TF}]^m}, \quad \text{m} > 0, \; \theta > 0 \qquad \text{Equation [3]}$$

where m is the degree of regulation (a steepness parameter) and threshold θ is related to the reaction rate. The function ranges from 0 to 1, increases with [TF], approaches 1 as [TF]→ ∞, and increases the expression rate (activation). A value for m was chosen based on the

physiological ranges of the model parameters (194, 195). Hill coefficient m = 2 and threshold parameter θ = 3 were used based on the previous report in reconstructing nonlinear dynamic models of gene regulation (**Figure 4.2A**)(165).

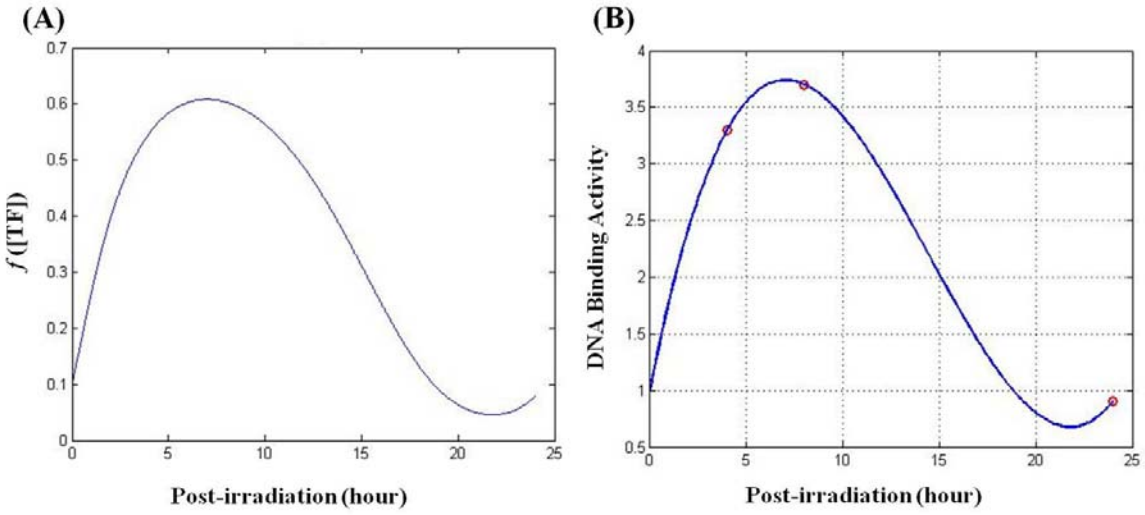

Figure 4.2. (A) Regulation Functions: $f([TF])$ and (B) Fitted [TF]: $[TF] = 0.0019t^3 - 0.0822t^2 + 0.8733t + 1$.

In this study, experimental data for [TF] were available only at times 0, 4, 8, and 24 h. In order to obtain time continuous [TF] data, the 3rd order polynominal equation for [TF] was developed by using the polyfit Matlab command (**Figure 4.2B**).

Experimental data of mRNA (x_1) and protein concentrations (x_2) of TNF-α, and NF-κB binding activity [TF] in the hippocampus at 0, 4, 8, 24 h after irradiation are given in **Table 4.1.** Values for x_1, x_2, and [TF] at 4, 8, 24 h post-irradiation were normalized by the values at 0 h post-irradiation (control group), respectively.

Post-irradiation (hour)	mRNA Concentration (x_1)	Protein Concentration (x_2)	Transcription factor Concentration ([TF])
0	1.0	1.0	1.0
4	15	23	3.3
8	8.5	8.3	3.7
24	2.4	3.6	0.9

Table 4.1. Experimental Data in Rat Hippocampus

4.3.2 Parameter Estimation of ODE Systems

In Equation [2], there were four unknown parameters: κ_1, κ_2, γ_1, and γ_2. Four measured values at 0, 4, 8, and 24 h were available to estimate these unknown parameters. Therefore, optimized parameters were obtained by using the Matlab command "fminsearch." This command is often used for parameter estimation in the dynamic system when constraints for unknown parameters are not provided. In this study, this command estimated the unknown parameters by minimizing the objective function J (Equation [4]) which is the summation of the squared error between predicted values by the model with changing unknown parameter values and the experimental data points. The mRNA and protein expression of TNF-α data were then compared with predicted values.

$$J = \sum_{i=1}^{4} \left\{ \left[\left(x_1^{\text{model}} \right)_i - \left(x_1^{\text{expt}} \right)_i \right]^2 + \left[\left(x_2^{\text{model}} \right)_i - \left(x_2^{\text{expt}} \right)_i \right]^2 \right\} \qquad \text{Equation [4]}$$

where subscript 1 and 2 state mRNA and protein, respectively; x^{model} is a value predicted by the modified model and x^{expt} is the measured value at time point t_i; $i = 1, 2, 3, 4$; $t_i = 0, 4, 8, 24$ h.

4.3.3 Algorithm

In the present study, we first estimated four unknown parameters and then predicted x_2 values based on obtained parameters. This work was performed by following steps.

Step 1. Initial conditions for κ_1, κ_2, γ_1, and γ_2 were arbitrarily selected to give a starting point for calculation.

Step 2. These values were used to calculate x_1 and x_2 values in the model by employing the Matlab command "ODE113" to solve non-stiff differential equations.

Step 3. The objective function J was calculated using predicted values for x_1 and x_2 and experimental data for x_1 and x_2 in the hippocampus at times 0, 4, 8, and 24 h.

Step 4. Values for κ_1, κ_2, γ_1, and γ_2 were changed by an algorithm of the Matlab command "fminsearch". Then **Step 2** and **Step 3** were performed iteratively until it finds optimized values for the unknown parameters to minimize J.

Step 5. Optimized parameters, κ_1, κ_2, γ_1, and γ_2, were identified by **Step 2-4**.

Step 6. Solution for x_2 was found by solving the Equation [2-b].

Step 7. x_2 values were predicted by using solution from Step 6 with estimated κ_2 and γ_2, and measured cortex x_1 data at times 0, 4, 8, and 24 h.

4.4 Results and Discussion

4.4.1 Parameter Estimation

Estimated synthesis and degradation rates were shown in **Table 4.2.**

κ_1	κ_2	γ_1	γ_2
89	8.4	5.5	5.0

Table 4.2. Estimated Parameter Values (h^{-1})

Experimental data of TNF-α mRNA and protein expression in rat hippocampus after a single dose of 10 Gy are shown as "o" in **Figure 4.3**. Simulated results of Equation [2] with estimated parameters (solid line) show the time series of mRNA concentration x_1 and protein concentration x_2 in the hippocampus within 24 h post-irradiation. In this study, the number of measured data points, four, is too small to estimate optimized parameters accurately. The use of a small number of data leads to multiple optimized local parameters at different initial conditions. In other words, the optimization algorithm is very sensitive to the initial conditions of parameters. Therefore, in order to have a stable and accurate parameter estimation, a higher number of data points is necessary. In addition, preliminary simulation results showed that estimated values for κ_2, γ_1, and γ_2 were smaller than 10 (h^{-1}). According to the simulation results, initial conditions for these

parameters were set as 1 and not changed through simulations, while the value for κ_1 in the initial condition was changed to reduce test cases. The transcription rate κ_1 was varied from 1 to 130 by steps of 10 in this study. One of the optimized results is shown in **Figure 4.3**.

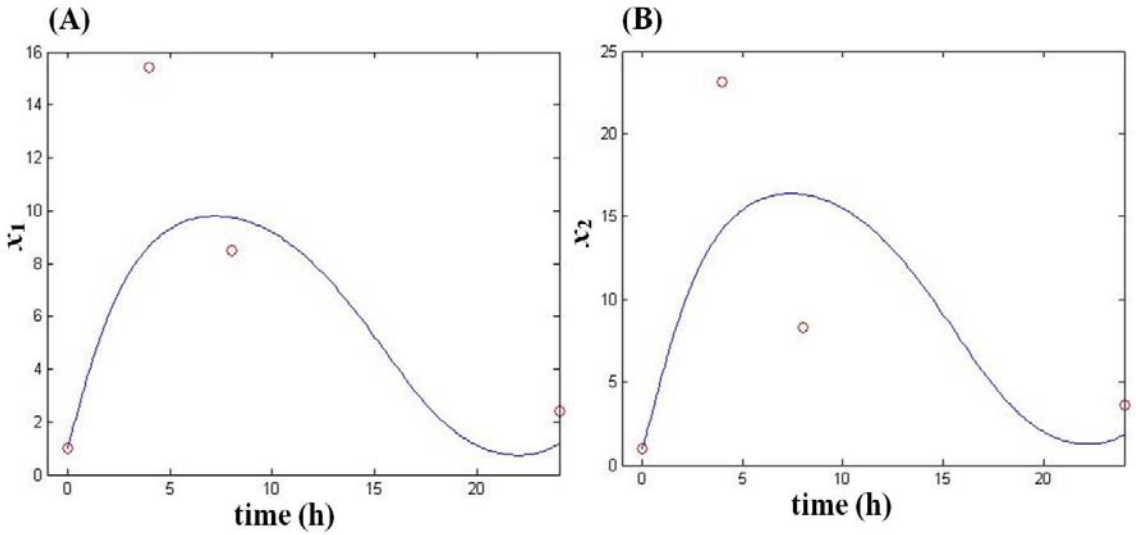

Figure 4.3. Simulated Results Using Estimated Parameters. (A) mRNA and (B) Protein. o and solid line indicate experimental data points and simulated data with model, respectively.

4.4.2 Limitation of Model

Qualitatively, the curves shown in **Figure 4.3** match the experimentally measured transient increases in TNF-α mRNA and protein. However, the model predicts that both of these transient effects should be maximal at around 7 h, whereas the experimental data appears to reach a maximum before 5 h. This discrepancy reflects either the accuracy of the data or of the model. The experimental data (**Table 4.1**) suggests that [TF] reaches a maximum after TNF-α mRNA and protein concentrations are decreasing. In contrast, the model is built on the assumption that [TF] stimulates x_1, which in turn stimulates x_2 (**Figure 4.1**). Therefore, the model requires that [TF] (**Figure 4.2A**) is maximal before x_1 (**Figure 4.3A**), and that x_1 must be maximal before x_2 (**Figure 4.3B**). Thus, a weakness of the model may be the TNF-α mRNA regulation by NF-kB. Indeed, other factors, such as suppressors of cytokine signaling (SOCS)-1 and SOCS-3 (repressors for NF-κB signal) may be involved in down-regulating TNF-α mRNA (196, 197)

(**Figure 4.4**). These may explain the result showing an increased TNF-α expression in response to irradiation was decreased at 8 h post-irradiation, even though NF-κB maximum activity was observed 8 h irradiation.

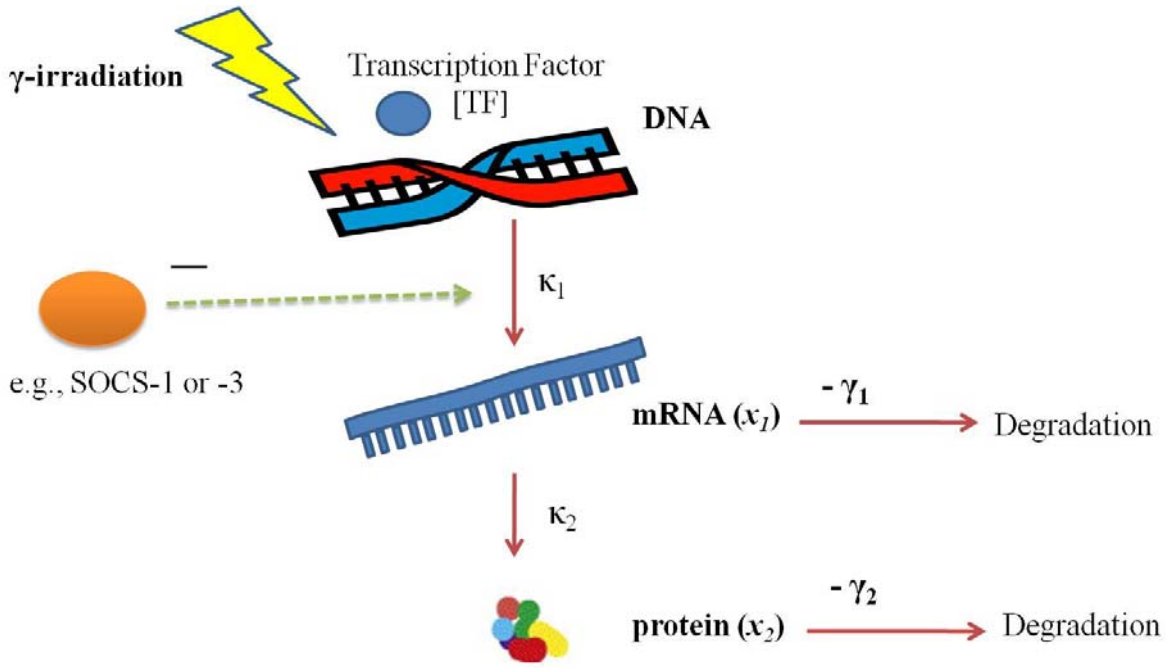

Figure 4.4. Modified Model Schematic for a Genetic Regulatory System

4.5 Conclusion

We modified the proposed nonlinear model based on reaction kinetics and reconstructed the model in time series experimental data of binding activity of transcription factor, mRNA expression, and protein expression in hippocampus following irradiation. However, more case studies with increased data points and addition of a negative feedback loop (**Figure 4.4**) are necessary to develop more accurate models. In addition, the nonlinear model validation can be also made using experimental data in different brain region (cortex) proposed in Chapter 3.

CHAPTER 5:

AGING ATTENUATES RADIATION-INDUCED EXPRESSION OF PRO-INFLAMMATORY MEDIATORS IN RAT BRAIN

*Reprinted from Lee WH, Sonntag WE, Lee YW. *Neuroscience Letters*, 476:89-93 (2010), with permission from Elsevier (198).

AGING ATTENUATES RADIATION-INDUCED EXPRESSION OF PRO-INFLAMMATORY MEDIATORS IN RAT BRAIN

5.1 Abstract

Purpose: The present study was designed to examine the effect of aging on radiation-induced expression of pro-inflammatory mediators in rat brain.

Materials and methods: Male F344×BN rats (4, 16, and 24 months of age) received either whole brain irradiation with a single dose of 10Gy γ-rays or sham-irradiation, and were maintained for 4, 8, and 24 h post-irradiation. The mRNA expression levels of various pro-inflammatory mediators such as cytokines, adhesion molecules, chemokine, and matrix metalloproteinase were analyzed by quantitative real-time reverse transcription-polymerase chain reaction (RT-PCR).

Results: The acute inflammatory responses to irradiation, including overexpression of tumor necrosis factor-α (TNF-α), interleukin-1β (IL-1β), interleukin-6 (IL-6), intercellular adhesion molecule-1 (ICAM-1), vascular cell adhesion molecule-1 (VCAM-1), E-selectin, monocyte chemoattractant protein-1 (MCP-1), and matrix metalloproteinase-9 (MMP-9) were markedly attenuated in the hippocampus of middle-aged and old rats compared with young groups. Specifically, a significant age-dependent decrease in TNF-α expression was detected 8 and 24 h after irradiation and a similar age-related attenuation was observed in IL-1β, ICAM-1, and VCAM-1 expression 4 and 8 h post-irradiation. MCP-1 expression was reduced 4 h post-irradiation and MMP-9 expression at 8 h post-irradiation.

Conclusion: These results provide evidence for the first time that radiation-induced pro-inflammatory responses in the brain are suppressed in aged animals.

Key words: *Aging; pro-inflammatory mediators; brain inflammation; whole brain irradiation*

5.2 Introduction

It is well documented that an impaired immune response is associated with aging. Gon et al. (110) demonstrated that the serum concentrations of pro-inflammatory cytokines including TNF-α and IL-1β were significantly lower in elderly patients with pneumonia compared with those in young patients. They also found that peripheral blood monocytes from healthy normal elderly subjects produced less amounts of these cytokines than those from healthy normal young subjects in response to lipopolysaccharide (LPS) stimulation (110). In addition, IL-1 production by LPS-stimulated co-cultures of peritoneal macrophages and splenic T cells from old mice were markedly reduced when compared with cells of young mice (111) and TNF-α-induced MMP-9 expression was decreased in aortic smooth muscle cells derived from old mice (112). Finally, mononuclear cells from elderly patients displayed a marked decrease in mitogen-stimulated production of interferon-γ (IFN- γ) and IL-2 (113). These studies provide evidence that an age-dependent impairment of immune response results in diminished inflammatory responses to extracellular stimuli.

Radiation therapy has been commonly used for the treatment of brain tumors. About 200,000 individuals are treated with partial large field or whole brain irradiation every year in the US (199). The prevailing evidence suggests that aging is an important prognostic factor in determining the response of brain tumors to radiation therapy (114). Previous clinical studies showed that the use of high dose radiation therapy for brain tumors resulted in significantly lower survival rates for patients older than 70 years of age compared with those for patients aged 70 and younger (115, 116). In addition, Rosenblum et al. (117) reported that stem cells obtained from patients over the age of 50 with brain tumors were less sensitive to radiation than those from patients 50 years old or younger. Although the mechanisms for this effect have not been established, these studies clearly demonstrate that aging exerts a profound effect on the efficacy of radiation therapy for treatment of brain tumors.

It has been suggested that acute inflammatory responses in cancer patients undergoing radiation therapy may have beneficial effects. Indeed, a number of previous studies have demonstrated that an enhanced production of pro-inflammatory cytokines in response to

radiation is a necessary component of normal tissue repair processes (13, 14). Although it is generally accepted that the immune responses and the effectiveness of radiation therapy decline with age, the association among aging, inflammation, and radiation therapy remains to be further investigated. Therefore, the present study was designed to examine the effect of age on radiation-induced expression of pro-inflammatory mediators, including several cytokines (e.g., TNF-α, IL-1β, and IL-6), adhesion molecules (e.g., E-selectin, ICAM-1, and VCAM-1), the chemokine MCP-1, and MMP-9 in rat brain.

5.3 Materials and Methods

5.3.1 Animals

Male young (4 months of age), middle-aged (16 months of age), and old (24 months of age) F344×BN rats were obtained from the NIA colony at Harlan Laboratories, Inc. (Indianapolis, IN). Animals were housed on a 12/12 light-dark cycle with food and water provided *ad libitum*. Animal experiments were carried out in accordance with the National Institute of Health Guide for the Care and Use of Laboratory Animals (NIH Publications No. 80-23 revised 1996) and adequate measures were taken to minimize pain or discomfort. All studies were approved by the Institutional Animal Care and Use Committee.

5.3.2 *Irradiation*

Whole brain irradiation procedures were carried out as described previously with minor modifications (171). Briefly, rats were anesthetized with a ketamine/xylazine mixture (80/12 mg/kg body weight) and received either whole brain irradiation with a single dose of 10Gy γ-rays or sham-irradiation. Whole brain irradiation was performed in a ^{137}Cs irradiator using lead and Cerrobend shielding devices to collimate the beam so that the whole rat brain, including the brain stem, was irradiated. Control rats were anesthetized but not irradiated. The animals were maintained for 4, 8, and 24 h post-irradiation. The brains were rapidly removed and the hippocampus was dissected, immediately frozen in liquid nitrogen, and stored at -80 °C until analysis.

5.3.3 Real-Time Reverse Transcriptase-Polymerase Chain Reaction (RT-PCR)

Quantitative real-time RT-PCR was employed for gene expression analyses (171). Total RNA was isolated and reverse transcribed. Amplification of individual genes was performed on the Applied Biosystems 7300 System using TaqMan® Universal PCR Master Mix and a standard thermal cycler protocol. TaqMan® Gene Expression Assay Reagents for rat TNF-α, IL-1β, IL-6, ICAM-1, VCAM-1, E-selectin, MCP-1, MMP-9, and GAPDH (housekeeping gene) were used for specific probes and primers of PCR amplifications. The threshold cycle (C_T) was determined and relative quantification was calculated by the comparative C_T method.

5.3.4 Statistical Analysis

The statistical analysis of data was completed using SigmaStat 3.5 (SPSS Inc., Chicago, IL). One-way analysis of variance (ANOVA) was used to compare mean responses among the treatments. For each endpoint, the treatment means were compared using the Bonferroni least significant difference procedure. Statistical probability of $p<0.05$ was considered significant.

5.4 Results

5.4.1 The Effect of Aging on Radiation-Induced Expression of the Pro-Inflammatory Cytokines in Rat Brain

A single dose of whole brain irradiation dramatically increased mRNA expression levels of TNF-α (**Figure 5.1A**), IL-1β (**Figure 5.1B**), and IL-6 (**Figure 5.1C**) in hippocampus collected from rat brains for all age groups compared to their sham irradiated controls. However, in response to radiation induction of TNF-α and IL-6 was markedly attenuated at all time points in middle-aged and old rats compared with young animals. A significant age-dependent attenuation of TNF-α expression was detected in rat brains 8 h after irradiation (young rats, 9.1-fold induction; middle-aged rats, 3.3-fold induction; and old rats, 2.3-fold induction) and 24 h after irradiation (young rats, 1.8-fold induction; middle-aged rats, 1.1-fold induction; and old rats, 0.5-

fold induction). A similar age-dependent decrease in IL-1β expression in response to irradiation was observed 4 and 8 h after irradiation while the influence of age was not significant at the 24 h time point.

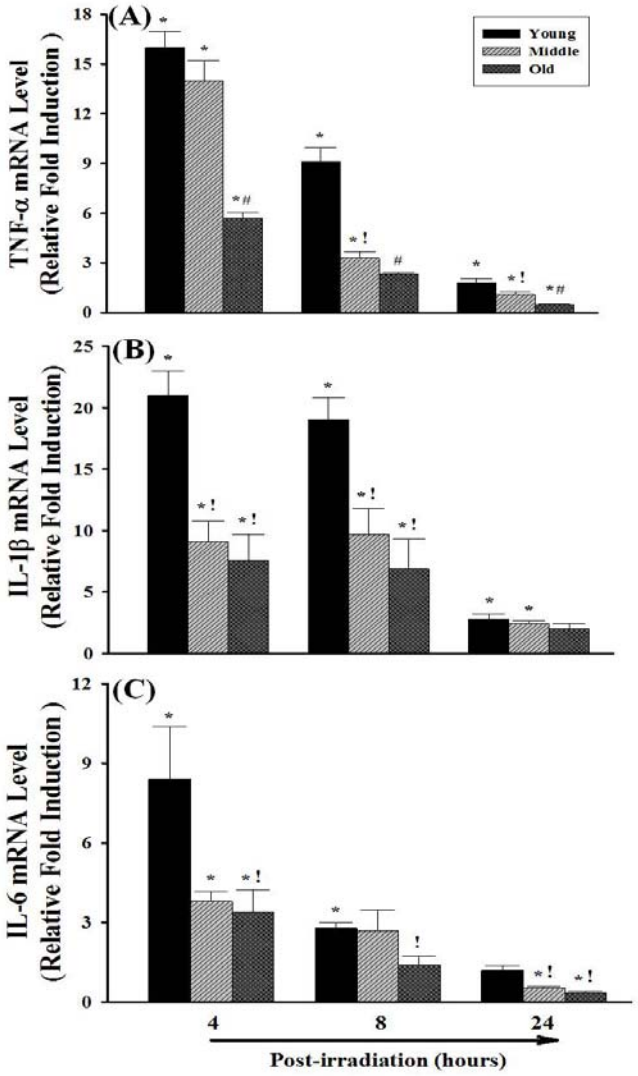

Figure 5.1. Effect of Aging on mRNA Expression of Pro-Inflammatory Cytokines in Rat Brain in Response to Whole Brain Irradiation. F344 x BN rats (4, 16, and 24 months of age; n=4) received either whole brain irradiation with a single dose of 10 Gy or sham-irradiation, and were maintained for 4, 8, or 24 h post-irradiation. The mRNA expression levels of TNF-α (A), IL-1β (B), and IL-6 (C) in hippocampus were determined by quantitative real-time RT-PCR. Values represent mean±SEM for each group. *$p<0.05$ vs. age-matched control; !$p<0.05$ vs. young rats; #$p<0.05$ vs. young and middle-aged rats.

5.4.2 The Effect of Aging on Radiation-Induced Expression of the Adhesion Molecules in Rat Brain

A significant up-regulation of ICAM-1 (**Figure. 5.2A**), VCAM-1 (**Figure. 5.2B**), and E-selectin (**Figure. 5.2C**) mRNA expression was observed 4 and 8 h after irradiation in all age-groups compared with age-matched sham-irradiated controls. In contrast, expression levels of these adhesion molecules 4 and 8 h after irradiation were profoundly lower in middle-aged and old rats than those in young groups. A significant age-dependent attenuation of ICAM-1 and VCAM-1 expression was observed 4 h after irradiation (young rats, 21-fold induction; middle-aged rats, 14-fold induction; and old rats, 8.2-fold induction) and 8 h after irradiation (young rats, 2.6-fold induction; middle-aged rats, 2.2-fold induction; and old rats, 1.6-fold induction), respectively.

5.4.3 The Effect of Aging on Radiation-Induced Expression of the Chemokine in Rat Brain

Radiation resulted in a significant and dramatic up-regulation of MCP-1 mRNA expression in hippocampus in all age-groups compared with their age-matched sham-irradiated controls (**Figure. 5.3**). Aging attenuated radiation-induced MCP-1 expression in brain at all age time points studied. A significant age-dependent impairment in MCP-1 expression was detected in rat brains 4 h after irradiation (young rats, 391-fold induction; middle-aged rats, 169-fold induction; and old rats, 98-fold induction).

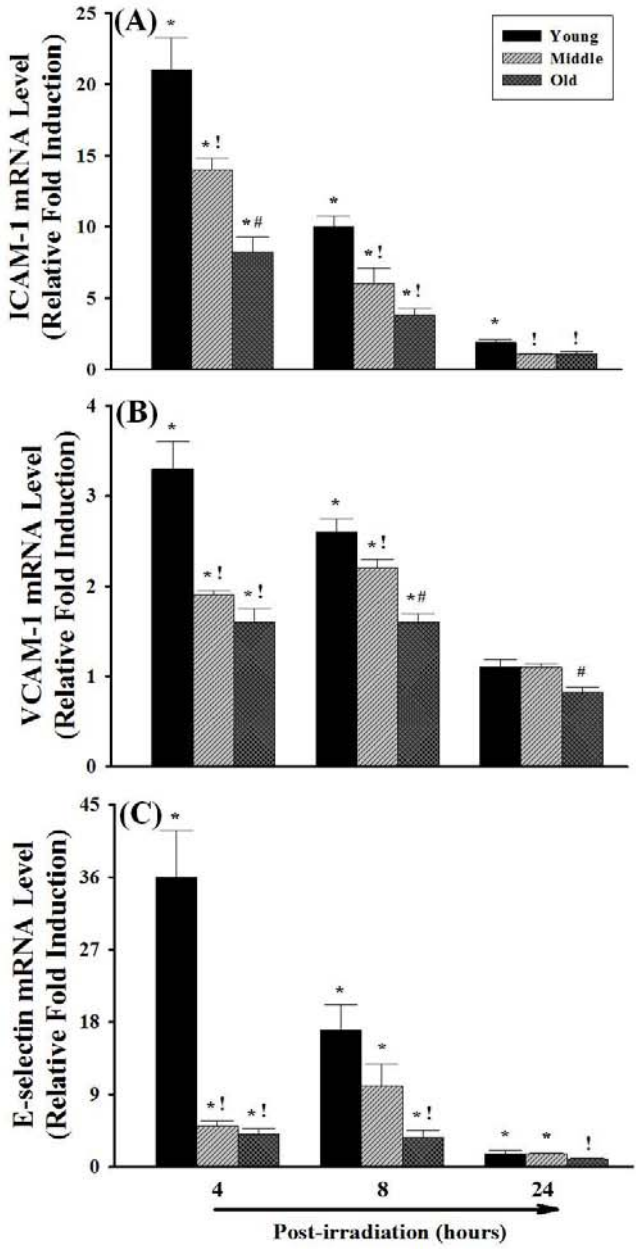

Figure 5.2. Effect of Aging on mRNA Expression of Adhesion Molecules in Rat Brain in Response to Whole Brain Irradiation. Experiments were carried out as described in Figure 5.1. The mRNA levels of ICAM-1 (A), VCAM-1 (B), and E-selectin (C) in hippocampus were determined by quantitative real-time RT-PCR. Values represent mean±SEM for each group. *$p<0.05$ vs. age-matched control; !$p<0.05$ vs. young rats; #$p<0.05$ vs. young and middle-aged rats.

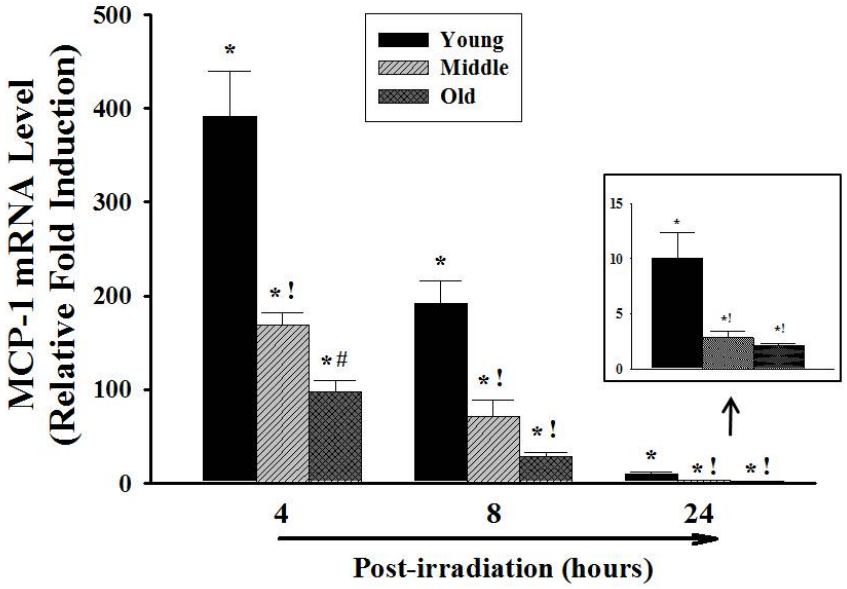

Figure 5.3. Effect of Aging on MCP-1 mRNA Expression in Rat Brain in Response to Whole Brain Irradiation. Experiments were carried out as described in Figure 5.1. The mRNA level of MCP-1 was determined by quantitative real-time RT-PCR. Values represent mean±SEM for each group. *$p<0.05$ vs. age-matched control; !$p<0.05$ vs. young rats; #$p<0.05$ vs. young and middle-aged rats.

5.4.4 The Effect of Aging on Radiation-Induced Expression of MMP-9 in Rat Brain

Irradiation significantly up-regulated MMP-9 mRNA expression for all age groups 8 h after irradiation compared with their age-matched sham-irradiated controls (**Figure. 5.4**). Previous *in vitro* and *in vivo* data demonstrated that irradiation increases mRNA expression and gelatinolytic activity of MMP-9 in brain (143, 200). Our recent *in situ* zymography result also showed strong gelatinolytic activity in rat brains after irradiation (unpublished data). These studies suggest that radiation-induced MMP-9 mRNA expression is consistent with the increase in MMP-9 activity in brain. Regardless of age, MMP-9 expression levels were not significantly different between sham and irradiated rat brains 4 and 24 h after irradiation. However, there was a significant age-dependent attenuation of radiation-induced MMP-9 expression in rat brains 8 h after irradiation (young rats, 2.4-fold induction; middle-aged rats, 1.6-fold induction; and old rats, 1.3-fold induction). Interestingly, the mRNA expression pattern of MMP-9 is different from those of the other genes investigated in the present study. Since pro-inflammatory cytokines are known to up-regulate MMP-9 expression (201), it is possible that irradiation may indirectly result in overexpression of MMP-9 through induction of these cytokines. However, the exact mechanisms of the late response of irradiation-induced MMP-9 expression remain unclear and should be further investigated.

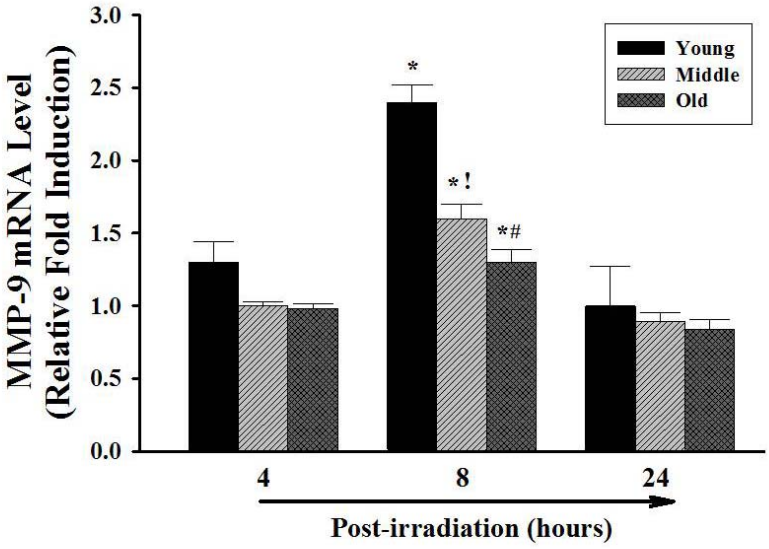

Figure 5.4. Effect of Aging on MMP-9 mRNA Expression in Rat Brain in Response to Whole Brain Irradiation. Experiments were carried out as described in Figure 5.1. The mRNA level of MMP-9 was determined by quantitative real-time RT-PCR. Values represent mean±SEM for each group. *$p<0.05$ vs. age-matched control; !$p<0.05$ vs. young rats; #$p<0.05$ vs. young and middle-aged rats.

5.5 Discussion

It is commonly accepted that chronic overexpression of pro-inflammatory mediators has detrimental effects on the brain (7). However, more recent evidence demonstrated that acute overexpression of pro-inflammatory mediators may represent a coordinated response to promote regeneration and repair processes of damaged areas in irradiated brain (105). In the present study, we examined the effect of aging on acute expression of pro-inflammatory mediators, including cytokines (e.g., TNF-α, IL-1β, and IL-6), adhesion molecules (e.g., E-selectin, ICAM-1, and VCAM-1), the chemokine MCP-1, and MMP-9 in response to irradiation. A rat model of whole brain irradiation with a single dose of 10Gy was chosen because it is the lowest dose to have a clear radiation effect (31) and is below the threshold for vascular changes, demyelination, or radionecrosis (32). Finally this dose is close to a clinically relevant dose in humans since the rat brain is more resistant to radiation injury than human brain (32). We found that the expression of all pro-inflammatory mediators evaluated in the present study were significantly up-regulated in response to radiation compared with sham-irradiated control groups regardless of age. In contrast, a significant age-dependent attenuation of inflammatory responses to acute radiation exposure was observed. These data are consistent with the age-related impairments in immune and inflammatory responses to stimulation described in response to other acute stresses (109, 202, 203). It is possible that reduced production of pro-inflammatory mediators in response to irradiation compromises the normal host defense mechanisms by decreasing the number of inflammatory cells in damaged brain tissue and subsequently leading to impaired repair/remodeling responses in old individuals. In addition, results from the present study may provide potential cellular and molecular mechanisms responsible for poor outcomes (e.g., survival and improvement in neurological function) in response to radiation therapy in elderly brain tumor patients.

It is widely accepted that basal expression levels of pro-inflammatory mediators including TNF-α, IL-1β, and IL-6 are significantly elevated in the aged brain compared with younger subjects (109). In contrast, advancing age results in a marked decrease in inflammatory responses induced by extracellular stimuli. A negative correlation between age and monocyte production of these cytokines in response to IFN-γ or LPS has been observed among different

age groups of animals (203). It was also found that LPS administration resulted in a significant attenuation of TNF-α and IL-6 mRNA expression in brains of old mice compared with those of young mice (109). Finally, Bruunsgaard et al. (202) demonstrated an impaired production of pro-inflammatory cytokines including TNF-α and IL-1β in response to LPS stimulation in elderly humans. Consistent with these previous reports, the present study also showed that aging is associated with an enhanced basal expression level of pro-inflammatory mediators and a diminished inflammatory response in brain to extracellular stimuli.

The pro-inflammatory pathways triggered by overexpression of inflammatory mediators have been implicated in the pathophysiological process of brain injury and subsequent progression of neurological disorders (65). For example, amyloid beta (Aβ) peptides contribute to Alzheimer's disease (AD) pathology through an inflammatory cascade in the brain *via* production of cytokines (e.g., IL-1β, TNF-α, and IL-6) and chemokines (e.g., MIP-1α and MIP-β) (204). It was also found that increased production of IL-1β, TNF-α, and IL-6 was observed in the brains of patients diagnosed with AD (205). The destructive processes including neurodegeneration, gliosis, and progressive neurological disease are mediated by overexpression of IFN-α, TNF-α, IL-1β, or IL-6 (206). Furthermore, treatment with non-steroidal anti-inflammatory drugs (NSAIDs) markedly reduced the prevalence of AD in patients, raising the possibility that an inflammatory environment in the brain has a significant role in the pathogenesis of central nervous system diseases (66).

On the contrary, more recent evidence suggests that acute overexpression of pro-inflammatory mediators are part of a complex pathway to resolve tissue injury (101, 102). For example, neuroprotective effects of pro-inflammatory cytokines, such as promotion of neuronal differentiation and survival, induction of neurotropic factors, and induction of anti-inflammatory mediators, were observed after acute traumatic brain injury (TBI) (207). The beneficial role of cytokines in the pathophysiology of TBI is also supported by animal studies indicating that cytokine knockout mice and cytokine-receptor knockout mice exhibited higher mortality and enhanced tissue damage after experimental TBI (104, 207). In addition, the protective role of pro-inflammatory mediators in the early stages of wound healing has been extensively reported. For example, enhanced production of cytokines (e.g., IL-6, TNF-α, and IL-1β) (105), adhesion

molecules (e.g., ICAM-1 and VCAM-1) (106), chemokines (e.g., MCP-1) (107), and MMPs (e.g., MMP-9) (108) at the wound site promotes healing process of injured brain tissues. These studies provide compelling evidence that the acute induction of pro-inflammatory mediators in brain is an essential part of a pathway that induces a protective response to brain injury.

5.6 Conclusions

In conclusion, the present study demonstrated for the first time that whole brain irradiation-induced acute inflammatory responses, including overexpression of pro-inflammatory cytokines (e.g., TNF-α, IL-1β, and IL-6), adhesion molecules (e.g., ICAM-1, VCAM-1, and E-selectin), the chemokine MCP-1, and MMP-9, in rat brain are significantly impaired in aged animals. The impaired response to irradiation with age appears to reveal a generalized attenuation of the cellular response to damage and a reduced capacity of aging tissues to induce essential repair systems necessary for cellular maintenance. Additionally, these data contribute to a better understanding of age-dependent changes in radiation-mediated immune and inflammatory responses in brain and may lead to the development of effective treatment strategies for brain tumor patients who are undergoing radiation therapy.

5.7 Acknowledgments

The project described was supported by Grant Number R01NS056218 from the National Institute of Neurological Disorders and Stroke.

CHAPTER 6:

IRRADIATION ALTERS MMP-2/TIMP-2 SYSTEM AND COLLAGEN TYPE IV DEGRADATION IN BRAIN

***Lee WH**, Warrington JP, Sonntag WE, Lee YW. *International Journal of Radiation Oncology Biology Physics*, 2010; Submitted on July, 2010.

IRRADIATION ALTERS MMP-2/TIMP-2 SYSTEM AND COLLAGEN TYPE IV DEGRADATION IN BRAIN

6.1 Abstract

Purpose: Blood-brain barrier (BBB) disruption is one of major consequences of radiation-induced tissue injury in the central nervous system. In the present study, we examined the effects of whole brain irradiation on matrix metalloproteinases (MMPs)/tissue inhibitors of metalloproteinases (TIMPs) and extracellular matrix (ECM) degradation in the brain.

Methods and Materials: Animals received either whole brain irradiation (a single dose of 10Gy γ-rays for rats or a fractionated dose of 40Gy γ-rays total for mice) or sham-irradiation, and were maintained for 4, 8, and 24 h following irradiation. The mRNA expression levels of MMPs and TIMPs in the brain were analyzed by real-time reverse transcriptase-polymerase chain reaction (RT-PCR). The functional activity of MMPs was measured by *in situ* zymography and degradation of ECM was visualized by collagen type IV immunofluorescence staining.

Results: A significant increase in mRNA expression levels of MMP-2, MMP-9, and TIMP-1 was observed in irradiated brains compared to sham-irradiated controls. *In situ* zymography revealed a strong gelatinolytic activity in the brain 24 h post-irradiation and the enhanced gelatinolytic activity mediated by irradiation was significantly attenuated in the presence of anti-MMP-2 antibody. A significant reduction in collagen type IV immunoreactivity was also detected in the brain at 24 h after irradiation. In contrast, the levels of collagen type IV were not significantly changed at 4 and 8 h after irradiation compared with the sham-irradiated controls.

Conclusion: The present study demonstrates for the first time that radiation induces an imbalance between MMP-2 and TIMP-2 levels and suggests that degradation of collagen type IV, a major ECM component of BBB basement membrane, may have a role in the pathogenesis of brain injury.

Key words: *Whole brain irradiation; MMPs; TIMPs; ECM; collagen type IV*

6.2 Introduction

Radiation therapy continues to be a main treatment modality in the therapeutic management of brain tumors (208, 209). About 200,000 individuals are treated with either partial large field or whole brain irradiation every year in the United States (210). The use of radiotherapy for treatment of brain tumors, however, is limited by the risk of radiation-induced injury to normal brain tissue that can subsequently lead to devastating functional deficits several months to years after treatment (1, 3). Recent randomized, prospective trials also provide evidence that the addition of whole brain radiation therapy to stereotactic radiosurgery may cause a significant reduction in learning and memory in patients with brain metastasis (4). At present, there is sparse information on the etiology of radiation-induced damage to normal tissue in brain.

The extracellular matrix (ECM) is a complex of various proteins and proteoglycans, including collagens, laminin, fibronectin, and tenascin, which constitute the basal lamina of the blood-brain barrier (BBB) (131). Besides acting as a physical barrier to the passage of macromolecules and cells, ECM separates adjacent tissues, provides mechanical support for cell attachment, and serves as a substratum for cell migration and a medium of communication between cells (129, 131). A number of previous studies have demonstrated that degradation and consequent rearrangement of ECM are critically involved in the breakdown of the BBB (132-134). Despite a crucial role for ECM degradation in the BBB breakdown, the involvement of ECM remodeling in the pathophysiology of radiation-induced brain injury has not yet been investigated.

Matrix metalloproteinases (MMPs), a large family of ECM-degrading enzymes, have been implicated in the pathophysiological processes of neurodegenerative diseases by causing BBB disruption (137, 138). The potential role of MMPs in brain injury in response to irradiation, however, remains largely unknown while evidence demonstrates that MMPs are associated with radiation-induced damage to various other tissues (138, 140-142).

In the present study, we examined the critical role of MMPs in radiation-induced ECM degradation in brain to define the molecular mechanisms of BBB disruption and subsequent brain injury by whole brain irradiation. Our results provide the first novel evidence to demonstrate that MMP-2 plays a pivotal role in radiation-induced ECM degradation in brain.

6.3 Methods and Materials

6.3.1 Animals

Fisher 344-Brown Norway (F344×BN) male rats and C57BL/6 male mice were purchased from Harlan Laboratories (Indianapolis, IN) and Jackson Laboratory (Bar Harbor, ME), respectively. Animals were housed on a 12/12 light-dark cycle with food and water provided *ad libitum*. Animal care was conducted in accordance with the NIH Guide for the Care and Use of Laboratory Animals and this study was approved by the Institutional Animal Care and Use Committee.

6.3.2 Whole Brain Irradiation and Tissue Sample Preparation

A single dose of whole brain irradiation procedure was carried out as described previously (171). For this procedure, rats were anesthetized by ketamine/xylazine (i.p., 80/12 mg/kg) and received a single dose of 10Gy (dose rate of 4.23Gy/min) using a ^{137}Cs γ-irradiator. Control rats were anesthetized but not irradiated. The animals were maintained for 4, 8, and 24 h post-irradiation. For real-time reverse transcriptase-polymerase chain reaction (RT-PCR), the rat brains were rapidly removed and two different brain regions (hippocampus and cortex) were dissected and immediately frozen in liquid nitrogen. For immunofluorescence staining and *in situ* zymography, the whole brains were rapidly removed after perfusion and immediately frozen in liquid nitrogen.

Fractionated whole brain irradiation was performed in mice as described previously (39). Briefly, mice were anesthetized by ketamine/xylazine (i.p., 20/3 mg/kg) and received a clinical fractionated dose of whole brain irradiation (total cumulative dose of 40Gy in eight fractions of

5Gy, twice a week for four weeks) using a ^{137}Cs γ-irradiator. Mice in the control group were only anesthetized. The mice were maintained for 4, 8, and 24 h after the last fractionated dose of whole brain irradiation. The mouse brains were rapidly removed after perfusion and hemisected at the midline. Brains were then immediately frozen in liquid nitrogen.

6.3.3 Real-Time Reverse Transcriptase-Polymerase Chain Reaction (RT-PCR)

Quantitative real-time RT-PCR using TaqMan® probes and primers (Applied Biosystems, Foster City, CA) were employed for gene expression analyses as described previously (171). Amplification of individual genes was performed on the Applied Biosystems 7300 Real-Time PCR System using TaqMan® Universal PCR Master Mix and a standard thermal cycler protocol. TaqMan® Gene Expression Assay Reagents for rat MMP-2, rat MMP-3, rat MMP-7, rat MMP-9, rat MMP-10, rat MMP-12, rat TIMP-1, rat TIMP-2, rat glyceraldehyde-3-phosphate dehydrogenase (GAPDH), mouse MMP-2, mouse TIMP-2, and mouse GAPDH were used for specific probes and primers of PCR amplifications. The threshold cycle (C_T) was determined and relative quantification was calculated by the comparative C_T method as described previously (171).

6.3.4 In Situ Zymography

To detect and localize net gelatinolytic activity of MMPs in brain sections, *in situ* zymography was carried out as described previously (211). Briefly, 100 μg/ml fluorescein-conjugated DQ gelatin (Molecular Probes, Eugene, OR) was mixed with 0.2 % agarose melted in reaction buffer at pH 7.6 (50 mM Tris-HCl, pH 7.5, 0.15M NaCl, 5 mM $CaCl_2$ and 0.2 mM sodium azide). The brain sections (20 μm) were incubated with the reaction mixture prepared above for 24 h at 37 °C in a moist dark chamber. The sections were then briefly washed with ice cold PBS and distilled water. Slides were mounted in Vectashield mounting medium (Vector Laboratories, Burlingame, CA) and examined using a Zeiss AXIO Imager A1m fluorescence microscope (Carl Zeiss MicroImaging, Thornwood, NY). Negative controls were prepared by incubation of tissue sections with non-immune rabbit serum (normal rabbit-IgG, Santa Cruz Biotechnology, Santa Cruz, CA) instead of the primary antibody, and rabbit anti-MMP-2 and

rabbit anti-MMP-9 polyclonal antibodies (Santa Cruz Biotechnology) were added to the reaction to inhibit metalloproteinase activities. Images were acquired with 200× objective by AxioCam MRc5 Digital Imaging System. The MMP activity of acquired digital images was quantified with ImageJ software (NIH, Bethesda, MD).

6.3.5 Immunofluorescence Staining

The brain sections (20-μm) were fixed in 4 % paraformaldehyde for 15 min at room temperature, rinsed with PBS, and incubated in 0.5% Triton X-100 for 15 min. After washing with PBS, the non-specific binding sites were blocked with 3 % bovine serum albumin (BSA) in PBS for 1 h at room temperature, followed by incubation with the primary antibody, goat anti-collagen type IV antibody (Southern Biotechnology, Birmingham, AL) diluted 1/500 in 1.5 % BSA, overnight at 4 °C. Sections were washed with PBS and incubated with secondary antibody, bovine anti-goat IgG conjugated with Texas Red (Santa Cruz Biotechnology), diluted 1/100 in PBS in the dark for 1 h. After washing with PBS, the sections were mounted in Vectashield mounting medium and examined using a Zeiss AXIO Imager A1m fluorescence microscope. Images were acquired with 100× objective by AxioCam MRc5 Digital Imaging System. The fluorescence intensity of acquired digital images was quantified by ImageJ software.

6.3.6 Statistical Analysis

The statistical analysis of data was completed using SigmaStat 3.5 (SPSS, Chicago, IL). One-way analysis of variance (ANOVA) was used to compare mean responses among the treatments. For each endpoint, the treatment means were compared using the Bonferroni least significant difference procedure. Statistical probability of $p<0.05$ was considered significant.

6.4 Results

6.4.1 A Single Dose of Whole Brain Irradiation Up-regulates mRNA Expression of MMP-2, MMP-9, and TIMP-1 in Rat Brain

To examine whether a single dose of whole brain irradiation affects the MMPs/TIMPs system in brain, the mRNA expression levels of MMP-2, MMP-3, MMP-7, MMP-9, MMP-10, MMP-12, TIMP-1, and TIMP-2 were determined by quantitative real-time RT-PCR. As indicated in **Figure 6.1A**, a significant up-regulation of MMP-2 mRNA expression was observed at 24 h post-irradiation in hippocampus (3.1-fold induction) and 8 and 24 h post-irradiation in cortex (3.0-fold and 6.4-fold) collected from irradiated rats compared to the sham-irradiated controls. In addition, a single dose of whole brain irradiation significantly increased mRNA expression levels of MMP-9 in hippocampus (1.6-fold at 4 h, 2.8-fold at 8 h, and 1.7-fold at 24 h post-irradiation) and cortex (1.9-fold at 8 h post-irradiation) (**Figure 6.1B**). In contrast, irradiation did not alter mRNA expression levels of MMPs-3, -7, -10, and -12 (data not shown). Furthermore, irradiation significantly up-regulated mRNA expression of TIMP-1 (**Figure 6.1C**), a specific endogenous inhibitor of MMP-9, in hippocampus and cortex at 4 h (9.2-fold and 5.5-fold), 8 h (16-fold and 7.9-fold), and 24 h (15-fold and 6.1-fold) post-irradiation, while the mRNA expression of TIMP-2, a specific endogenous inhibitor of MMP-2, was not affected by irradiation (**Figure 6.1D**). These results suggest that irradiation differentially regulates MMPs/TIMPs system in brain.

6.4.2 A Single Dose of Whole Brain Irradiation Enhances the Gelatinase Activity of MMPs in Rat Brain

To determine whether irradiation-mediated increases in MMP-2 and MMP-9 mRNA levels translate to elevated protein expression and functional activity, the histological distribution of the gelatinase activity was determined by *in situ* zymography using FITC-labeled DQ-gelatin. As illustrated in **Figure 6.2**, a strong gelatinolytic activity was observed in rat brains 24 h after irradiation, whereas very little activity was detected in sham-irradiated control rat brains as well as in brains 4 and 8 h post-irradiation (**Figure 6.2A-6.2D**). Quantitative analysis also demonstrated a significant increase in gelatinase activity in brains 24 h after irradiation compared to the sham-irradiated control rat brains (**Figure 6.2E**). In addition, anti-rat MMP-2 and MMP-9 neutralizing antibodies were employed to further elucidate the critical role of either MMP-2 or MMP-9 in radiation-induced gelatinase activity. These antibodies were selected for their abilities to neutralize the biological activity of MMP-2 and MMP-9, respectively. As shown

in **Figure 6.3**, enhanced gelatinase activity in irradiated brain was significantly attenuated in the presence of MMP-2 neutralizing antibody (**Figure 6.3B** and **6.3E**). Interestingly, incubation with MMP-9 neutralizing antibody (**Figure 6.3C** and **6.3E**) and normal non-immune IgG (negative control, **Figure 6.3D**) did not exert any significant effects on radiation-induced gelatinolytic activity. These data demonstrate that irradiation-induced MMP-2 expression is critically involved in enhanced gelatinase activity in brain.

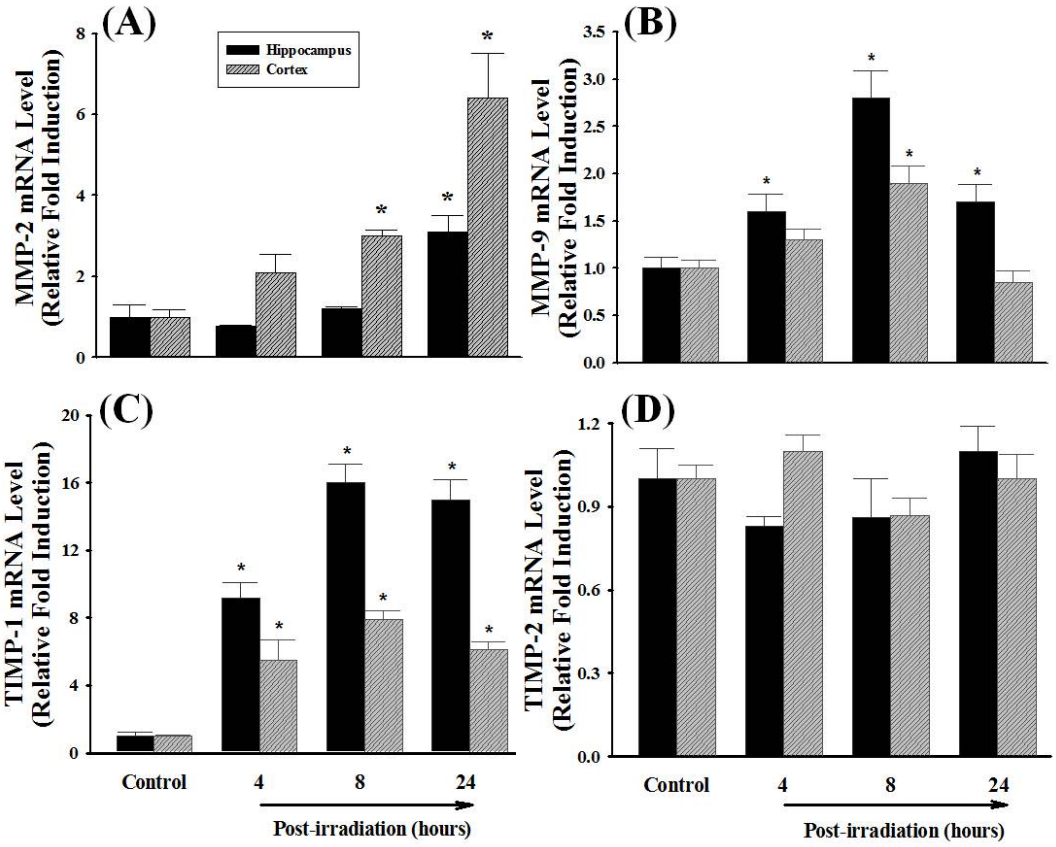

Figure 6.1. Effect of a Single Dose of Whole Brain Irradiation on mRNA Expression of MMPs and TIMPs in Rat Brain. Compared with sham-irradiated controls, a single dose of whole brain irradiation up-regulated mRNA expression of MMP-2 (A), MMP-9 (B), and TIMP-1 (C) in hippocampus and cortex, while the mRNA expression of TIMP-2 (D) was not affected by irradiation. Data shown are mean ± SEM for each group (n=4). *Statistically significant from control ($p<0.05$).

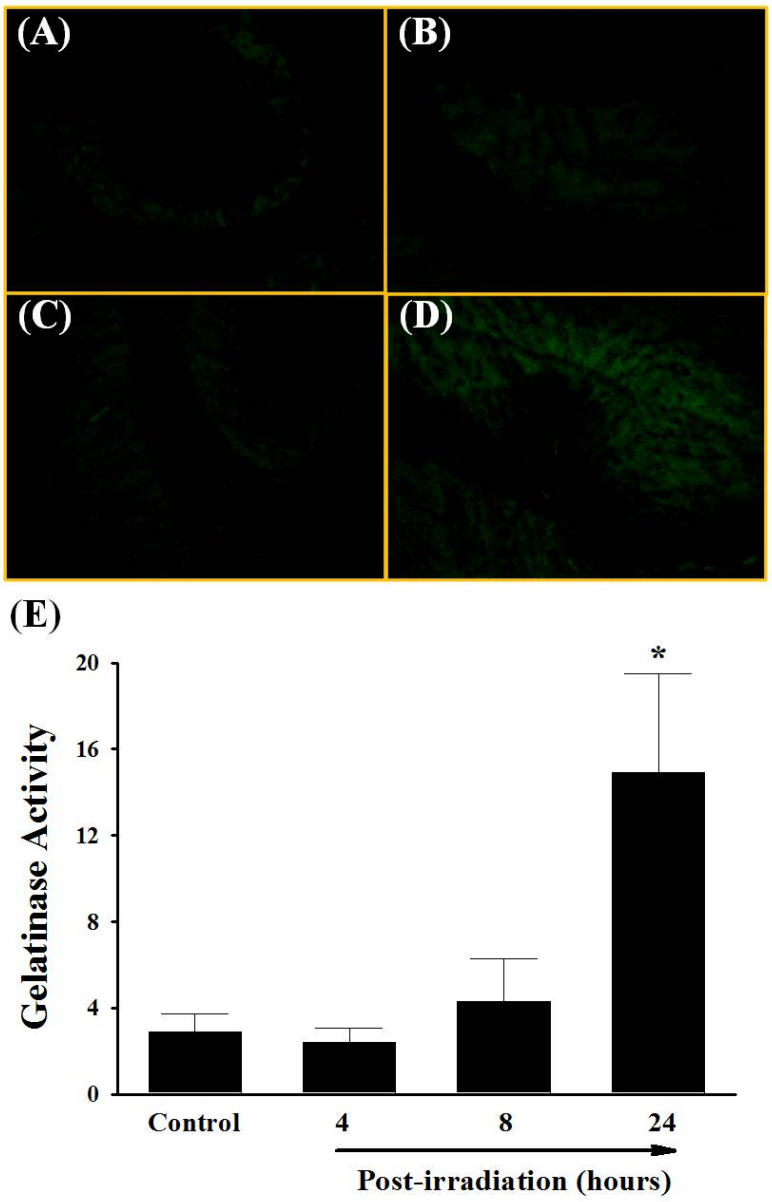

Figure 6.2. Effect of a Single Dose of Whole Brain Irradiation on Gelatinase Activity in Rat Brain. A: sham-irradiation (Control); B: 4 h post-irradiation; C: 8 h post-irradiation; D: 24 h post- irradiation; E: quantitative analysis of fluorescence intensity. The localization of green fluorescence indicates gelatinolytic activity of MMPs in rat brain (A-D). Quantitative analysis indicated a significant increase in gelatinase activity in brain 24 h after whole brain irradiation compared to sham-irradiated controls (E). Magnification of the images (A-D) is 200×. Data shown are mean ± SEM for each group (n=4). *Statistically significant from control ($p<0.05$).

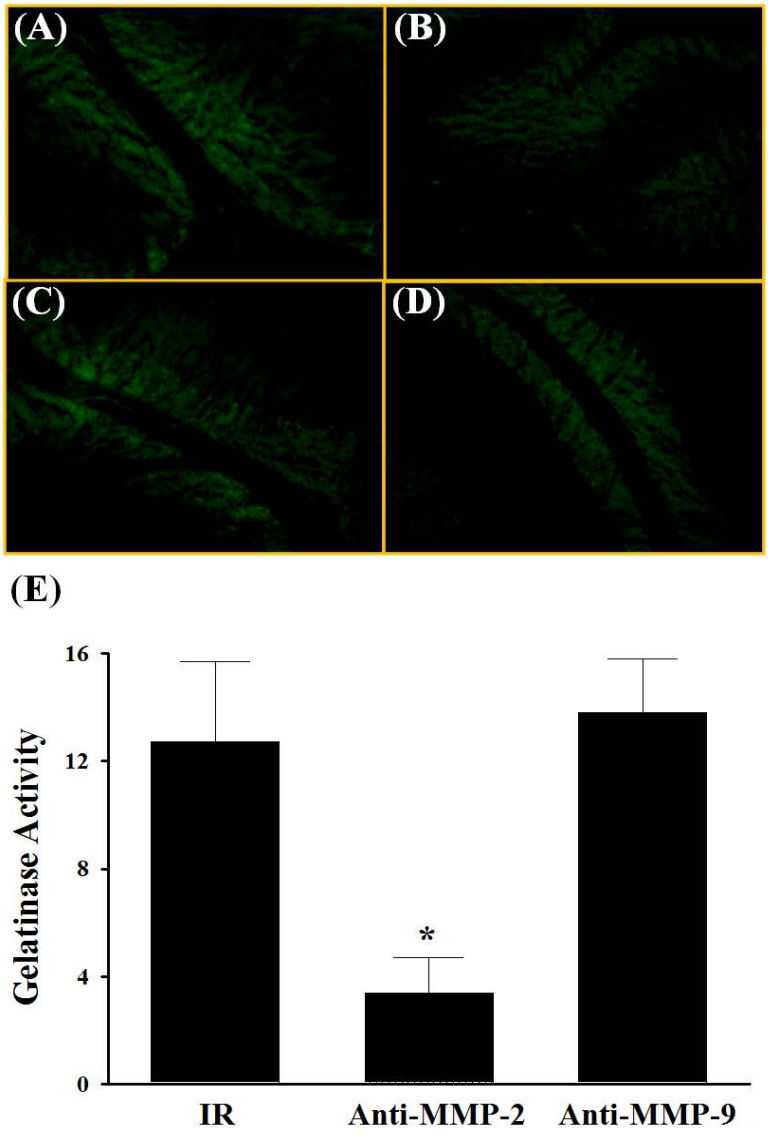

Figure 6.3. Effect of MMP-2 and MMP-9 Neutralizing Antibodies on Radiation-Induced Gelatinase Activity in Rat Brain. A: 24 h post-irradiation; B: 24 h post-irradiation with anti-MMP-2 antibody; C: 24 h post-irradiation with anti-MMP-9 antibody; D: 24 h post-irradiation with normal non-immune IgG; E: quantitative analysis of fluorescence intensity. The localization of green fluorescence indicates gelatinolytic activity of MMPs in rat brain (A-D). Enhanced gelatinase activity in brains 24 h after a single dose of whole brain irradiation (IR) was significantly attenuated in the presence of MMP-2 neutralizing antibody (Anti-MMP-2) (E). Magnification of the images (A-D) is 200×. Data shown are mean ± SEM for each group (n=4). *Statistically significant from irradiated brain ($p<0.05$).

6.4.3 A Single Dose of Whole Brain Irradiation Degrades ECM in Rat Brain

To investigate whether a single dose of whole brain irradiation mediates degradation of ECM, the expression levels of collagen type IV, one of the major ECM components of BBB basement membrane, in brains were visualized by immunofluorescence staining. As illustrated in **Figure 6.4**, a significant reduction in collagen type IV immunoreactivity was detected in brains 24 h after irradiation compared with sham-irradiated control brains. In contrast, the expression levels of collagen type IV were not significantly changed in rat brains 4 and 8 h after irradiation.

6.4.4 Fractionated Whole Brain Irradiation Mediates Induction of MMP-2 mRNA Expression, Increase in Gelatinase Activity, and Degradation of ECM in Mouse Brain

In addition to a single dose of whole brain irradiation, the present study also examined the effect of a clinically relevant regimen of fractionated whole brain irradiation on MMP-2 expression and ECM degradation in brains from mice. Quantitative real-time RT-PCR showed that irradiation resulted in a significant up-regulation of MMP-2 mRNA expression in mouse brains at 4, 8, and 24 h after the completion of a fractionated dose of whole brain irradiation. Specifically, the mRNA expression levels of MMP-2 in mouse brains were increased by 2.1-fold at 4 h, 2.2-fold at 8 h, and 2.1-fold at 24 h after irradiation (**Figure 6.5A**). In contrast, fractionated whole brain irradiation did not affect mRNA expression levels of TIMP-2 (**Figure 6.5B**). Fractionated whole brain irradiation also significantly increased gelatinase activity by 16.5-fold at 24 h post-irradiation compared to the sham-irradiated control brains (**Figure 6.6A, 6.6B** and **6.6E**). In contrast, radiation-mediated increase in gelatinase activity in the brain was significantly attenuated in the presence of a neutralizing antibody against MMP-2 (**Figure 6.6C** and **6E**). The negative control experiment with normal non-immune IgG did not show any significant effect on gelatinolytic activity in irradiated brain (**Figure 6.6D**). We further examined the effect of fractionated whole brain irradiation on ECM degradation in mouse brain. As depicted in **Figure 6.7**, a significantly reduced collagen type IV immunoreactivity was observed in mouse brain at 24 h after fractionated whole brain irradiation compared with those determined in sham-irradiated controls.

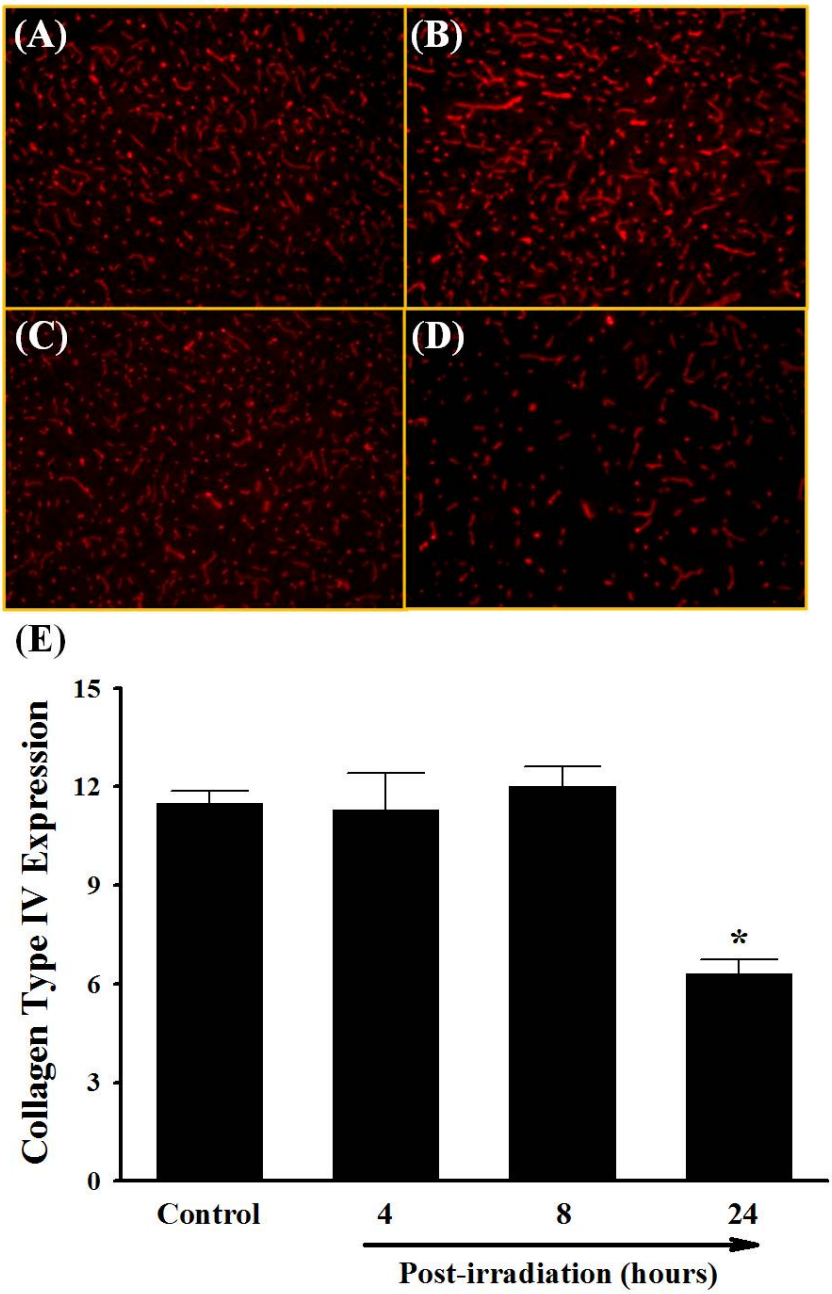

Figure 6.4. Effect of a Single Dose of Whole Brain Irradiation on Collagen Type IV Expression in Rat Brain. A: sham-irradiation (Control); B: 4 h post-irradiation; C: 8 h post-irradiation; D: 24 h post-irradiation; E: quantitative analysis of fluorescence intensity. Immunoreactivity of collagen type IV was visualized in rat brain (A-D). A single dose of whole brain irradiation markedly and significantly reduced the protein expression levels of collagen type IV in rat brains 24 h after irradiation (E). Magnification of the images (A-D) is 100×. Data shown are mean ± SEM for each group (n=4). *Statistically significant from control ($p<0.05$).

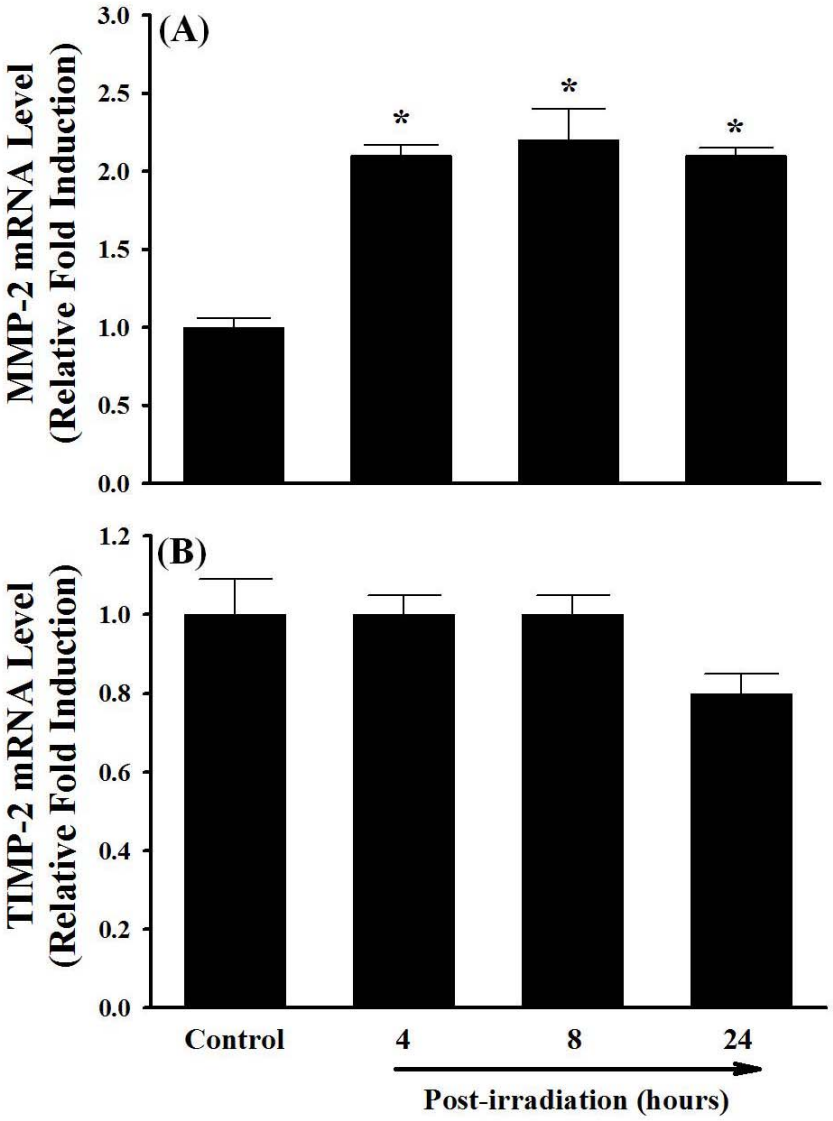

Figure 6.5. Effect of Fractionated Whole Brain Irradiation on mRNA Expression of MMP-2 and TIMP-2 in Mouse Brain. Compared with sham-irradiated controls, fractionated whole brain irradiation up-regulated mRNA expression of MMP-2 (A) in mouse brain, while the expression of TIMP-2 was not affected by irradiation (B). Data shown are mean ± SEM for each group (n=4). *Statistically significant from control ($p<0.05$).

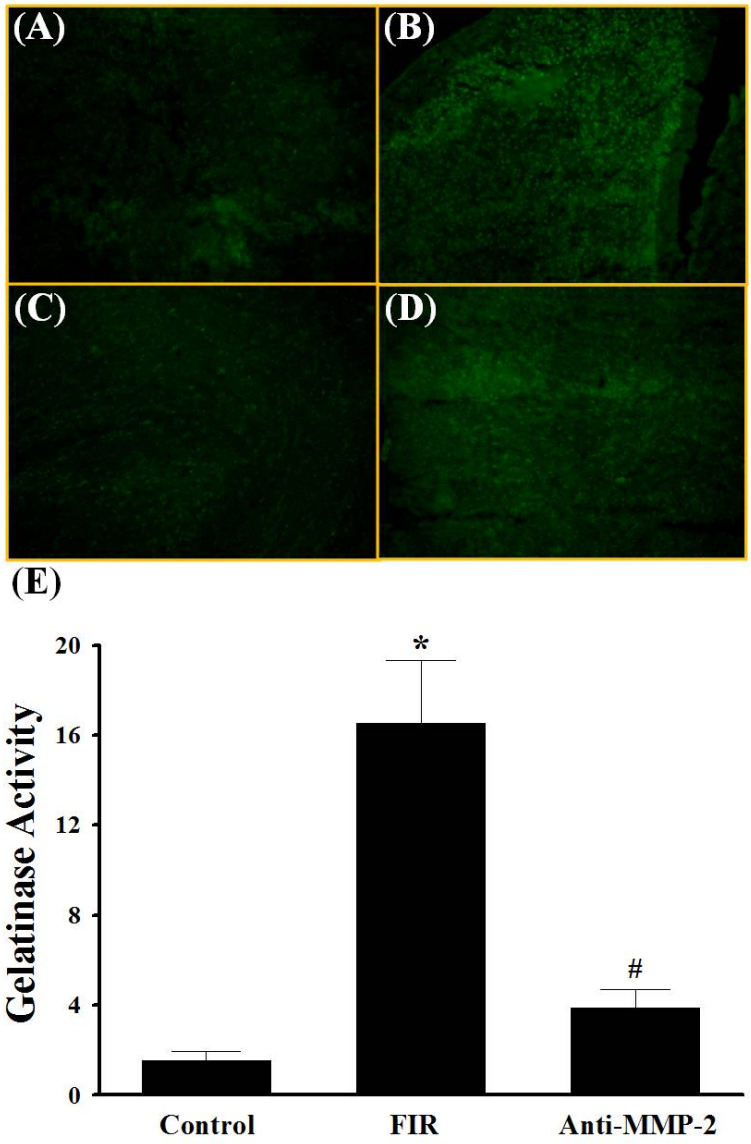

Figure 6.6. Effect of MMP-2 Neutralizing Antibody on Radiation-Induced Gelatinase Activity in Mouse Brain. A: sham-irradiation (Control); B: 24 h post-irradiation; C: 24 h post-irradiation with anti-MMP-2 antibody; D: 24 h post-irradiation with normal non-immune IgG; E: quantitative analysis of fluorescence intensity. The localization of green fluorescence demonstrates the gelatinolytic activities of MMPs in mouse brain (A-D). A significant increase in gelatinase activity in brains 24 h after fractionated whole brain irradiation (FIR) was markedly and significantly attenuated in the presence of MMP-2 neutralizing antibody (Anti-MMP-2) (E). Magnification of the images (A-D) is 200×. Data shown are mean ± SEM for each group (n=4). *Statistically significant from control ($p<0.05$). #Statistically significant from the irradiated brain ($p<0.05$).

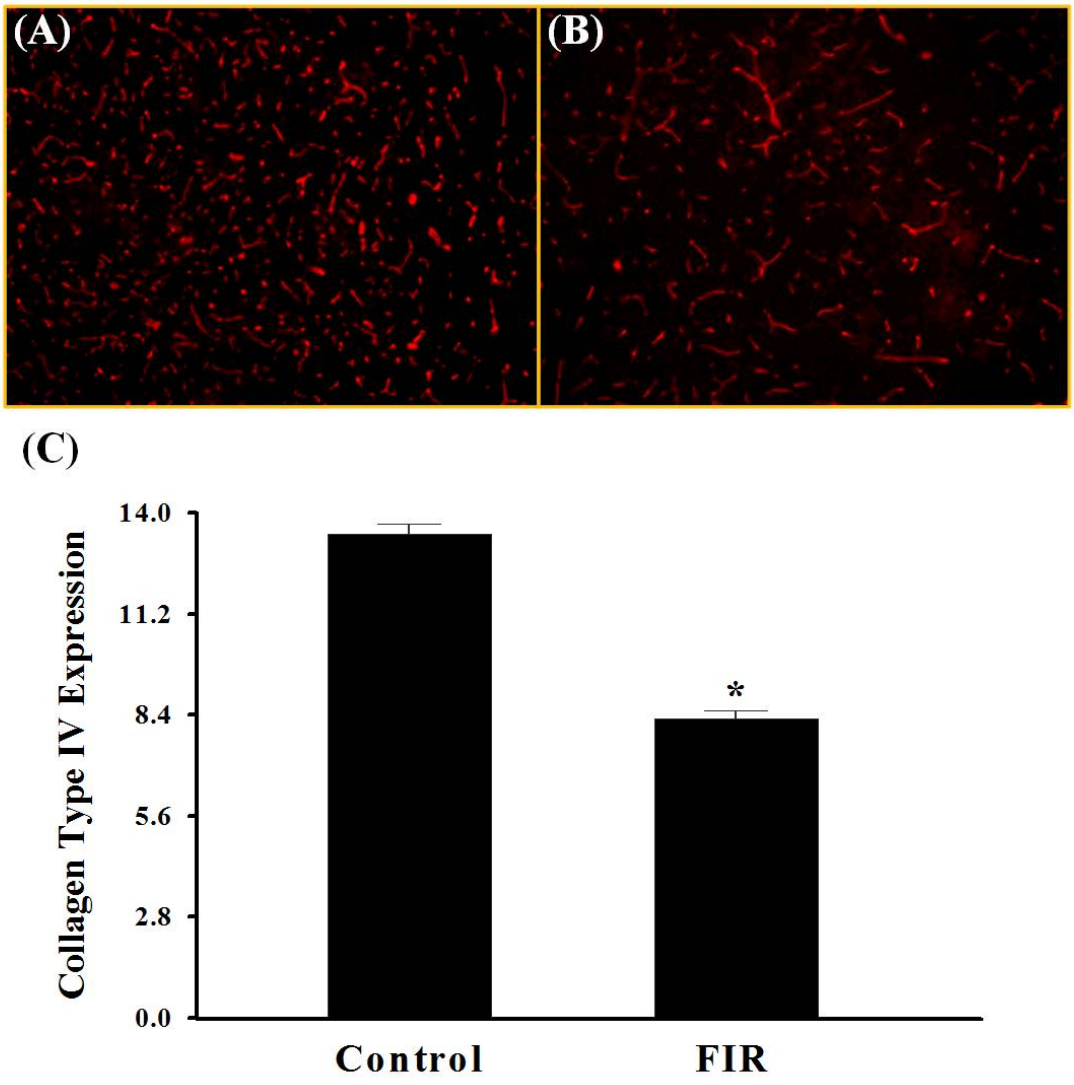

Figure 6.7. Effect of Fractionated Whole Brain Irradiation on Collagen Type IV Expression in Mouse Brain. A: sham-irradiation (Control); B: 24 h post-irradiation; C: quantitative analysis of fluorescence intensity. Immunoreactivity of collagen type IV was visualized in mouse brain (A and B). Fractionated whole brain irradiation significantly reduced the protein expression levels of collagen type IV in brains 24 h after irradiation (FIR) (C). Magnification of the images (A and B) is 100×. Data shown are mean ± SEM for each group (n=4). *Statistically significant from control ($p<0.05$).

6.5 Discussion

The present study provides compelling evidence that whole brain irradiation induces an imbalance between MMPs and TIMPs expression, increases gelatinase activity, and degrades collagen type IV in the brain. Initially, an animal model of whole brain irradiation with a single dose of 10Gy was selected because it is the lowest dose to have a clear radiation effect and is under the threshold for vascular changes, demyelination, or radionecrosis (171). Studies were also conducted after a fractionated dose of whole brain irradiation to assess a clinical relevance (37, 38). A significant and marked decrease in collagen type IV immunoreactivity as well as a strong gelatinase activity was detected in the brain 24 h after irradiation. In addition, an enhanced gelatinolytic activity mediated by irradiation was significantly attenuated in the presence of anti-MMP-2 antibody, highlighting the contribution of MMP-2 to the radiation-induced alterations of ECM components in the brain. To our knowledge, these results demonstrated for the first time that a radiation-induced imbalance between MMP-2 and TIMP-2 expression may have an important role in the pathogenesis of brain injury by degrading ECM components of the BBB basement membrane.

In a variety of physiologic and pathophysiologic conditions, MMPs become activated and play a key role in degradation of the ECM proteins (139). Recent evidence from *in vivo* and *in vitro* studies has identified that ionizing irradiation up-regulates MMPs expression in various tissues. For example, enhanced activity of MMP-2 and MMP-9 was observed in lung after thoracic irradiation (140). Araya *et al.* (141) have reported a significant elevation of MMP-2 production in human airway epithelial cells after irradiation. Additionally, previous clinical studies showed that use of pelvic radiation therapy for prostate cancer patients resulted in significant increases in MMP-2 and MMP-9 activity in rectal mucosa (142). It was also found that abdominal irradiation led to a significant elevation in MMP-2 and MMP-14 levels in rat ileum (138). These findings are also supported by *in vitro* study from Nirmala *et al*. (143) demonstrating that radiation-induced increased expression levels of MMP-2 and MMP-9 may be involved in the alteration of the CNS microvasculature by regulating glial-endothelial cells interaction. Furthermore, our previous study showed that whole brain irradiation significantly up-regulated MMP-9 mRNA expression for all age groups in rat brain (198). Alterations in the

levels of other MMPs after irradiation in normal brain, however, remain to be further investigated. In the present study, we examined effects of whole brain irradiation on various MMPs in brain. MMP-2, MMP-3, MMP-7, MMP-9, MMP-10, and MMP-12 were chosen because previous studies have demonstrated the pivotal role of these MMPs in ECM degradation of the BBB basement membrane such as collagen type IV, laminin, and fibronectin (137, 139).

The enzymatic activity of MMPs is inactivated by TIMPs, the endogenous inhibitors with a higher affinity for specific MMPs (144). For example, TIMP-1 forms a specific complex with MMP-9, whereas MMP-2 is bound by TIMP-2. Therefore, the balance between MMPs and TIMPs is considered necessary for normal homeostasis during periods of development and plasticity in the CNS (133, 134). Since our data demonstrated the selective induction of MMP-2 and MMP-9 in irradiated brains, we further examined the effects of whole brain irradiation on TIMP-1 and TIMP-2 expression in the brain. TIMP-1 mRNA expression was found to up-regulated in the irradiated rat colon while the mRNA level of TIMP-2 was unchanged (147). In lung epithelial cells, radiation increased MMP-2 mRNA but had no effect on TIMP-2 indicating the balance between the MMP-2 and TIMP-2 was in favor of MMP-2 promoting proteolysis (141). Our own data indicate that whole brain irradiation resulted in a significant increase in TIMP-1 mRNA expression in the brain at 4, 8, and 24 h after irradiation. We could speculate that radiation-mediated up-regulation of TIMP-1 expression was counterbalanced by overexpression of MMP-9 in irradiated brain suggesting that the balance of MMP-9/TIMP-1 levels remains unchanged. In contrast, mRNA expression of TIMP-2 was not affected by either a single dose or fractionated whole brain irradiation in the brain. It is possible that the balance in the relative ratio of MMP-2 to TIMP-2 levels was altered in favor of a persistent enzymatic activity of MMP-2. Our data from neutralizing antibody experiment further supports the critical role of MMP-2 in radiation-mediated increase in gelatinase activity.

Even though the present study has demonstrated that irradiation induces MMP-2, MMP-9, and TIMP-1 expression throughout the rat brain, it should be noted that the time course for induction and maximal response were regionally specific. Indeed, the expression levels of MMP-9 and TIMP-1 induced by irradiation were higher in hippocampus whereas the enhanced expression of MMP-2 was detected in irradiated cortex. Similar regional specificity in response

to irradiation was observed in our recent report that irradiation induces regionally specific alterations in pro-inflammatory mediator expression in rat brain (171). These data suggest that elevated levels of specific MMPs and TIMPs within each brain region are unique and may contribute to selective activation of biochemical pathways that contribute to the functional deficiencies after whole brain irradiation although the exact mechanisms of regional specificity of radiation-induced expression of MMPs and TIMPs remain unsolved.

Collagen type IV is the major ECM constituent of the BBB basement membrane and a known substrate of MMP-2 and MMP-9 (141). Previous studies have demonstrated an essential role for collagen type IV degradation in BBB disruption and brain injury. Scholler *et al.* (212) have shown that a significant decrease in microvascular collagen type IV immunoreactivity following subarachnoid hemorrhage is correlated with increased BBB permeability and may be, at least in part, responsible for ischemic brain edema. Additionally, acute loss of basal lamina antigens including collagen type IV during cerebral ischemia/reperfusion injury may offer an explanation for understanding decreased microvascular integrity as well as development of hemorrhagic complications of acute stroke (213). Even though the importance of collagen type IV degradation in BBB disruption and brain injury was suggested previously, the mechanism by which proteases are involved in compromising the integrity of the BBB has not yet been fully understood. Studies from Rosenberg *et al*. (132, 214) provide evidence suggesting the potential role of MMP-2 and collagen type IV in BBB breakdown. These investigators showed that direct intracerebral administration of MMP-2 resulted in an increase in collagen type IV degradation and BBB permeability, and inhibition of MMP-2 (by injection of TIMP-2) prevented BBB disruption. These results support our observations that collagen type IV degradation in the irradiated brain may be mediated through enhanced MMP-2 expression and activity. Further studies using combined pharmacological (e.g., selective MMP-2 inhibitors) and genetic approaches (e.g., MMP-2 knockout mice), however, are needed to elucidate a mechanistic link between MMP-2 expression and collagen type IV degradation in brain after irradiation.

6.6 Conclusions

In conclusion, we provide the first direct evidence indicating that whole brain irradiation mediates degradation of collagen type IV, a major ECM component of the BBB basement membrane, by altering the balance of MMP-2 and TIMP-2 levels in the brain. These findings may contribute to defining a new cellular and molecular basis for radiation-mediated BBB disruption and subsequent brain injury that will lead to new opportunities for preventive and therapeutic interventions for brain tumor patients who are undergoing radiotherapy.

6.7 Acknowledgments

The project described was supported by Grant Number R01NS056218 from the National Institute of Neurological Disorders and Stroke.

CHAPTER 7:

IRRADIATION INDUCES VESSEL RAREFACTION BY DIFFERENTIAL REGULATION OF ANG-1, TIE-2, ANG-2, AND VEGF IN RAT BRAIN

*Lee WH, Warrington JP, Sonntag WE, Lee YW. Irradiation induces vessel rarefaction by differential regulation of Ang-1, Tie-2, Ang-2, and VEGF in rat brain. *International Journal of Radiation Oncology Biology Physics*, 2010; In preparation

7.1 Abstract

Purpose: It has been hypothesized that radiation-induced brain injury is mediated by cerebrovascular rarefaction. The present study was designed to investigate the molecular mechanisms of radiation-induced vessel rarefaction in the brain.

Methods and Materials: Four month old F344×BN rats received either whole brain irradiation with a single dose of 10Gy γ-rays or sham-irradiation, and were maintained for 4, 8, and 24 h following irradiation. A series of immunofluorescence staining was employed to visualize endothelial cell (EC) density, EC proliferation, and EC apoptosis in brain. The mRNA and protein expression levels of angiogenic factors, such as vascular endothelial growth factor (VEGF), angiopoietin-1 (Ang-1), Ang-2, endothelial receptor tyrosine kinase (Tie-2), in brain were determined by real-time reverse transcriptase-polymerase chain reaction (RT-PCR), enzyme-linked immunosorbent assay (ELISA), and immunofluorescence staining.

Results: Significantly reduced levels of CD31-immunoreactive cells were detected in irradiated rat brains compared with sham-irradiated controls, indicating that whole brain irradiation decreases EC density in the brain. Double immunofluorescence staining also revealed that whole brain irradiation significantly suppressed EC proliferation and increased EC apoptosis in rat brain. In addition, a significant decrease in mRNA and protein expression of Ang-1, Tie-2, and VEGF was observed in irradiated rat brains compared with sham-irradiated controls. However, whole brain irradiation significantly up-regulated Ang-2 expression in rat brain.

Conclusion: The present study provides the novel evidence that whole brain irradiation differentially regulates expression of Ang-1, Tie-2, Ang-2 and VEGF, which may affect vessel rarefaction by decreasing EC proliferation and increasing EC apoptosis in brain.

Key words: *Whole brain irradiation; VEGF; Ang-1; Ang-2; Tie-2; vessel rarefaction*

7.2 Introduction

Radiation therapy has been commonly used as the standard treatment for brain tumors. Approximately 200,000 patients with brain tumors are treated with either partial large field or whole brain irradiation each year in the United States (215). On the other hand, whole brain irradiation therapy may cause a significant reduction in learning and memory in brain tumor patients as long-term consequences of treatment (1, 3, 4). Although a number of *in vitro* and *in vivo* studies have demonstrated the pathogenesis of radiation-mediated brain injury (3, 38, 61, 171, 216), the cellular and molecular mechanisms by which irradiation induces brain injury remain largely unknown.

Vessel rarefaction, defined as a decrease in vascular density, has been implicated in the onset and progression of various pathological processes (17-19). Previous studies have shown that irradiation induces both acute and late changes in the vasculature (20-22). For example, Ljubimova et al. (20) found a decrease in endothelial cell (EC) density in rat brain within 24 h after large single doses of irradiation. In addition, an initial marked decline and a subsequent slow loss of EC number were observed after 24 h and between 26 and 52 weeks after a single dose of X-rays to the rat brain, respectively (160). Furthermore, a substantial decrease in vessel density and length was detected in irradiated rat brains 10 weeks after fractionated whole brain irradiation (38). These studies provide robust evidence indicating that radiation-induced early and persistent damages to the microvasculature may be responsible for vessel rarefaction leading to the late delayed brain injury. The molecular mechanisms of radiation-induced vessel rarefaction in the brain, however, remain to be further investigated.

Regulation of vascular system is characterized by a dynamic temporally and spatially coordinated interaction of vasculogenesis, angiogenesis, and vessel regression (217, 218). Under physiological conditions, a controlled balance between vascular endothelial growth factor (VEGF), a prototypical angiogenesis factor, and a new class of angiogenic regulators, such as angiopoietin-1 (Ang-1), Ang-2, and Tie-2, is essential for stable vascular endothelium. The potential contribution of these angiogenic factors to the radiation-induced vessel rarefaction in brain, however, has not yet been explored.

In the present study, we examined the molecular mechanisms of radiation-induced vessel rarefaction in rat brain. Our results demonstrated for the first time that differential regulation of Ang-1, Ang-2, Tie-2, and VEGF may be responsible for a decrease in EC proliferation and an increase in EC apoptosis in irradiated brain.

7.3 Methods and Materials

7.3.1 Animals

Fisher 344-Brown Norway (F344×BN) male rats were purchased from Harlan Laboratories (Indianapolis, IN), and housed on a 12/12 light-dark cycle with food and water provided *ad libitum*. Animal care was conducted in accordance with the NIH Guide for the Care and Use of Laboratory Animals and this study was approved by the Institutional Animal Care and Use Committee.

7.3.2 Whole Brain Irradiation and Tissue Sample Preparation

A single dose of whole brain irradiation procedure was carried out as described previously with minor modifications (171). Briefly, whole brain irradiation was performed in a ^{137}Cs γ-irradiator using lead and Cerrobend shielding devices to collimate the beam so that the whole rat brain, including the brain stem, was irradiated. Rats were anesthetized by ketamine/xylazine (i.p., 80/12 mg/kg body weight) and received 10Gy at an average dose rate of 4.23Gy/min. Control rats were anesthetized but not irradiated. The animals were maintained for 4, 8, and 24 h post-irradiation. For real-time reverse transcriptase-polymerase chain reaction (RT-PCR), the rat brains were rapidly removed and two different brain regions (hippocampus and cortex) were dissected, and then immediately frozen in liquid nitrogen. For immunofluorescence staining, the whole brains were rapidly removed after perfusion and immediately frozen in liquid nitrogen.

7.3.3 Real-time RT-PCR

Quantitative real-time RT-PCR using TaqMan® probes and primers (Applied Biosystems, Foster City, CA) were employed for gene expression analyses as described previously (171). Amplification of individual genes was performed on the Applied Biosystems 7300 Real-Time PCR System using TaqMan® Universal PCR Master Mix and a standard thermal cycler protocol. TaqMan® Gene Expression Assay Reagents for rat Ang-1, Tie-2, Ang-2, VEGF, and glyceraldehydes-3-phosphate dehydrogenase GAPDH (housekeeping gene) were used for specific probes and primers of PCR amplifications. The threshold cycle (C_T) was determined and relative quantification was calculated by the comparative C_T method as described previously (171).

7.3.4 Enzyme-Linked Immunosorbent Assay (ELISA)

Tissue homogenates from rat brain were prepared as described previously (171). Briefly, both hippocampus and cortex were homogenized in 1 ml of ice-cold PBS and stored overnight at -80 ºC. After three freeze-thaw cycles were performed, the homogenates were centrifuged for 5 min at 5,000 × g at 4 ºC. Supernatants were frozen immediately on dry ice and stored at -80 °C until analysis. Protein concentrations of brain tissue homogenates were determined as described by Bradford (176). The protein expression levels of VEGF in brain tissue homogenates were determined by using Quantikine® VEGF Immunoassay Kit following to the manufacturer's protocols (R&D Systems, Minneapolis, MN).

7.3.5 Immunofluorescence Staining

Freshly excised brains were embedded in Tissue-Tek O.C.T. compound (*Sakura* Finetek USA Inc., Torrance, CA) and stored at -80 °C. Frozen tissues were cut into 20-µm sections using a Microm HM 550 cryostat (MICROM International GmbH, Walldorf, Germany) and mounted on Superfrost/Plus microscope slides (Fisher Scientific, Pittsburgh, PA). The brain sections were then fixed in 4 % paraformaldehyde for 15 min at room temperature, rinsed with PBS three times for 5 min each, and incubated in 0.5 % Triton X-100 for 15 min to permeabilize tissues for optimal staining. After washing with PBS three times, the sections were then incubated with 3 % bovine serum albumin (BSA) in PBS for 1 h at room temperature to block non-specific binding

of the antibodies, followed by incubation with the primary antibody, such as goat anti-Ang-1 polyclonal antibody, goat anti-Ang-2 polyclonal antibody, or rabbit anti-Tie-2 polyclonal antibody (Santa Cruz Biotechnology, Santa Cruz, CA) diluted 1/500 in 1.5 % BSA, overnight at 4 °C. Sections were washed three times with PBS and incubated with secondary antibody, such as donkey anti-goat IgG conjugated with Alexa Fluor 488 or goat anti-rabbit IgG conjugated with Alexa Fluor 555 (Invitrogen, Carlsbad, CA) diluted 1/400 in PBS in the dark for 1 h. After washing three times with PBS, the sections were mounted in Vectashield Mounting Medium (Vector Laboratories Inc, Burlingame, CA) and sealed with a coverslip. The slides were examined on a Zeiss AXIO Imager A1m fluorescence microscope (Carl Zeiss MicroImaging, Inc., Thornwood, NY). Images were acquired with 100× objective by AxioCam MRc5 Digital Imaging System. The fluorescence intensity of acquired digital images was quantified by Image J Software.

7.3.6 Double Immunofluorescence Staining

For the detection of EC proliferation, rat brain sections were stained with rabbit monoclonal anti-Ki67 antibody (cell proliferation marker; Abcam, Cambridge, MA) and mouse monoclonal anti-CD31 antibody (EC marker; BD Pharmingen, San Jose, CA) followed by Alexa Fluor 555-conjugated goat anti-rabbit IgG and Alexa Fluor 488-conjugated donkey anti-mouse IgG (Invitrogen), respectively. For the detection of EC apoptosis, rat brain sections were incubated with rabbit polyclonal anti-cleaved caspase-3 antibody (apoptotic cell marker; Cell Signaling Technology, Inc., Danvers, MA) and mouse monoclonal anti-CD31 antibody before staining with secondary antibodies such as Alexa Fluor 555-conjugated goat anti-rabbit IgG and Alexa Fluor 488-conjugated donkey anti-mouse IgG. After washing three times with PBS, the sections were mounted in Vectashield mounting medium and sealed with a coverslip. The slides were examined on a Zeiss AXIO Imager A1m fluorescence microscope. Images were acquired with 100× objective by AxioCam MRc5 Digital Imaging System. The fluorescence intensity of acquired digital images was quantified by ImageJ software (NIH, Bethesda, MD).

7.3.7 Statistical Analysis

Routine statistical analysis of data was completed using SigmaStat 3.5 (SPSS Inc., Chicago, IL). One-way analysis of variance (ANOVA) was used to compare mean responses among the treatments. For each endpoint, the treatment means were compared using Bonferroni least significant difference procedure. Statistical probability of $p<0.05$ was considered significant.

7.4 Results

7.4.1 Effect of Whole Brain Irradiation on EC Density, EC Proliferation, and EC Apoptosis in Rat Brain

A series of immunofluorescence staining for CD31, a specific marker for EC, were performed to investigate whether whole brain irradiation affects EC density in brain. Significantly reduced levels of CD31-immunoreactive cells were detected in irradiated rat brains compared with sham-irradiated controls (**Figures 7.1** and **7.2**), indicating that whole brain irradiation decreases EC density in brain. To elucidate the potential mechanisms of a decrease in EC density in irradiated brain, EC proliferation and EC apoptosis were measured. Double immunofluorescence staining for CD31 (EC marker) and for Ki67 (cell proliferation marker) was performed to identify proliferating EC in brain. Large numbers of double-immunoreactive cells (proliferating EC) were observed in sham-irradiated control brains (**Figure 7.1C**). The number of proliferating EC, however, decreases dramatically in rat brains 4 and 8 h after irradiation (**Figure 7.1F** and **7.1I**) and barely proliferating EC were detectable in 24 h post-irradiated rat brains (**Figure 7.1L**). In addition, double immunofluorescence staining for CD31 (EC marker) and for cleaved caspase-3 (apoptotic cell marker) was conducted to measure apoptotic EC in brain. In sham-irradiated control brains, the colocalization of CD31 and cleaved caspase-3 (apoptotic EC) was sparsely detected (**Figure 7.2C**). In contrast, more apoptotic EC were observed in rat brains 4 h after irradiation (**Figure 7.2F**) and maintained at maximum levels 8 and 24 h post-irradiation (**Figure 7.2I** and **7.2L**). Quantitative analysis further confirmed that whole brain irradiation significantly decreased EC proliferation (**Figure 7.1M**) and increased EC apoptosis (**Figure 7.2M**) in rat brain. These results suggest that irradiation-induced decrease in EC proliferation and increase in EC apoptosis may be responsible for a decrease in EC density in irradiated brain.

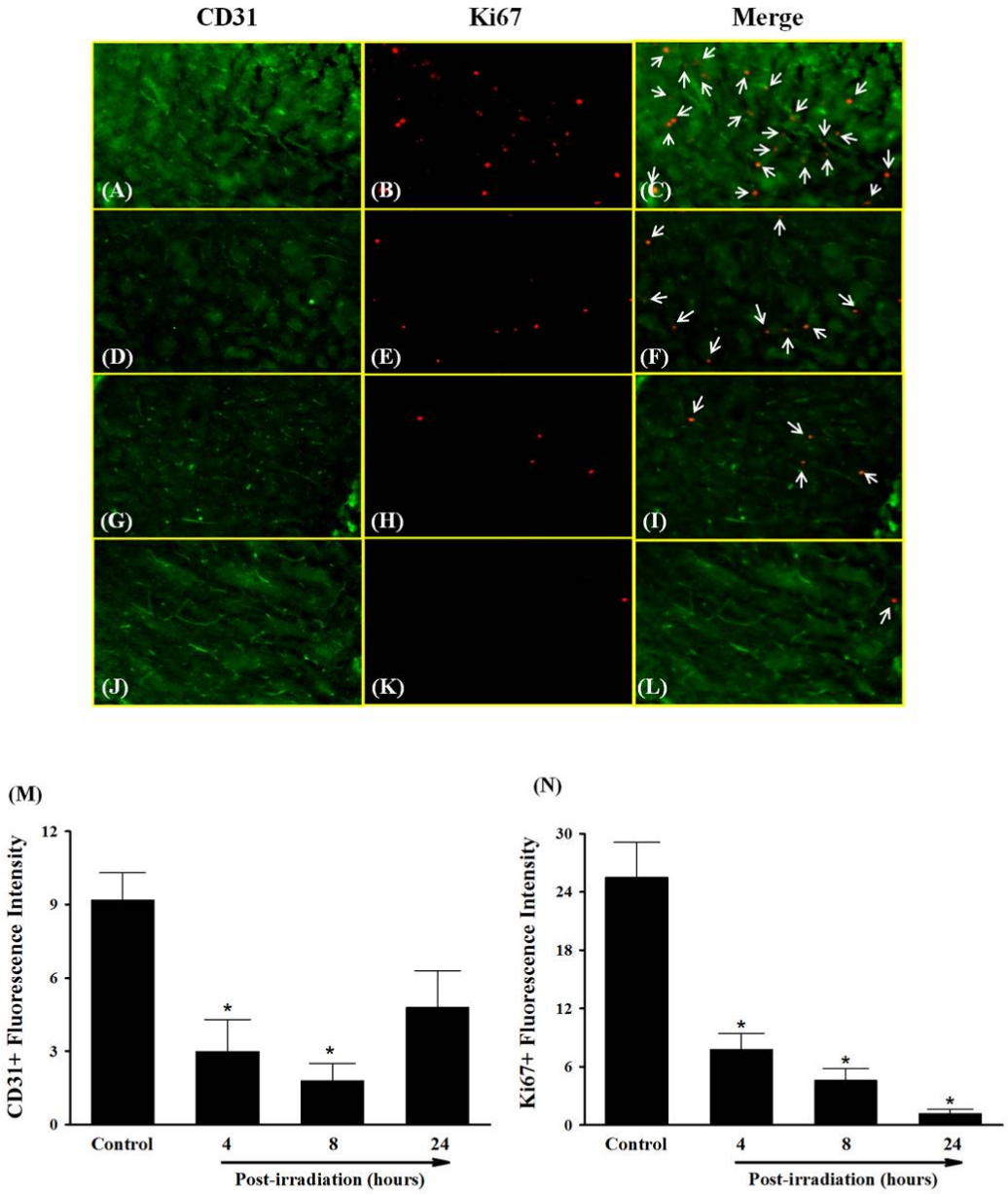

Figure 7.1. Effect of Whole Brain Irradiation on Endothelial Cell Proliferation in Rat Brain. Irradiation markedly and significantly reduced proliferating endothelial cells in rat brain compared with sham-irradiated controls. (A-L): Representative images showing double immunofluorescence staining for CD31 in green and Ki67 in red. A-C: Sham-irradiation (Control); D-F: 4 h post-irradiation; G-I: 8 h post-irradiation; J-L: 24 h post-irradiation. Arrows in merged images indicate proliferating endothelial cells. Magnification of the images is 100×. (M and N): Quantitative analysis of fluorescence intensity. Data shown are means ± SEM of 4 determinations. *Statistically significant from control ($P < 0.05$).

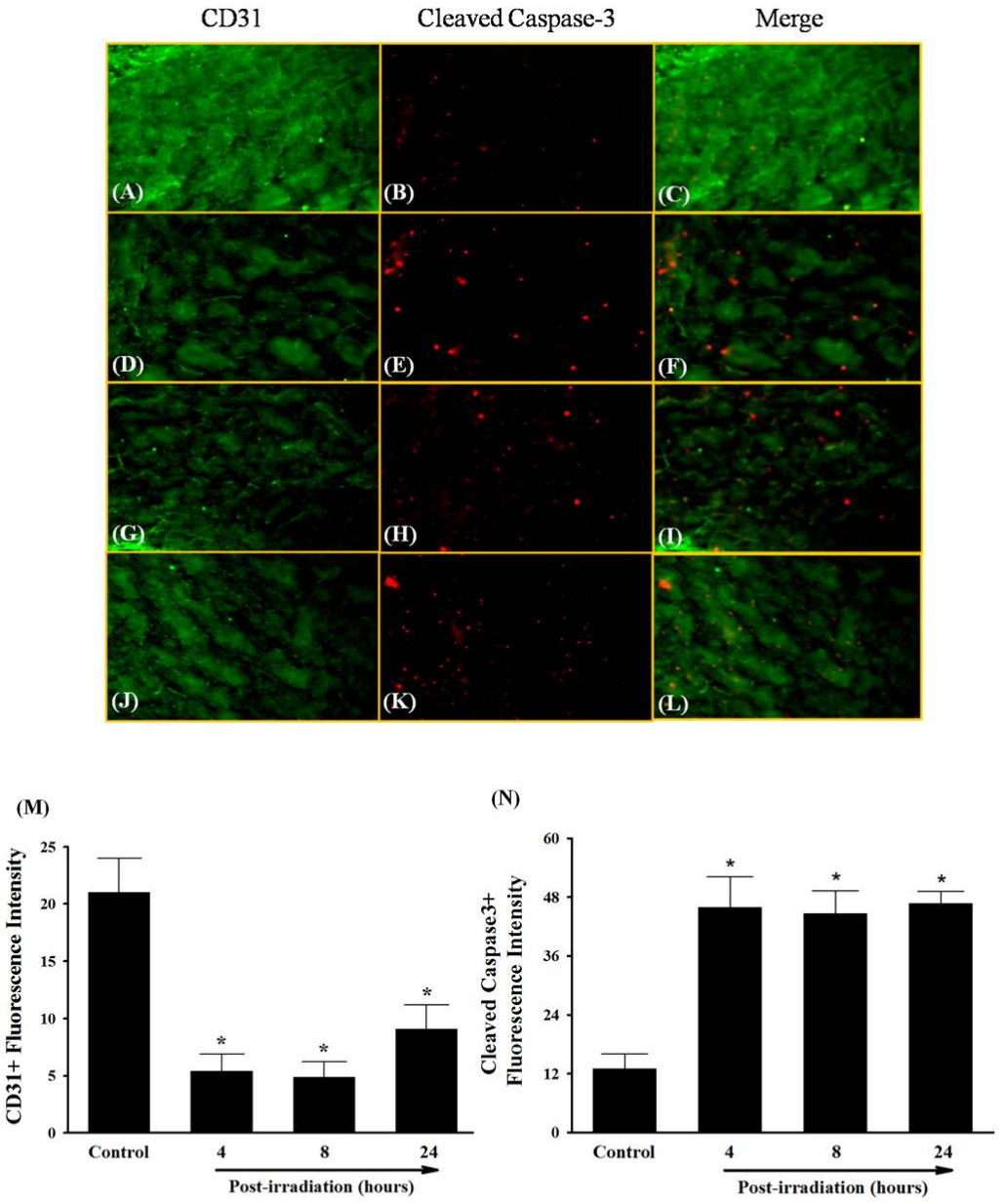

Figure 7.2. Effect of Whole Brain Irradiation on Endothelial Cell Apoptosis in Rat Brain. Irradiation markedly and significantly increased apoptotic endothelial cells in rat brain compared with sham-irradiated controls. (A-L): Representative images showing double immunofluorescence staining for CD31 in green and cleaved caspase-3 in red. A-C: Sham-irradiation (Control); D-F: 4 h post-irradiation; G-I: 8 h post-irradiation; J-L: 24 h post-irradiation. Arrows in merged images indicate apoptotic endothelial cells. Magnification of the images is 100×. (M and N): Quantitative analysis of fluorescence intensity. Data shown are means ± SEM of 4 determinations. *Statistically significant from control ($P < 0.05$).

7.4.2 Effect of Whole Brain Irradiation on mRNA and Protein Expression of Angiogenic Factors in Rat Brain

The mRNA expression levels of VEGF, Ang-1, Tie-2, and Ang-2 were analyzed by quantitative real-time RT-PCR to examine effect of whole brain irradiation on a variety of angiogenic factors in rat brain. As shown in **Figure 7.3A**, VEGF mRNA expression was significantly suppressed in hippocampus at 8 h (0.69-fold) and 24 h (0.58-fold) post-irradiation. A significant down-regulation of Ang-1 mRNA was also observed in hippocampus (0.66-fold) and cortex (0.77-fold) 8 h post-irradiation (**Figure 7.3B**). In addition, whole brain irradiation resulted in a significant reduction in Tie-2 mRNA expression in hippocampus and cortex 4 h (0.62- and 0.71-fold) and 8 h (0.39- and 0.46-fold) after irradiation (**Figure 7.3C**). In contrast, a significant and dramatic increase in Ang-2 mRNA expression was observed at 4 h post-irradiation (2.5-fold induction in hippocampus and 3.4-fold induction in cortex), reached a maximum at 8 h post-irradiation (10.4-fold induction in hippocampus and 13.5-fold induction in cortex), and maintained at significantly higher levels at 24 h post-irradiation (3.5-fold induction in hippocampus and 4.0-fold induction in cortex) (**Figure 7.3D**).

The quantitative sandwich enzyme immunoassay and immunofluorescence staining were employed to determine whether radiation-mediated changes in mRNA levels of angiogenic factors translate to protein expression in hippocampal and cortical regions isolated from rat brains. As indicated in **Figure 7.4**, high expression levels of VEGF protein were found in sham-irradiated control rats (310 pg/mg protein in hippocampus and 294 pg/mg protein in cortex). However, consistent with the gene expression data (**Figure 7.1A**), whole brain irradiation resulted in a significant decrease in VEGF protein expression in hippocampus (1.9-fold at 24 h post-irradiation) and cortex (1.3-fold at 8 h post-irradiation). A strong Ang-1 immunoreactivity was detected in sham-irradiated control rat brains as well as in brains 4 h post-irradiation, whereas the minimum immunoreactivity of Ang-1 protein was found 8 and 24 h after irradiation (**Figure 7.5A-7.5D**). Quantitative analysis also demonstrated a significant reduction in Ang-1 protein expression in rat brains 8 and 24 h after irradiation compared with sham-irradiated control brains (**Figure 7.5E**). In addition, whole brain irradiation significantly decreased the protein expression levels of Tie-2 in rat brains 4, 8, and 24 h after irradiation (**Figure 7.6**). On

the other hand, a marked increase in Ang-2 immunoreactivity was observed in rat brains 24 h after irradiation (**Figure 7.7**). These results demonstrate that irradiation differentially regulates mRNA and protein expression of angiogenic factors in brain.

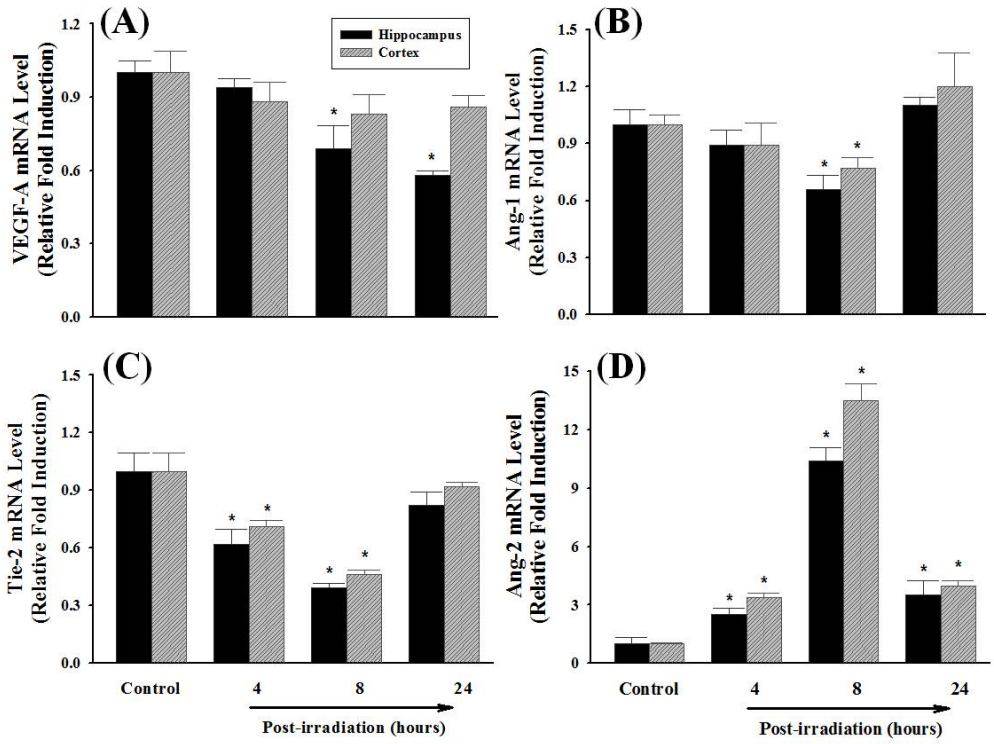

Figure 7.3. Effect of Whole Brain Irradiation on the mRNA Expression of VEGF, Ang-1, Tie-2, and Ang-2 in Rat Brain. Compared with sham-irradiated controls, irradiation down-regulated mRNA expressions of VEGF (A), Ang-1 (B), and Tie-2 (C) in hippocampus and cortex, while the mRNA expression of Ang-2 (D) was up-regulated by irradiation. Data shown are means ± SEM of 4 determinations. *Statistically significant from control ($P < 0.05$).

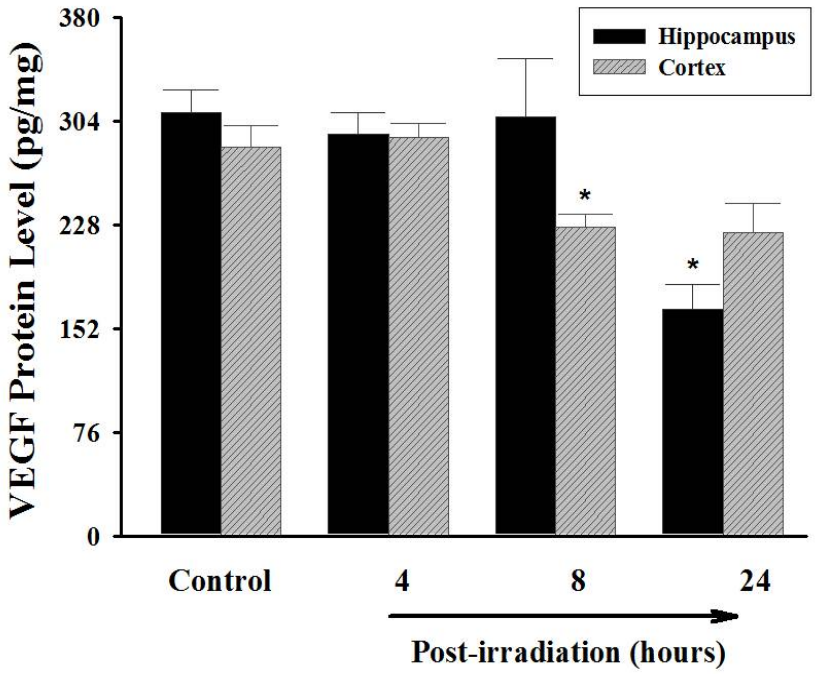

Figure 7.4. Effect of Whole Brain Irradiation on VEGF Protein Expression in Rat Brain. Irradiation significantly attenuated protein expression levels of VEGF in hippocampus and cortex compared with sham-irradiated controls. Data shown are means ± SEM of 4 determinations. *Statistically significant from control ($P < 0.05$).

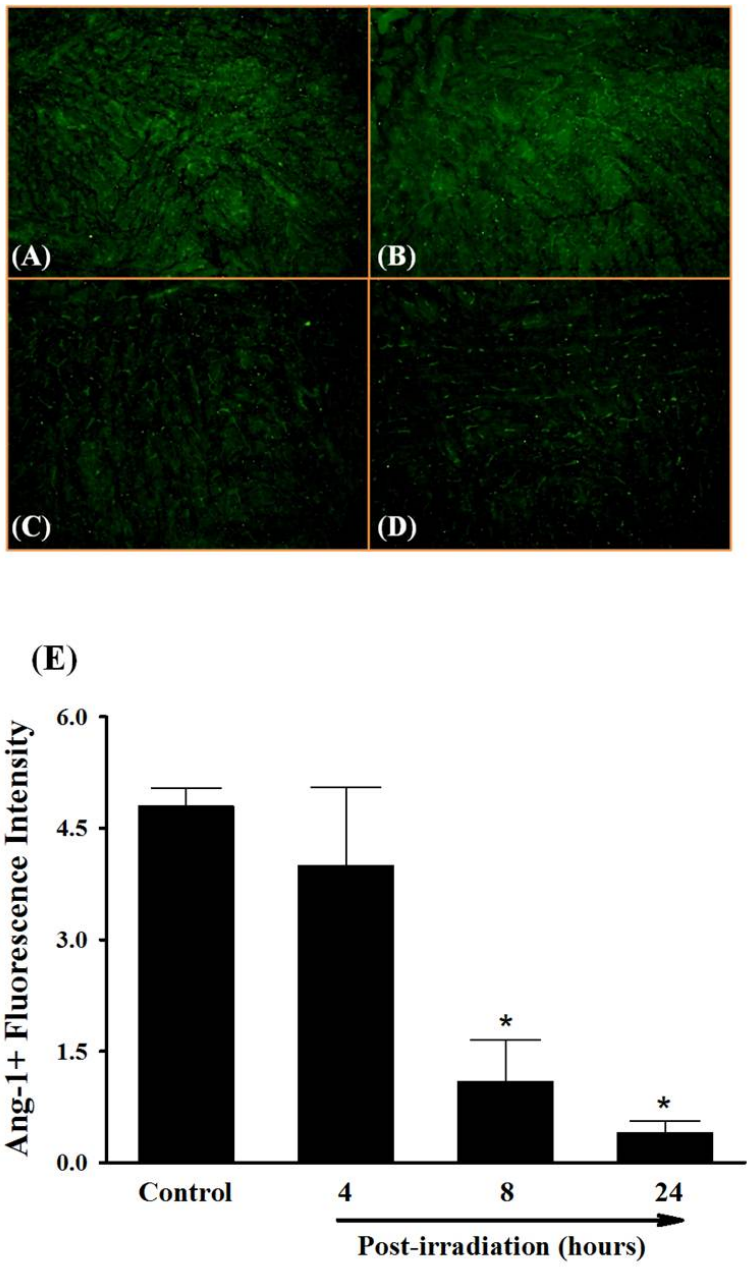

Figure 7.5. Effect of Whole Brain Irradiation on Ang-1 Protein Expression in Rat Brain. Irradiation markedly and significantly reduced Ang-1 protein expression in rat brain compared with sham-irradiated controls. (A-D): Representative images showing immunoreactivity of Ang-1. A: Sham-irradiation (Control); B: 4 h post-irradiation; C: 8 h post-irradiation; D: 24 h post-irradiation. Magnification of the images is 100×. (E): Quantitative analysis of fluorescence intensity. Data shown are means ± SEM of 4 determinations. *Statistically significant from control ($P < 0.05$).

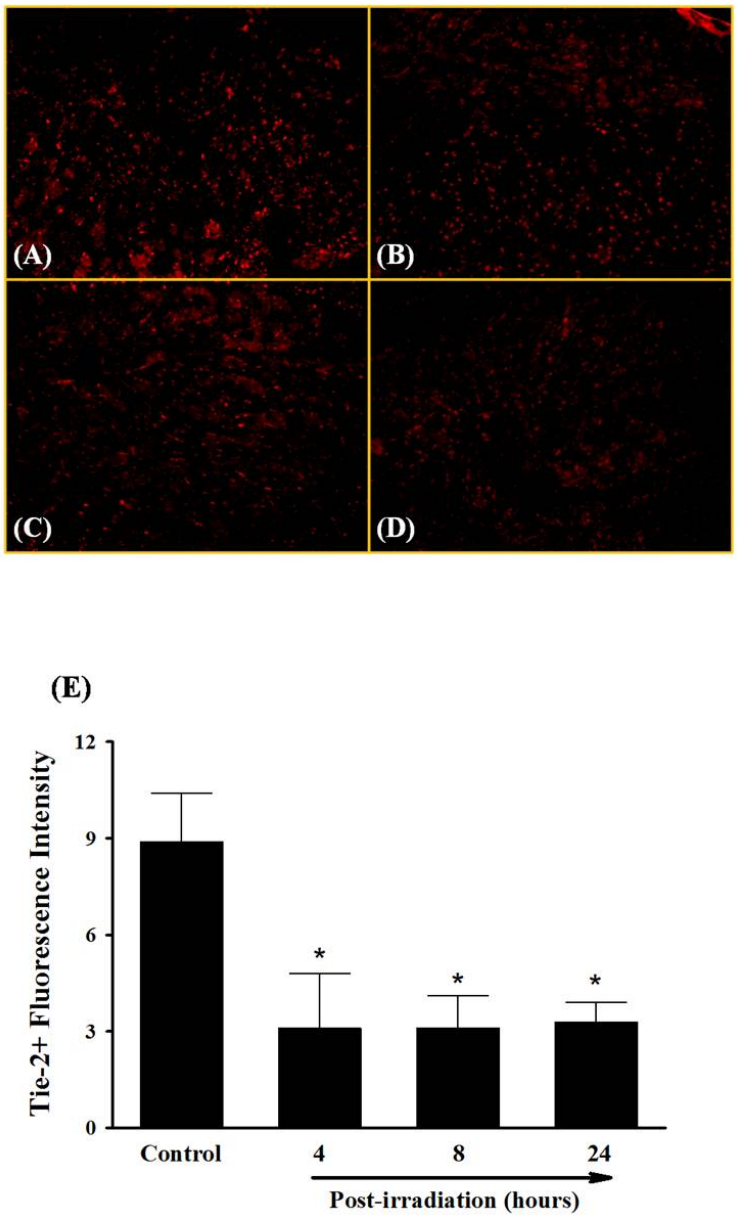

Figure 7.6. Effect of Whole Brain Irradiation on Tie-2 Protein Expression in Rat Brain. Irradiation markedly and significantly reduced Tie-2 protein expression in rat brain compared with sham-irradiated controls. (A-D): Representative images showing immunoreactivity of Tie-2. A: Sham-irradiation (Control); B: 4 h post-irradiation; C: 8 h post-irradiation; D: 24 h post-irradiation. Magnification of the images is 100×. (E): Quantitative analysis of fluorescence intensity. Data shown are means ± SEM of 4 determinations. *Statistically significant from control ($P < 0.05$).

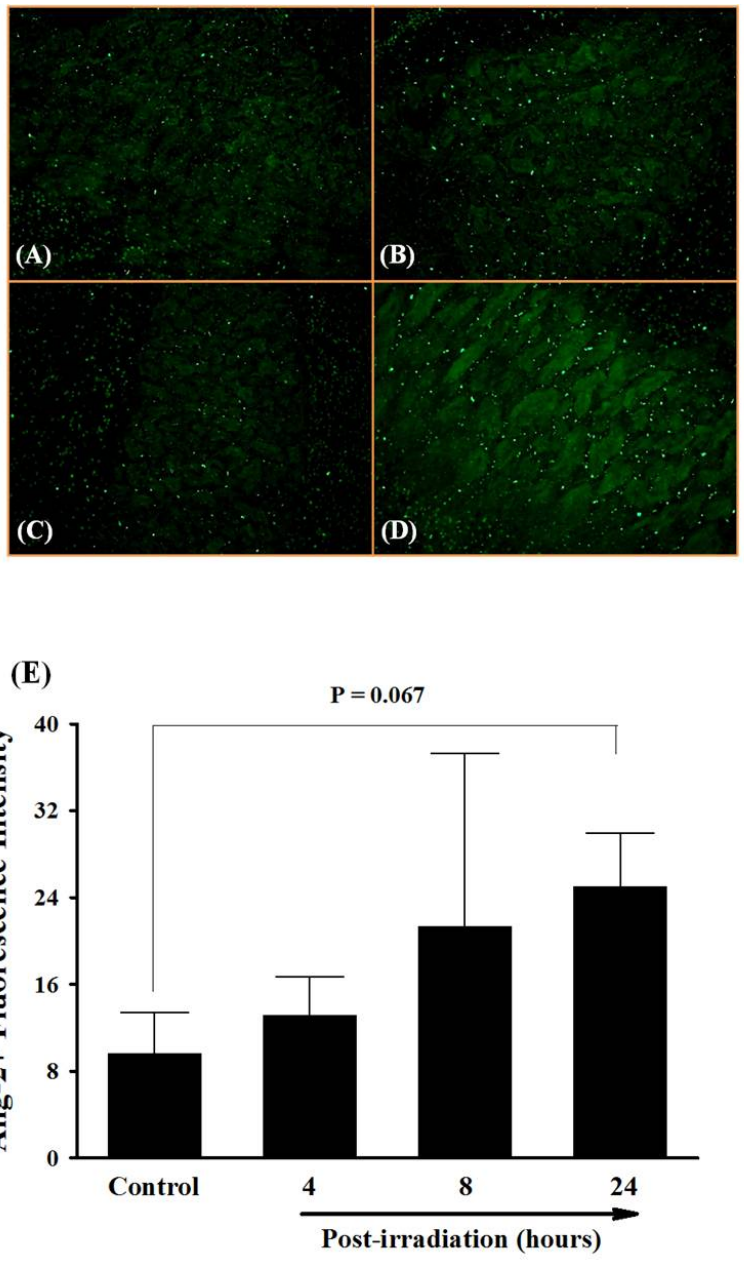

Figure 7.7. Effect of Whole Brain Irradiation on Ang-2 Protein Expression in Rat Brain. Irradiation markedly increased Ang-2 protein expression in rat brain compared with sham-irradiated controls. (A-D): Representative images showing immunoreactivity of Ang-2. A: Sham-irradiation (Control); B: 4 h post-irradiation; C: 8 h post-irradiation; D: 24 h post-irradiation. Magnification of the images is 100×. (E): Quantitative analysis of fluorescence intensity. Data shown are means ± SEM of 4 determinations.

7.5 Discussion

An intimate and coordinated relationship of Ang-1, Ang-2, Tie-2, and VEGF plays a key role in regulating various aspects of physiological angiogenesis. The present study demonstrates that whole brain irradiation decreases EC proliferation, increases EC apoptosis, and differentially regulates the expression of angiogenic factors such as Ang-1, Ang-2, Tie-2, and VEGF in rat brain.

It has been proposed that radiation-induced brain damage is a consequence of injury to the vascular endothelium (22). For example, a single dose of irradiation resulted in the rapid reduction in the number of EC within 24 h in rat brain and a slow loss of EC persisted over several months (20). Similar patterns of EC loss have been also reported in irradiated rat brain (219). Recent evidence has demonstrated that EC apoptosis may be responsible for the radiation-induced decrease in endothelial cell density. Pena et al. (161) reported that EC apoptosis was observed in mouse brain and spinal cord between 4 and 24 h after single-dose irradiation. It was also found that an increased number of apoptotic EC at 24 h post-irradiation was associated with a decrease in vessel density in rat spinal cord (220). In agreement with previous reports, the present study also demonstrated that whole brain irradiation resulted in a significant increase in EC apoptosis in rat brain. In addition to EC apoptosis, we examined EC proliferation and found out that whole brain irradiation significantly decreased the number of proliferating EC in rat brain. These data suggest that radiation-mediated increased EC apoptosis and decreased EC proliferation may contribute to vascular damage in the brain. The exact mechanisms of vessel rarefaction in irradiated brain, however, remain largely unknown.

Angiogenesis plays a critical role not only in physiological processes such as embryonic development and wound healing, but also in the development of a number of pathological conditions including inflammation and tumor progression (148, 221, 222). These events are characterized by the temporally and spatially coordinated interaction among EC, angiogenic factors, and surrounding extracellular matrix protein (148). One of the most important angiogenic factors is VEGF which has a potent and specific activity for the vascular endothelium (149). VEGF and its receptors serve to initiate EC proliferation, EC migration, and production of

new capillary sprouts, which subsequently promote vasculogenesis and angiogenesis (150, 151). VEGF is also considered as a survival factor for EC by protecting them from apoptosis (149, 223). In addition to VEGF, recent studies have suggested that other angiogenic factors such as Ang-1, Tie-2, and Ang-2 play a pivotal role in both physiological and pathological angiogenesis (152). Under physiological condition (**Figure 7.8A**), Ang-1 is necessary for vessel maturation and stabilization by binding its physiological receptor, Tie-2 (156). Ang-2, a functional antagonist of Ang-1, competitively inhibits interaction between Ang-1 and Tie-2. By blocking cell signaling pathways initiated by Ang-1/Tie-2 system, Ang-2 leads to a loosening of tight vascular structure which allows EC to be more sensitive and responsive toward the other angiogenic factors such as VEGF (158, 159). In the presence of high levels of VEGF, Ang-2 facilitates angiogenic process by increasing EC proliferation, EC migration, and vessel sprouting. On the other hand, in the absence of the activating signal from VEGF, Ang-2 promotes EC apoptosis and eventually leads to regression of vessels (159). These studies suggest that dynamic interplay among Ang-1, Ang-2, Tie-2, and VEGF is critically associated with physiological angiogenesis. In the present study, significantly lower levels of mRNA and protein expression of Ang-1, Tie-2, and VEGF were detected in irradiated rat brain. In contrast, whole brain irradiation significantly up-regulated Ang-2 mRNA and protein expression in rat brain. These results suggest that whole brain irradiation may decreases vessel integrity and maturation by causing imbalance in the relative ratio of Ang-1 to Ang-2 levels in brain. Additionally, alterations in the balance of Ang-2/VEGF in irradiated rat brain may initiate vessel rarefaction by decreasing EC proliferation and increasing EC apoptosis in brain (**Figure 7.8B**). Taken together, differential regulation of angiogenic factors such as Ang-1, Ang-2, Tie-2, and VEGF may be responsible for vessel immaturation and regression subsequently.

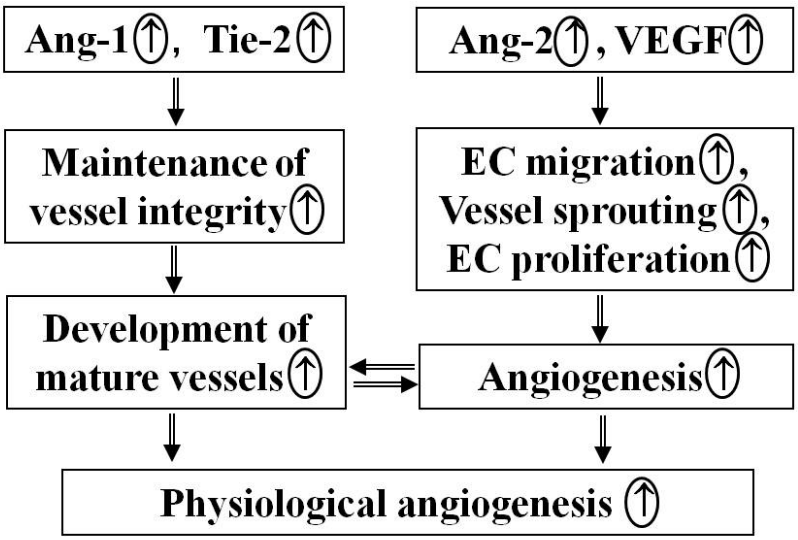

Figure 7.8A. Dynamic Interaction among Ang-1, Ang-2, Tie-2, and VEGF in the Regulation of Physiological Angiogenesis.

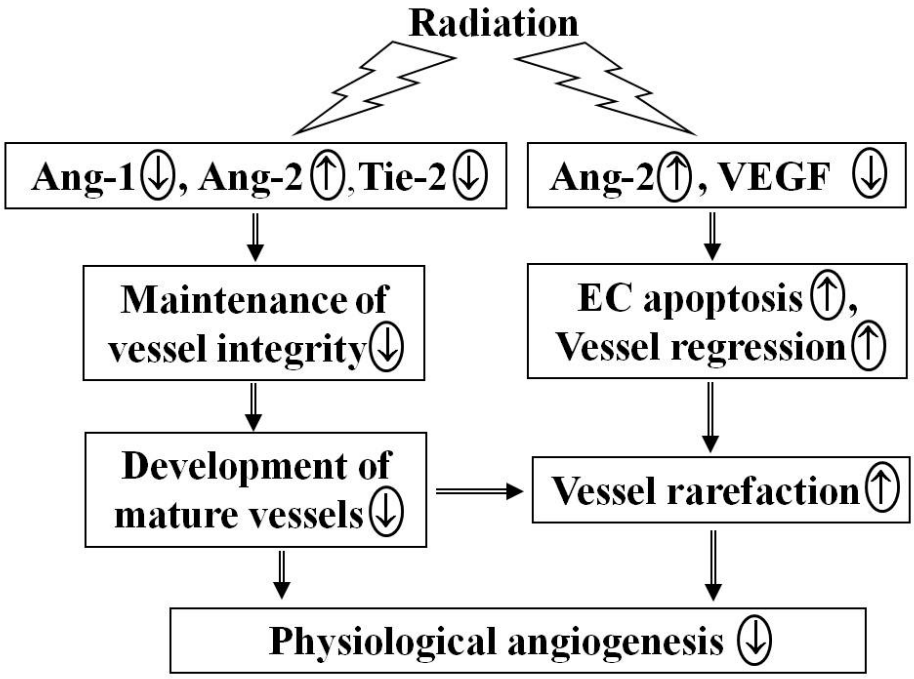

Figure 7.8B. Effect of Whole Brain Irradiation on Dynamic Interaction among Ang-1, Ang-2, Tie-2, and VEGF in the Regulation of Physiological Angiogenesis.

7.6 Conclusions

In conclusion, the present study demonstrated the first evidence that differential regulation of Ang-1, Ang-2, Tie-2, and VEGF may be responsible for vessel rarefaction by decreasing EC proliferation and increasing EC apoptosis in irradiated rat brain. These findings may contribute to defining cellular and molecular mechanisms by which irradiation alters physiological angiogenesis that will lead to new opportunities for preventive and therapeutic interventions for patients with brain tumors who receive radiation therapy.

7.7 Acknowledgments

The project described was supported by Grant Number R01NS056218 from the National Institute of Neurological Disorders and Stroke.

CHAPTER 8: CONCLUSIONS AND FUTURE WORK

8.1 Conclusions

Radiation therapy continues to be a main treatment modality in the therapeutic management of brain tumors (208, 209). The use of radiotherapy for treatment of brain tumors, however, is limited by the risk of radiation-induced injury to normal brain tissue that can subsequently lead to devastating functional deficits several months to years after treatment (1-3). At present, there is sparse information on the etiology of radiation-induced damage to normal brain tissue. Additionally, the specific mechanisms by which irradiation causes brain injury in normal tissues have not yet been fully understood. Therefore, the prime goal of this work was to determine the molecular mechanisms responsible for radiation-induced brain injury. The following main conclusions have been achieved:

1. The effects of whole brain irradiation on pro-inflammatory pathways in the brain were examined. This study demonstrated that irradiation induces regionally specific alterations in pro-inflammatory environments through activation of pro-inflammatory transcription factors (e.g., AP-1, NF-κB, and CREB) and overexpression of pro-inflammatory mediators (e.g., TNF-α, IL-1β, MCP-1) in brain.

2. A mathematical model describing radiation-induced mRNA and protein expression kinetics of TNF-α in hippocampus was reconstructed. This study suggested that more case studies with increased data points and addition of a negative feedback loop are necessary to develop more accurate models.

3. The effects of aging on radiation-induced impairment of immune responses in brain were examined. This study demonstrated that radiation-induced acute inflammatory responses, such as overexpression of pro-inflammatory cytokines (e.g., TNF-α, IL-1β, and IL-6), adhesion molecules (e.g., ICAM-1, VCAM-1, and E-selectin), chemokine MCP-1, and MMP-9, are significantly impaired in aged brain.

4. The critical role of MMPs/TIMPs system in radiation-induced ECM degradation in brain was examined. This study demonstrated that whole brain irradiation mediates degradation of collagen type IV, a major ECM component of the BBB basement membrane, by altering the balance of MMP-2 and TIMP-2 levels in brain.

5. The critical role of radiation-induced differential regulation of angiogenic factors in vessel rarefaction in brain was examined. This study demonstrated that differential regulation of Ang-1, Ang-2, Tie-2, and VEGF may be responsible for vessel rarefaction by decreasing EC proliferation and increasing EC apoptosis in irradiated brain.

The results of these studies support our main hypothesis that whole brain irradiation induces brain injury by triggering pro-inflammatory pathways, degrading extracellular matrix, and altering physiologic angiogenesis. These findings may contribute to defining a new cellular and molecular basis for radiation-induced brain injury. Additionally, this work may lead to new opportunities for preventive and therapeutic interventions for patients with brain tumors who receive radiation therapy.

8.2 Future Work

The ultimate goal of this work is to determine the cellular and molecular mechanisms related to the etiology of cognitive impairment that occurs in response to whole brain irradiation. In order to aid in understanding of the pathophysiological mechanisms responsible for radiation-induced brain injury and the successful development of novel strategies for prevention and treatment of radiation-induced brain injury, there are several areas of study that need to be further explored. The following research areas are of considerable research interest for future work:

1. Effects of aging on radiation-induced ECM degradation and vessel rarefaction in brain

It was demonstrated in Chapter 5 that the expression of all pro-inflammatory mediators were significantly up-regulated in response to whole brain irradiation compared with sham-irradiated

control groups regardless of age. In contrast, a significant age-dependent attenuation of inflammatory responses to acute radiation exposure was observed. However, the effects of aging on radiation-induced ECM degradation and vessel rarefaction in brain have not yet been investigated. Based on data from Chapter 5, it is anticipated that radiation-induced alteration in MMPs/TIMPs system, ECM degradation, differential regulation of angiogenic factors, and vessel rarefaction in brain will be significantly influenced by age. Results from this study will contribute to development of therapeutic strategies for brain tumor patients with different ages who receive radiation therapy.

2. *Role of MMP-2 in radiation-induced collagen type IV degradation in brain*

It was demonstrated in Chapter 6 that whole brain irradiation induces an imbalance between MMPs and TIMPs expression, increases gelatinase activity, and degrades collagen type IV in brain. It was also shown that collagen type IV degradation in the irradiated brain may be mediated through enhanced MMP-2 expression and activity. However, the mechanistic link between MMP-2 activity and ECM degradation remains unclear and needs to be further investigated. Selective MMP-2 inhibitors and MMP-2 knockout mice could be employed as in-depth pharmacological and genetic approaches. It is anticipated that MMP-2 plays a crucial role in radiation-induced collagen type IV degradation in brain. Results from this study will contribute to elucidating a mechanistic links among MMP-2 expression, collagen type IV degradation, and BBB disruption in brain after irradiation.

3. Experimental studies of acute radiation-induced cognitive dysfunction in a mouse model

It was demonstrated in Chapter 3 that elevated levels of pro-inflammatory mediators may lead to the decline in tissue function after whole brain irradiation. It was also demonstrated in Chapter 6 that MMP-2 plays a pivotal role in the pathogenesis of brain injury by degrading ECM components of the BBB basement membrane. However, whether radiation-mediated early inflammatory responses and enhanced MMP-2 activity observed in this work have a causal relationship with delayed injury to the brain, especially cognitive dysfunction, remain to be further investigated. Therefore, the role of pro-inflammatory environments and MMP-2 activity

in radiation-induce brain injury can be further examined by administering anti-inflammatory drugs or a neutralizing anti-MMP-2 monoclonal antibody before whole brain irradiation, respectively. After irradiation, animals can be evaluated for spatial learning (behavioral testing) using the Morris Water Maze. It is anticipated that pro-inflammatory environment and MMP-2 play a crucial role in radiation-induced cognitive dysfunction in brain. Results from this study will contribute to the development a potential preventive approach for radiation-induced brain injury.

REFERENCES

1. Sheline GE, Wara WM, Smith V. Therapeutic irradiation and brain injury. *Int J Radiat Oncol Biol Phys* 1980;6:1215-1228.
2. Moulder JE, Cohen EP. Future strategies for mitigation and treatment of chronic radiation-induced normal tissue injury. *Semin Radiat Oncol* 2007;17:141-148.
3. Denham JW, Hauer-Jensen M. The radiotherapeutic injury--a complex 'wound'. *Radiother Oncol* 2002;63:129-145.
4. Chang EL, Wefel JS, Hess KR, Allen PK, Lang FF, Kornguth DG, Arbuckle RB, Swint JM, Shiu AS, Maor MH, Meyers CA. Neurocognition in patients with brain metastases treated with radiosurgery or radiosurgery plus whole-brain irradiation: a randomised controlled trial. *Lancet Oncol* 2009;10:1037-1044.
5. Hong JH, Chiang CS, Campbell IL, Sun JR, Withers HR, McBride WH. Induction of acute phase gene expression by brain irradiation. *Int J Radiat Oncol Biol Phys* 1995;33:619-626.
6. Chiang CS, Hong JH, Stalder A, Sun JR, Withers HR, McBride WH. Delayed molecular responses to brain irradiation. *Int J Radiat Biol* 1997;72:45-53.
7. Gaber MW, Sabek OM, Fukatsu K, Wilcox HG, Kiani MF, Merchant TE. Differences in ICAM-1 and TNF-alpha expression between large single fraction and fractionated irradiation in mouse brain. *Int J Radiat Biol* 2003;79:359-366.
8. Baluna RG, Eng TY, Thomas CR. Adhesion molecules in radiotherapy. *Radiat Res* 2006;166:819-831.
9. Olschowka JA, Kyrkanides S, Harvey BK, O'Banion MK, Williams JP, Rubin P, Hansen JT. ICAM-1 induction in the mouse CNS following irradiation. *Brain Behav Immun* 1997;11:273-285.
10. Szallasi Z. Genetic network analysis in light of massively parallel biological data acquisition. *Pac Symp Biocomput* 1999:5-16.
11. de Jong H. Modeling and simulation of genetic regulatory systems: a literature review. *J Comput Biol* 2002;9:67-103.
12. Tyson JJ, Othmer HG. The dynamics of feedback control circuits in biochemical pathways. Vol 5: Theoretical Biology; 1978. pp. 1-62.
13. Sepah SC, Bower JE. Positive affect and inflammation during radiation treatment for breast and prostate cancer. *Brain Behav Immun* 2009;23:1068-1072.

14. Stone HB, Coleman CN, Anscher MS, McBride WH. Effects of radiation on normal tissue: consequences and mechanisms. *Lancet Oncol* 2003;4:529-536.
15. Baker DG, Krochak RJ. The response of the microvascular system to radiation: a review. *Cancer Invest* 1989;7:287-294.
16. Rubin P, Gash DM, Hansen JT, Nelson DF, Williams JP. Disruption of the blood-brain barrier as the primary effect of CNS irradiation. *Radiother Oncol* 1994;31:51-60.
17. Goligorsky MS. Microvascular rarefaction: The decline and fall of blood vessels. *Organogenesis* 2010;6:1-10.
18. Prasad A, Dunnill GS, Mortimer PS, MacGregor GA. Capillary rarefaction in the forearm skin in essential hypertension. *J Hypertens* 1995;13:265-268.
19. Rakusan K, Moravec J, Hatt PY. Regional capillary supply in the normal and hypertrophied rat heart. *Microvasc Res* 1980;20:319-326.
20. Ljubimova NV, Levitman MK, Plotnikova ED, Eidus L. Endothelial cell population dynamics in rat brain after local irradiation. *Br J Radiol* 1991;64:934-940.
21. Dimitrievich GS, Fischer-Dzoga K, Griem ML. Radiosensitivity of vascular tissue. I. Differential radiosensitivity of capillaries: a quantitative in vivo study. *Radiat Res* 1984;99:511-535.
22. Roth NM, Sontag MR, Kiani MF. Early effects of ionizing radiation on the microvascular networks in normal tissue. *Radiat Res* 1999;151:270-277.
23. Walker EM, Jr., Nillas MS, Mangiarua EI, Cansino S, Morrison RG, Perdue RR, Triest WE, Wright GL, Studeny M, Wehner P, Rice KM, Blough ER. Age-associated changes in hearts of male Fischer 344/Brown Norway F1 rats. *Ann Clin Lab Sci* 2006;36:427-438.
24. Hebda-Bauer EK, Morano MI, Therrien B. Aging and corticosterone injections affect spatial learning in Fischer-344 X Brown norway rats. *Brain Res* 1999;827:93-103.
25. Chiang CS, Liu WC, Jung SM, Chen FH, Wu CR, McBride WH, Lee CC, Hong JH. Compartmental responses after thoracic irradiation of mice: strain differences. *Int J Radiat Oncol Biol Phys* 2005;62:862-871.
26. Schindler MK, Forbes ME, Robbins ME, Riddle DR. Aging-dependent changes in the radiation response of the adult rat brain. *Int J Radiat Oncol Biol Phys* 2008;70:826-834.

27. Shi L, Molina DP, Robbins ME, Wheeler KT, Brunso-Bechtold JK. Hippocampal neuron number is unchanged 1 year after fractionated whole-brain irradiation at middle age. *Int J Radiat Oncol Biol Phys* 2008;71:526-532.

28. Lindsay KJ, Coates PJ, Lorimore SA, Wright EG. The genetic basis of tissue responses to ionizing radiation. *Br J Radiol* 2007;80 Spec No 1:S2-6.

29. Acharya MM, Christie LA, Lan ML, Donovan PJ, Cotman CW, Fike JR, Limoli CL. Rescue of radiation-induced cognitive impairment through cranial transplantation of human embryonic stem cells. *Proc Natl Acad Sci U S A* 2009;106:19150-19155.

30. Kim SH, Lim DJ, Chung YG, Cho TH, Lim SJ, Kim WJ, Suh JK. Expression of TNF-alpha and TGF-beta 1 in the rat brain after a single high-dose irradiation. *J Korean Med Sci* 2002;17:242-248.

31. Voges J, Treuer H, Sturm V, Buchner C, Lehrke R, Kocher M, Staar S, Kuchta J, Muller RP. Risk analysis of linear accelerator radiosurgery. *Int J Radiat Oncol Biol Phys* 1996;36:1055-1063.

32. Monje ML, Mizumatsu S, Fike JR, Palmer TD. Irradiation induces neural precursor-cell dysfunction. *Nat Med* 2002;8:955-962.

33. Hodges H, Katzung N, Sowinski P, Hopewell JW, Wilkinson JH, Bywaters T, Rezvani M. Late behavioural and neuropathological effects of local brain irradiation in the rat. *Behav Brain Res* 1998;91:99-114.

34. Calvo W, Hopewell JW, Reinhold HS, Yeung TK. Time- and dose-related changes in the white matter of the rat brain after single doses of X rays. *Br J Radiol* 1988;61:1043-1052.

35. Monje ML, Palmer T. Radiation injury and neurogenesis. *Curr Opin Neurol* 2003;16:129-134.

36. Shi L, Adams MM, Long A, Carter CC, Bennett C, Sonntag WE, Nicolle MM, Robbins M, D'Agostino R, Brunso-Bechtold JK. Spatial learning and memory deficits after whole-brain irradiation are associated with changes in NMDA receptor subunits in the hippocampus. *Radiat Res* 2006;166:892-899.

37. Fowler JF. Brief summary of radiobiological principles in fractionated radiotherapy. *Seminars in Radiation Oncology* 1992;2:16-21.

38. Brown WR, Thore CR, Moody DM, Robbins ME, Wheeler KT. Vascular damage after fractionated whole-brain irradiation in rats. *Radiat Res* 2005;164:662-668.

39. Conner KR, Payne VS, Forbes ME, Robbins ME, Riddle DR. Effects of the AT1 receptor antagonist L-158,809 on microglia and neurogenesis after fractionated whole-brain irradiation. *Radiat Res* 2010;173:49-61.
40. Buckner JC, Brown PD, O'Neill BP, Meyer FB, Wetmore CJ, Uhm JH. Central nervous system tumors. *Mayo Clin Proc* 2007;82:1271-1286.
41. Chandana SR, Movva S, Arora M, Singh T. Primary brain tumors in adults. *Am Fam Physician* 2008;77:1423-1430.
42. Hess KR. Extent of resection as a prognostic variable in the treatment of gliomas. *J Neurooncol* 1999;42:227-231.
43. Simpson JR, Horton J, Scott C, Curran WJ, Rubin P, Fischbach J, Isaacson S, Rotman M, Asbell SO, Nelson JS. Influence of location and extent of surgical resection on survival of patients with glioblastoma multiforme: results of three consecutive Radiation Therapy Oncology Group (RTOG) clinical trials. *Int J Radiat Oncol Biol Phys* 1993;26:239-244.
44. American Brain Tumor Foundation; 2008.
45. Jacob F, Monod J. Genetic regulatory mechanisms in the synthesis of proteins. *J Mol Biol* 1961;3:318-356.
46. Cohadon F. Indications for surgery in the management of gliomas. *Adv Tech Stand Neurosurg* 1990;17:189-234.
47. Brian Andrews BTA. Intensive Care in Neurosurgery: Thieme Medical Publishers; 2002.
48. Fadul C, Wood J, Thaler H, Galicich J, Patterson RH, Jr., Posner JB. Morbidity and mortality of craniotomy for excision of supratentorial gliomas. *Neurology* 1988;38:1374-1379.
49. Hegi ME, Diserens AC, Gorlia T, Hamou MF, de Tribolet N, Weller M, Kros JM, Hainfellner JA, Mason W, Mariani L, Bromberg JE, Hau P, Mirimanoff RO, Cairncross JG, Janzer RC, Stupp R. MGMT gene silencing and benefit from temozolomide in glioblastoma. *N Engl J Med* 2005;352:997-1003.
50. Stupp R, Mason WP, van den Bent MJ, Weller M, Fisher B, Taphoorn MJ, Belanger K, Brandes AA, Marosi C, Bogdahn U, Curschmann J, Janzer RC, Ludwin SK, Gorlia T, Allgeier A, Lacombe D, Cairncross JG, Eisenhauer E, Mirimanoff RO. Radiotherapy plus concomitant and adjuvant temozolomide for glioblastoma. *N Engl J Med* 2005;352:987-996.

51. Trebilcock GU, Ponnappan U. Evidence for lowered induction of nuclear factor kappa B in activated human T lymphocytes during aging. *Gerontology* 1996;42:137-146.
52. Markman M. Regional Chemotherapy: Clinical Research and Practice. Vol 2: Springer-Verlag New York, LLC; 1999.
53. Fowler JF. The linear-quadratic formula and progress in fractionated radiotherapy. *Br J Radiol* 1989;62:679-694.
54. Walker MD, Strike TA, Sheline GE. An analysis of dose-effect relationship in the radiotherapy of malignant gliomas. *Int J Radiat Oncol Biol Phys* 1979;5:1725-1731.
55. Walker MD, Alexander E, Jr., Hunt WE, MacCarty CS, Mahaley MS, Jr., Mealey J, Jr., Norrell HA, Owens G, Ransohoff J, Wilson CB, Gehan EA, Strike TA. Evaluation of BCNU and/or radiotherapy in the treatment of anaplastic gliomas. A cooperative clinical trial. *J Neurosurg* 1978;49:333-343.
56. Andersen AP. Postoperative irradiation of glioblastomas. Results in a randomized series. *Acta Radiol Oncol Radiat Phys Biol* 1978;17:475-484.
57. Bucci MK, Bevan A, Roach M, 3rd. Advances in radiation therapy: conventional to 3D, to IMRT, to 4D, and beyond. *CA Cancer J Clin* 2005;55:117-134.
58. Denham JW, Hauer-Jensen M. The radiotherapeutic injury-a complex 'wound'. *Radiother Oncol* 2002;63:129-145.
59. Tofilon PJ, Fike JR. The radioresponse of the central nervous system: a dynamic process. *Radiat Res* 2000;153:357-370.
60. Schultheiss TE, Stephens LC. Invited review: permanent radiation myelopathy. *Br J Radiol* 1992;65:737-753.
61. Lamproglou I, Chen QM, Boisserie G, Mazeron JJ, Poisson M, Baillet F, Le Poncin M, Delattre JY. Radiation-induced cognitive dysfunction: an experimental model in the old rat. *Int J Radiat Oncol Biol Phys* 1995;31:65-70.
62. Yoneoka Y, Satoh M, Akiyama K, Sano K, Fujii Y, Tanaka R. An experimental study of radiation-induced cognitive dysfunction in an adult rat model. *Br J Radiol* 1999;72:1196-1201.
63. Keyeux A, Brucher JM, Ochrymowicz-Bemelmans D, Charlier AA. Late effects of X irradiation on regulation of cerebral blood flow after whole-brain exposure in rats. *Radiat Res* 1997;147:621-630.

64. McGeer PL, McGeer EG. The inflammatory response system of brain: implications for therapy of Alzheimer and other neurodegenerative diseases. *Brain Res Brain Res Rev* 1995;21:195-218.

65. Dheen ST, Kaur C, Ling EA. Microglial activation and its implications in the brain diseases. *Curr Med Chem* 2007;14:1189-1197.

66. Akiyama H, Barger S, Barnum S, Bradt B, Bauer J, Cole GM, Cooper NR, Eikelenboom P, Emmerling M, Fiebich BL, Finch CE, Frautschy S, Griffin WS, Hampel H, Hull M, Landreth G, Lue L, Mrak R, Mackenzie IR, McGeer PL, O'Banion MK, Pachter J, Pasinetti G, Plata-Salaman C, Rogers J, Rydel R, Shen Y, Streit W, Strohmeyer R, Tooyoma I, Van Muiswinkel FL, Veerhuis R, Walker D, Webster S, Wegrzyniak B, Wenk G, Wyss-Coray T. Inflammation and Alzheimer's disease. *Neurobiol Aging* 2000;21:383-421.

67. Suo Z, Tan J, Placzek A, Crawford F, Fang C, Mullan M. Alzheimer's beta-amyloid peptides induce inflammatory cascade in human vascular cells: the roles of cytokines and CD40. *Brain Res* 1998;807:110-117.

68. Fiala M, Zhang L, Gan X, Sherry B, Taub D, Graves MC, Hama S, Way D, Weinand M, Witte M, Lorton D, Kuo YM, Roher AE. Amyloid-beta induces chemokine secretion and monocyte migration across a human blood--brain barrier model. *Mol Med* 1998;4:480-489.

69. Giri R, Selvaraj S, Miller CA, Hofman F, Yan SD, Stern D, Zlokovic BV, Kalra VK. Effect of endothelial cell polarity on beta-amyloid-induced migration of monocytes across normal and AD endothelium. *Am J Physiol Cell Physiol* 2002;283:C895-904.

70. McGeer PL, Yasojima K, McGeer EG. Inflammation in Parkinson's disease. *Adv Neurol* 2001;86:83-89.

71. Schulz JB, Falkenburger BH. Neuronal pathology in Parkinson's disease. *Cell Tissue Res* 2004;318:135-147.

72. Liu B, Hong JS. Role of microglia in inflammation-mediated neurodegenerative diseases: mechanisms and strategies for therapeutic intervention. *J Pharmacol Exp Ther* 2003;304:1-7.

73. Teismann P, Tieu K, Choi DK, Wu DC, Naini A, Hunot S, Vila M, Jackson-Lewis V, Przedborski S. Cyclooxygenase-2 is instrumental in Parkinson's disease neurodegeneration. *Proc Natl Acad Sci U S A* 2003;100:5473-5478.

74. Lee YW, Eum SY, Nath A, Toborek M. Estrogen-mediated protection against HIV Tat protein-induced inflammatory pathways in human vascular endothelial cells. *Cardiovasc Res* 2004;63:139-148.

75. Ross R. The pathogenesis of atherosclerosis: a perspective for the 1990s. *Nature* 1993;362:801-809.

76. Ross R. Atherosclerosis is an inflammatory disease. *Am Heart J* 1999;138:S419-420.

77. Dinarello CA. Biologic basis for interleukin-1 in disease. *Blood* 1996;87:2095-2147.

78. Locksley RM, Killeen N, Lenardo MJ. The TNF and TNF receptor superfamilies: integrating mammalian biology. *Cell* 2001;104:487-501.

79. Kishimoto T. Interleukin-6: from basic science to medicine--40 years in immunology. *Annu Rev Immunol* 2005;23:1-21.

80. Lee YW, Hennig B, Toborek M. Redox-regulated mechanisms of IL-4-induced MCP-1 expression in human vascular endothelial cells. *Am J Physiol Heart Circ Physiol* 2003;284:H185-192.

81. Lee YW, Hirani AA. Role of interleukin-4 in atherosclerosis. *Arch Pharm Res* 2006;29:1-15.

82. Lee YW, Son KW, Flora G, Hennig B, Nath A, Toborek M. Methamphetamine activates DNA binding of specific redox-responsive transcription factors in mouse brain. *J Neurosci Res* 2002;70:82-89.

83. Stanimirovic D, Zhang W, Howlett C, Lemieux P, Smith C. Inflammatory gene transcription in human astrocytes exposed to hypoxia: roles of the nuclear factor-kappaB and autocrine stimulation. *J Neuroimmunol* 2001;119:365-376.

84. Toborek M, Lee YW, Kaiser S, Hennig B. Measurement of inflammatory properties of fatty acids in human endothelial cells. *Methods Enzymol* 2002;352:198-219.

85. Lee YW, Hirani AA, Kyprianou N, Toborek M. Human immunodeficiency virus-1 Tat protein up-regulates interleukin-6 and interleukin-8 expression in human breast cancer cells. *Inflamm Res* 2005;54:380-389.

86. Bouloumie A, Marumo T, Lafontan M, Busse R. Leptin induces oxidative stress in human endothelial cells. *FASEB J* 1999;13:1231-1238.

87. Guha M, Bai W, Nadler JL, Natarajan R. Molecular mechanisms of tumor necrosis factor alpha gene expression in monocytic cells via hyperglycemia-induced oxidant stress-dependent and -independent pathways. *J Biol Chem* 2000;275:17728-17739.

88. Lakshminarayanan V, Drab-Weiss EA, Roebuck KA. H2O2 and tumor necrosis factor-alpha induce differential binding of the redox-responsive transcription factors AP-1 and NF-kappaB to the interleukin-8 promoter in endothelial and epithelial cells. *J Biol Chem* 1998;273:32670-32678.

89. Wung BS, Cheng JJ, Hsieh HJ, Shyy YJ, Wang DL. Cyclic strain-induced monocyte chemotactic protein-1 gene expression in endothelial cells involves reactive oxygen species activation of activator protein 1. *Circ Res* 1997;81:1-7.

90. Kyrkanides S, Moore AH, Olschowka JA, Daeschner JC, Williams JP, Hansen JT, Kerry O'Banion M. Cyclooxygenase-2 modulates brain inflammation-related gene expression in central nervous system radiation injury. *Brain Res Mol Brain Res* 2002;104:159-169.

91. Moore AH, Olschowka JA, Williams JP, Okunieff P, O'Banion MK. Regulation of prostaglandin E2 synthesis after brain irradiation. *Int J Radiat Oncol Biol Phys* 2005;62:267-272.

92. Behrends U, Peter RU, Hintermeier-Knabe R, Eissner G, Holler E, Bornkamm GW, Caughman SW, Degitz K. Ionizing radiation induces human intercellular adhesion molecule-1 in vitro. *J Invest Dermatol* 1994;103:726-730.

93. Gaugler MH, Squiban C, van der Meeren A, Bertho JM, Vandamme M, Mouthon MA. Late and persistent up-regulation of intercellular adhesion molecule-1 (ICAM-1) expression by ionizing radiation in human endothelial cells in vitro. *Int J Radiat Biol* 1997;72:201-209.

94. Hallahan D, Kuchibhotla J, Wyble C. Cell adhesion molecules mediate radiation-induced leukocyte adhesion to the vascular endothelium. *Cancer Res* 1996;56:5150-5155.

95. Molla M, Gironella M, Salas A, Miquel R, Perez-del-Pulgar S, Conill C, Engel P, Biete A, Pique JM, Panes J. Role of P-selectin in radiation-induced intestinal inflammatory damage. *Int J Cancer* 2001;96:99-109.

96. Molla M, Panes J. Radiation-induced intestinal inflammation. *World J Gastroenterol* 2007;13:3043-3046.
97. Han SK, Song JY, Yun YS, Yi SY. Effect of gamma radiation on cytokine expression and cytokine-receptor mediated STAT activation. *Int J Radiat Biol* 2006;82:686-697.
98. Hong JH, Chiang CS, Tsao CY, Lin PY, McBride WH, Wu CJ. Rapid induction of cytokine gene expression in the lung after single and fractionated doses of radiation. *Int J Radiat Biol* 1999;75:1421-1427.
99. Haveman J, Geerdink AG, Rodermond HM. TNF, IL-1 and IL-6 in circulating blood after total-body and localized irradiation in rats. *Oncol Rep* 1998;5:679-683.
100. Johnston CJ, Williams JP, Okunieff P, Finkelstein JN. Radiation-induced pulmonary fibrosis: examination of chemokine and chemokine receptor families. *Radiat Res* 2002;157:256-265.
101. Hagemann T, Balkwill F, Lawrence T. Inflammation and cancer: a double-edged sword. *Cancer Cell* 2007;12:300-301.
102. Wyss-Coray T, Mucke L. Inflammation in neurodegenerative disease--a double-edged sword. *Neuron* 2002;35:419-432.
103. Morganti-Kossmann MC, Rancan M, Stahel PF, Kossmann T. Inflammatory response in acute traumatic brain injury: a double-edged sword. *Curr Opin Crit Care* 2002;8:101-105.
104. Stahel PF, Shohami E, Younis FM, Kariya K, Otto VI, Lenzlinger PM, Grosjean MB, Eugster HP, Trentz O, Kossmann T, Morganti-Kossmann MC. Experimental closed head injury: analysis of neurological outcome, blood-brain barrier dysfunction, intracranial neutrophil infiltration, and neuronal cell death in mice deficient in genes for pro-inflammatory cytokines. *J Cereb Blood Flow Metab* 2000;20:369-380.
105. Kiecolt-Glaser JK, Loving TJ, Stowell JR, Malarkey WB, Lemeshow S, Dickinson SL, Glaser R. Hostile marital interactions, proinflammatory cytokine production, and wound healing. *Arch Gen Psychiatry* 2005;62:1377-1384.
106. Ashcroft GS, Horan MA, Ferguson MW. Aging alters the inflammatory and endothelial cell adhesion molecule profiles during human cutaneous wound healing. *Lab Invest* 1998;78:47-58.
107. DiPietro LA, Polverini PJ, Rahbe SM, Kovacs EJ. Modulation of JE/MCP-1 expression in dermal wound repair. *Am J Pathol* 1995;146:868-875.

108. Noble LJ, Donovan F, Igarashi T, Goussev S, Werb Z. Matrix metalloproteinases limit functional recovery after spinal cord injury by modulation of early vascular events. *J Neurosci* 2002;22:7526-7535.

109. Sharman KG, Sharman EH, Yang E, Bondy SC. Dietary melatonin selectively reverses age-related changes in cortical cytokine mRNA levels, and their responses to an inflammatory stimulus. *Neurobiol Aging* 2002;23:633-638.

110. Gon Y, Hashimoto S, Hayashi S, Koura T, Matsumoto K, Horie T. Lower serum concentrations of cytokines in elderly patients with pneumonia and the impaired production of cytokines by peripheral blood monocytes in the elderly. *Clin Exp Immunol* 1996;106:120-126.

111. Inamizu T, Chang MP, Makinodan T. Influence of age on the production and regulation of interleukin-1 in mice. *Immunology* 1985;55:447-455.

112. Moon SK, Cha BY, Lee YC, Nam KS, Runge MS, Patterson C, Kim CH. Age-related changes in matrix metalloproteinase-9 regulation in cultured mouse aortic smooth muscle cells. *Exp Gerontol* 2004;39:123-131.

113. Caruso C, Candore G, Cigna D, DiLorenzo G, Sireci G, Dieli F, Salerno A. Cytokine production pathway in the elderly. *Immunol Res* 1996;15:84-90.

114. Flowers A. Brain tumors in the older person. *Cancer Control* 2000;7:523-538.

115. Villa S, Vinolas N, Verger E, Yaya R, Martinez A, Gil M, Moreno V, Caral L, Graus F. Efficacy of radiotherapy for malignant gliomas in elderly patients. *Int J Radiat Oncol Biol Phys* 1998;42:977-980.

116. Peschel RE, Wilson L, Haffty B, Papadopoulos D, Rosenzweig K, Feltes M. The effect of advanced age on the efficacy of radiation therapy for early breast cancer, local prostate cancer and grade III-IV gliomas. *Int J Radiat Oncol Biol Phys* 1993;26:539-544.

117. Rosenblum ML, Gerosa M, Dougherty DV, Reese C, Barger GR, Davis RL, Levin VA, Wilson CB. Age-related chemosensitivity of stem cells from human malignant brain tumours. *Lancet* 1982;1:885-887.

118. Rubin LL, Staddon JM. The cell biology of the blood-brain barrier. *Annu Rev Neurosci* 1999;22:11-28.

119. Abbott NJ, Ronnback L, Hansson E. Astrocyte-endothelial interactions at the blood-brain barrier. *Nat Rev Neurosci* 2006;7:41-53.

120. Banerjee S, Bhat MA. Neuron-glial interactions in blood-brain barrier formation. *Annu Rev Neurosci* 2007;30:235-258.
121. Nordal RA, Wong CS. Molecular targets in radiation-induced blood-brain barrier disruption. *Int J Radiat Oncol Biol Phys* 2005;62:279-287.
122. Diserbo M, Agin A, Lamproglou I, Mauris J, Staali F, Multon E, Amourette C. Blood-brain barrier permeability after gamma whole-body irradiation: an in vivo microdialysis study. *Can J Physiol Pharmacol* 2002;80:670-678.
123. Delattre JY, Shapiro WR, Posner JB. Acute effects of low-dose cranial irradiation on regional capillary permeability in experimental brain tumors. *J Neurol Sci* 1989;90:147-153.
124. d'Avella D, Cicciarello R, Albiero F, Mesiti M, Gagliardi ME, Russi E, d'Aquino A, Tomasello F, d'Aquino S. Quantitative study of blood-brain barrier permeability changes after experimental whole-brain radiation. *Neurosurgery* 1992;30:30-34.
125. Groothuis DR, Wright DC, Ostertag CB. The effect of 125I interstitial radiotherapy on blood-brain barrier function in normal canine brain. *J Neurosurg* 1987;67:895-902.
126. Bernstein M, Marotta T, Stewart P, Glen J, Resch L, Henkelman M. Brain damage from 125I brachytherapy evaluated by MR imaging, a blood-brain barrier tracer, and light and electron microscopy in a rat model. *J Neurosurg* 1990;73:585-593.
127. Fike JR, Cann CE, Phillips TL, Bernstein M, Gutin PH, Turowski K, Weaver KA, Davis RL, Higgins RJ, DaSilva V. Radiation brain damage induced by interstitial 125I sources: a canine model evaluated by quantitative computed tomography. *Neurosurgery* 1985;16:530-537.
128. Mun-Bryce S, Rosenberg GA. Matrix metalloproteinases in cerebrovascular disease. *J Cereb Blood Flow Metab* 1998;18:1163-1172.
129. Tilling T, Engelbertz C, Decker S, Korte D, Huwel S, Galla HJ. Expression and adhesive properties of basement membrane proteins in cerebral capillary endothelial cell cultures. *Cell Tissue Res* 2002;310:19-29.
130. Rutka JT, Apodaca G, Stern R, Rosenblum M. The extracellular matrix of the central and peripheral nervous systems: structure and function. *J Neurosurg* 1988;69:155-170.
131. Paulsson M. Basement membrane proteins: structure, assembly, and cellular interactions. *Crit Rev Biochem Mol Biol* 1992;27:93-127.

132. Rosenberg GA, Estrada E, Kelley RO, Kornfeld M. Bacterial collagenase disrupts extracellular matrix and opens blood-brain barrier in rat. *Neurosci Lett* 1993;160:117-119.
133. Sellner J, Leib SL. In bacterial meningitis cortical brain damage is associated with changes in parenchymal MMP-9/TIMP-1 ratio and increased collagen type IV degradation. *Neurobiol Dis* 2006;21:647-656.
134. Sellner J, Simon F, Meyding-Lamade U, Leib SL. Herpes-simplex virus encephalitis is characterized by an early MMP-9 increase and collagen type IV degradation. *Brain Res* 2006;1125:155-162.
135. Tilling T, Korte D, Hoheisel D, Galla HJ. Basement membrane proteins influence brain capillary endothelial barrier function in vitro. *J Neurochem* 1998;71:1151-1157.
136. Visse R, Nagase H. Matrix metalloproteinases and tissue inhibitors of metalloproteinases: structure, function, and biochemistry. *Circ Res* 2003;92:827-839.
137. Romanic AM, White RF, Arleth AJ, Ohlstein EH, Barone FC. Matrix metalloproteinase expression increases after cerebral focal ischemia in rats: inhibition of matrix metalloproteinase-9 reduces infarct size. *Stroke* 1998;29:1020-1030.
138. Strup-Perrot C, Vozenin-Brotons MC, Vandamme M, Linard C, Mathe D. Expression of matrix metalloproteinases and tissue inhibitor metalloproteinases increases in X-irradiated rat ileum despite the disappearance of CD8a T cells. *World J Gastroenterol* 2005;11:6312-6321.
139. Planas AM, Sole S, Justicia C. Expression and activation of matrix metalloproteinase-2 and -9 in rat brain after transient focal cerebral ischemia. *Neurobiol Dis* 2001;8:834-846.
140. Yang K, Liu L, Zhang T, Wu G, Ruebe C, Hu Y. TGF-betal transgenic mouse model of thoracic irradiation: modulation of MMP-2 and MMP-9 in the lung tissue. *J Huazhong Univ Sci Technolog Med Sci* 2006;26:301-304.
141. Araya J, Maruyama M, Sassa K, Fujita T, Hayashi R, Matsui S, Kashii T, Yamashita N, Sugiyama E, Kobayashi M. Ionizing radiation enhances matrix metalloproteinase-2 production in human lung epithelial cells. *Am J Physiol Lung Cell Mol Physiol* 2001;280:L30-38.
142. Hovdenak N, Wang J, Sung CC, Kelly T, Fajardo LF, Hauer-Jensen M. Clinical significance of increased gelatinolytic activity in the rectal mucosa during external beam radiation therapy of prostate cancer. *Int J Radiat Oncol Biol Phys* 2002;53:919-927.

143. Nirmala C, Jasti SL, Sawaya R, Kyritsis AP, Konduri SD, Ali-Osman F, Rao JS, Mohanam S. Effects of radiation on the levels of MMP-2, MMP-9 and TIMP-1 during morphogenic glial-endothelial cell interactions. *Int J Cancer* 2000;88:766-771.
144. Lukes A, Mun-Bryce S, Lukes M, Rosenberg GA. Extracellular matrix degradation by metalloproteinases and central nervous system diseases. *Mol Neurobiol* 1999;19:267-284.
145. Aoudjit F, Masure S, Opdenakker G, Potworowski EF, St-Pierre Y. Gelatinase B (MMP-9), but not its inhibitor (TIMP-1), dictates the growth rate of experimental thymic lymphoma. *Int J Cancer* 1999;82:743-747.
146. Wang Z, Juttermann R, Soloway PD. TIMP-2 is required for efficient activation of proMMP-2 in vivo. *J Biol Chem* 2000;275:26411-26415.
147. Strup-Perrot C, Vozenin-Brotons MC, Vandamme M, Benderitter M, Mathe D. Expression and activation of MMP -2, -3, -9, -14 are induced in rat colon after abdominal X-irradiation. *Scand J Gastroenterol* 2006;41:60-70.
148. Clark R. Molecular and Cellular Biology of Wound Repair. 2 nd ed ed. New York: Springer-Verlag; 1996.
149. Ferrara N. Vascular endothelial growth factor: molecular and biological aspects. *Curr Top Microbiol Immunol* 1999;237:1-30.
150. Plate KH. Mechanisms of angiogenesis in the brain. *J Neuropathol Exp Neurol* 1999;58:313-320.
151. Breier G, Albrecht U, Sterrer S, Risau W. Expression of vascular endothelial growth factor during embryonic angiogenesis and endothelial cell differentiation. *Development* 1992;114:521-532.
152. Davis S, Aldrich TH, Jones PF, Acheson A, Compton DL, Jain V, Ryan TE, Bruno J, Radziejewski C, Maisonpierre PC, Yancopoulos GD. Isolation of angiopoietin-1, a ligand for the TIE2 receptor, by secretion-trap expression cloning. *Cell* 1996;87:1161-1169.
153. Witzenbichler B, Maisonpierre PC, Jones P, Yancopoulos GD, Isner JM. Chemotactic properties of angiopoietin-1 and -2, ligands for the endothelial-specific receptor tyrosine kinase Tie2. *J Biol Chem* 1998;273:18514-18521.
154. Koblizek TI, Weiss C, Yancopoulos GD, Deutsch U, Risau W. Angiopoietin-1 induces sprouting angiogenesis in vitro. *Curr Biol* 1998;8:529-532.

155. Hayes AJ, Huang WQ, Mallah J, Yang D, Lippman ME, Li LY. Angiopoietin-1 and its receptor Tie-2 participate in the regulation of capillary-like tubule formation and survival of endothelial cells. *Microvasc Res* 1999;58:224-237.

156. Sato TN, Tozawa Y, Deutsch U, Wolburg-Buchholz K, Fujiwara Y, Gendron-Maguire M, Gridley T, Wolburg H, Risau W, Qin Y. Distinct roles of the receptor tyrosine kinases Tie-1 and Tie-2 in blood vessel formation. *Nature* 1995;376:70-74.

157. Peters KG, Kontos CD, Lin PC, Wong AL, Rao P, Huang L, Dewhirst MW, Sankar S. Functional significance of Tie2 signaling in the adult vasculature. *Recent Prog Horm Res* 2004;59:51-71.

158. Valenzuela DM, Griffiths JA, Rojas J, Aldrich TH, Jones PF, Zhou H, McClain J, Copeland NG, Gilbert DJ, Jenkins NA, Huang T, Papadopoulos N, Maisonpierre PC, Davis S, Yancopoulos GD. Angiopoietins 3 and 4: diverging gene counterparts in mice and humans. *Proc Natl Acad Sci U S A* 1999;96:1904-1909.

159. Yancopoulos GD, Davis S, Gale NW, Rudge JS, Wiegand SJ, Holash J. Vascular-specific growth factors and blood vessel formation. *Nature* 2000;407:242-248.

160. Lyubimova N, Hopewell JW. Experimental evidence to support the hypothesis that damage to vascular endothelium plays the primary role in the development of late radiation-induced CNS injury. *Br J Radiol* 2004;77:488-492.

161. Pena LA, Fuks Z, Kolesnick RN. Radiation-induced apoptosis of endothelial cells in the murine central nervous system: protection by fibroblast growth factor and sphingomyelinase deficiency. *Cancer Res* 2000;60:321-327.

162. Lewin B. Genes VII: Oxford University Press; 1999.

163. Gardner TS, Faith, Jeremiah J. Reverse-engineering transcription control networks. *Physics of Life Reviews* 2005;2:65-88.

164. Gene regulatory networks (GRNs); http://genomicscience.energy.gov/science/generegulatorynetwork.shtml

165. Mazur J, Ritter D, Reinelt G, Kaderali L. Reconstructing nonlinear dynamic models of gene regulation using stochastic sampling. *BMC Bioinformatics* 2009;10:448.

166. Akutsu T, Miyano S, Kuhara S. Identification of genetic networks from a small number of gene expression patterns under the Boolean network model. *Pac Symp Biocomput* 1999:17-28.

167. Liang S, Fuhrman S, Somogyi R. Reveal, a general reverse engineering algorithm for inference of genetic network architectures. *Pac Symp Biocomput* 1998:18-29.
168. Chen T, He HL, Church GM. Modeling gene expression with differential equations. *Pac Symp Biocomput* 1999:29-40.
169. D'Haeseleer P, Wen X, Fuhrman S, Somogyi R. Linear modeling of mRNA expression levels during CNS development and injury. *Pac Symp Biocomput* 1999:41-52.
170. Cho KH, Shin SY, Lee HW, Wolkenhauer O. Investigations into the analysis and modeling of the TNF alpha-mediated NF-kappa B-signaling pathway. *Genome Res* 2003;13:2413-2422.
171. Lee WH, Sonntag WE, Mitschelen M, Yan H, Lee YW. Irradiation induces regionally specific alterations in pro-inflammatory environments in rat brain. *Int J Radiat Biol* 2010;86:132-144.
172. Blasi E, Barluzzi R, Bocchini V, Mazzolla R, Bistoni F. Immortalization of murine microglial cells by a v-raf/v-myc carrying retrovirus. *J Neuroimmunol* 1990;27:229-237.
173. Kim HJ, Jung KJ, Yu BP, Cho CG, Choi JS, Chung HY. Modulation of redox-sensitive transcription factors by calorie restriction during aging. *Mech Ageing Dev* 2002;123:1589-1595.
174. Deng X, Li H, Tang YW. Cytokine expression in respiratory syncytial virus-infected mice as measured by quantitative reverse-transcriptase PCR. *J Virol Methods* 2003;107:141-146.
175. Livak KJ, Schmittgen TD. Analysis of relative gene expression data using real-time quantitative PCR and the 2(-Delta Delta C(T)) Method. *Methods* 2001;25:402-408.
176. Bradford MM. A rapid and sensitive method for the quantitation of microgram quantities of protein utilizing the principle of protein-dye binding. *Anal Biochem* 1976;72:248-254.
177. Beg AA, Finco TS, Nantermet PV, Baldwin AS, Jr. Tumor necrosis factor and interleukin-1 lead to phosphorylation and loss of I kappa B alpha: a mechanism for NF-kappa B activation. *Mol Cell Biol* 1993;13:3301-3310.
178. Marquette C, Linard C, Galonnier M, Van Uye A, Mathieu J, Gourmelon P, Clarencon D. IL-1beta, TNFalpha and IL-6 induction in the rat brain after partial-body irradiation: role of vagal afferents. *Int J Radiat Biol* 2003;79:777-785.

179. Linard C, Ropenga A, Vozenin-Brotons MC, Chapel A, Mathe D. Abdominal irradiation increases inflammatory cytokine expression and activates NF-kappaB in rat ileal muscularis layer. *Am J Physiol Gastrointest Liver Physiol* 2003;285:G556-565.

180. Linard C, Marquette C, Mathieu J, Pennequin A, Clarencon D, Mathe D. Acute induction of inflammatory cytokine expression after gamma-irradiation in the rat: effect of an NF-kappaB inhibitor. *Int J Radiat Oncol Biol Phys* 2004;58:427-434.

181. Block ML, Zecca L, Hong JS. Microglia-mediated neurotoxicity: uncovering the molecular mechanisms. *Nat Rev Neurosci* 2007;8:57-69.

182. Xiao Z, Su Y, Yang S, Yin L, Wang W, Yi Y, Fenton BM, Zhang L, Okunieff P. Protective effect of esculentoside A on radiation-induced dermatitis and fibrosis. *Int J Radiat Oncol Biol Phys* 2006;65:882-889.

183. Son EW, Rhee DK, Pyo S. Gamma-irradiation-induced intercellular adhesion molecule-1 (ICAM-1) expression is associated with catalase: activation of Ap-1 and JNK. *J Toxicol Environ Health A* 2006;69:2137-2155.

184. Beetz A, Peter RU, Oppel T, Kaffenberger W, Rupec RA, Meyer M, van Beuningen D, Kind P, Messer G. NF-kappaB and AP-1 are responsible for inducibility of the IL-6 promoter by ionizing radiation in HeLa cells. *Int J Radiat Biol* 2000;76:1443-1453.

185. Brach MA, Hass R, Sherman ML, Gunji H, Weichselbaum R, Kufe D. Ionizing radiation induces expression and binding activity of the nuclear factor kappa B. *J Clin Invest* 1991;88:691-695.

186. Park JS, Qiao L, Su ZZ, Hinman D, Willoughby K, McKinstry R, Yacoub A, Duigou GJ, Young CS, Grant S, Hagan MP, Ellis E, Fisher PB, Dent P. Ionizing radiation modulates vascular endothelial growth factor (VEGF) expression through multiple mitogen activated protein kinase dependent pathways. *Oncogene* 2001;20:3266-3280.

187. Mori K, Tani M, Kamata K, Kawamura H, Urata Y, Goto S, Kuwano M, Shibata S, Kondo T. Mitogen-activated protein kinase, ERK1/2, is essential for the induction of vascular endothelial growth factor by ionizing radiation mediated by activator protein-1 in human glioblastoma cells. *Free Radic Res* 2000;33:157-166.

188. Zhou D, Yu T, Chen G, Brown SA, Yu Z, Mattson MP, Thompson JS. Effects of NF-kappaB1 (p50) targeted gene disruption on ionizing radiation-induced NF-kappaB

activation and TNFalpha, IL-1alpha, IL-1beta and IL-6 mRNA expression in vivo. *Int J Radiat Biol* 2001;77:763-772.

189. Raju U, Gumin GJ, Tofilon PJ. Radiation-induced transcription factor activation in the rat cerebral cortex. *Int J Radiat Biol* 2000;76:1045-1053.
190. Grosch S, Kaina B. Transcriptional activation of apurinic/apyrimidinic endonuclease (Ape, Ref-1) by oxidative stress requires CREB. *Biochem Biophys Res Commun* 1999;261:859-863.
191. Iwata E, Asanuma M, Nishibayashi S, Kondo Y, Ogawa N. Different effects of oxidative stress on activation of transcription factors in primary cultured rat neuronal and glial cells. *Brain Res Mol Brain Res* 1997;50:213-220.
192. Goodwin BC. Oscillatory behavior in enzymatic control processes. *Adv Enzyme Regul* 1965;3:425-438.
193. Yagil G, Yagil E. On the relation between effector concentration and the rate of induced enzyme synthesis. *Biophys J* 1971;11:11-27.
194. Wolf DM, Eeckman FH. On the relationship between genomic regulatory element organization and gene regulatory dynamics. *J Theor Biol* 1998;195:167-186.
195. Buchler NE, Gerland U, Hwa T. Nonlinear protein degradation and the function of genetic circuits. *Proc Natl Acad Sci U S A* 2005;102:9559-9564.
196. Nakagawa R, Naka T, Tsutsui H, Fujimoto M, Kimura A, Abe T, Seki E, Sato S, Takeuchi O, Takeda K, Akira S, Yamanishi K, Kawase I, Nakanishi K, Kishimoto T. SOCS-1 participates in negative regulation of LPS responses. *Immunity* 2002;17:677-687.
197. Rigby RJ, Simmons JG, Greenhalgh CJ, Alexander WS, Lund PK. Suppressor of cytokine signaling 3 (SOCS3) limits damage-induced crypt hyper-proliferation and inflammation-associated tumorigenesis in the colon. *Oncogene* 2007;26:4833-4841.
198. Lee WH, Sonntag WE, Lee YW. Aging attenuates radiation-induced expression of pro-inflammatory mediators in rat brain. *Neurosci Lett* 2010;476:89-93.
199. Liu Y, Xiao S, Liu J, Zhou H, Liu Z, Xin Y, Suo WZ. An experimental study of acute radiation-induced cognitive dysfunction in a young rat model. *AJNR Am J Neuroradiol* 2010;31:383-387.

200. Tabatabai G, Frank B, Mohle R, Weller M, Wick W. Irradiation and hypoxia promote homing of haematopoietic progenitor cells towards gliomas by TGF-beta-dependent HIF-1alpha-mediated induction of CXCL12. *Brain* 2006;129:2426-2435.

201. Nagase H, Woessner JF, Jr. Matrix metalloproteinases. *J Biol Chem* 1999;274:21491-21494.

202. Bruunsgaard H, Pedersen AN, Schroll M, Skinhoj P, Pedersen BK. Impaired production of proinflammatory cytokines in response to lipopolysaccharide (LPS) stimulation in elderly humans. *Clin Exp Immunol* 1999;118:235-241.

203. Wallace PK, Eisenstein TK, Meissler JJ, Jr., Morahan PS. Decreases in macrophage mediated antitumor activity with aging. *Mech Ageing Dev* 1995;77:169-184.

204. Yates SL, Burgess LH, Kocsis-Angle J, Antal JM, Dority MD, Embury PB, Piotrkowski AM, Brunden KR. Amyloid beta and amylin fibrils induce increases in proinflammatory cytokine and chemokine production by THP-1 cells and murine microglia. *J Neurochem* 2000;74:1017-1025.

205. Wood JA, Wood PL, Ryan R, Graff-Radford NR, Pilapil C, Robitaille Y, Quirion R. Cytokine indices in Alzheimer's temporal cortex: no changes in mature IL-1 beta or IL-1RA but increases in the associated acute phase proteins IL-6, alpha 2-macroglobulin and C-reactive protein. *Brain Res* 1993;629:245-252.

206. Akwa Y, Hassett DE, Eloranta ML, Sandberg K, Masliah E, Powell H, Whitton JL, Bloom FE, Campbell IL. Transgenic expression of IFN-alpha in the central nervous system of mice protects against lethal neurotropic viral infection but induces inflammation and neurodegeneration. *J Immunol* 1998;161:5016-5026.

207. Morganti-Kossman MC, Lenzlinger PM, Hans V, Stahel P, Csuka E, Ammann E, Stocker R, Trentz O, Kossmann T. Production of cytokines following brain injury: beneficial and deleterious for the damaged tissue. *Mol Psychiatry* 1997;2:133-136.

208. Tsao MN, Lloyd NS, Wong RK, Rakovitch E, Chow E, Laperriere N. Radiotherapeutic management of brain metastases: a systematic review and meta-analysis. *Cancer Treat Rev* 2005;31:256-273.

209. Kantor G, Laprie A, Huchet A, Loiseau H, Dejean C, Mazeron JJ. [Radiation therapy for glial tumors: technical aspects and clinical indications]. *Cancer Radiother* 2008;12:687-694.

210. Stone HB, Moulder JE, Coleman CN, Ang KK, Anscher MS, Barcellos-Hoff MH, Dynan WS, Fike JR, Grdina DJ, Greenberger JS, Hauer-Jensen M, Hill RP, Kolesnick RN, Macvittie TJ, Marks C, McBride WH, Metting N, Pellmar T, Purucker M, Robbins ME, Schiestl RH, Seed TM, Tomaszewski JE, Travis EL, Wallner PE, Wolpert M, Zaharevitz D. Models for evaluating agents intended for the prophylaxis, mitigation and treatment of radiation injuries. Report of an NCI Workshop, December 3-4, 2003. *Radiat Res* 2004;162:711-728.

211. Oh LY, Larsen PH, Krekoski CA, Edwards DR, Donovan F, Werb Z, Yong VW. Matrix metalloproteinase-9/gelatinase B is required for process outgrowth by oligodendrocytes. *J Neurosci* 1999;19:8464-8475.

212. Scholler K, Trinkl A, Klopotowski M, Thal SC, Plesnila N, Trabold R, Hamann GF, Schmid-Elsaesser R, Zausinger S. Characterization of microvascular basal lamina damage and blood-brain barrier dysfunction following subarachnoid hemorrhage in rats. *Brain Res* 2007;1142:237-246.

213. Hamann GF, Okada Y, Fitridge R, del Zoppo GJ. Microvascular basal lamina antigens disappear during cerebral ischemia and reperfusion. *Stroke* 1995;26:2120-2126.

214. Rosenberg GA, Kornfeld M, Estrada E, Kelley RO, Liotta LA, Stetler-Stevenson WG. TIMP-2 reduces proteolytic opening of blood-brain barrier by type IV collagenase. *Brain Res* 1992;576:203-207.

215. CBTRUS. Statistical Report: Primary Brain and Central Nervous System Tumors Diagnosed in the United States in 2004-2006; 2010.

216. Ramanan S, Zhao W, Riddle DR, Robbins ME. Role of PPARs in Radiation-Induced Brain Injury. *PPAR Res*;2010:234975.

217. Holash J, Wiegand SJ, Yancopoulos GD. New model of tumor angiogenesis: dynamic balance between vessel regression and growth mediated by angiopoietins and VEGF. *Oncogene* 1999;18:5356-5362.

218. Isner JM, Asahara T. Angiogenesis and vasculogenesis as therapeutic strategies for postnatal neovascularization. *J Clin Invest* 1999;103:1231-1236.

219. Calvo W, Hopewell JW, Reinhold HS, van den Berg AP, Yeung TK. Dose-dependent and time-dependent changes in the choroid plexus of the irradiated rat brain. *Br J Radiol* 1987;60:1109-1117.

220. Li YQ, Chen P, Jain V, Reilly RM, Wong CS. Early radiation-induced endothelial cell loss and blood-spinal cord barrier breakdown in the rat spinal cord. *Radiat Res* 2004;161:143-152.

221. Hanahan D. Signaling vascular morphogenesis and maintenance. *Science* 1997;277:48-50.

222. Miller JW, Adamis AP, Shima DT, D'Amore PA, Moulton RS, O'Reilly MS, Folkman J, Dvorak HF, Brown LF, Berse B. Vascular endothelial growth factor/vascular permeability factor is temporally and spatially correlated with ocular angiogenesis in a primate model. *Am J Pathol* 1994;145:574-584.

223. Alavi A, Hood JD, Frausto R, Stupack DG, Cheresh DA. Role of Raf in vascular protection from distinct apoptotic stimuli. *Science* 2003;301:94-96.